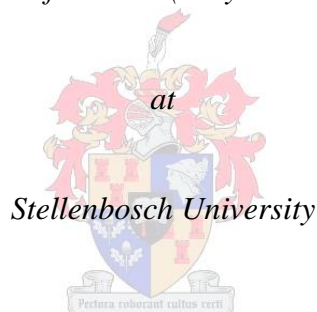**Synthesis and structure-property relationships of 3-methylene-2-pyrrolidone-based (co)polymers**

By

Ingrid Heyns

Thesis presented in fulfilment of the requirements for the degree of Masters of Science (Polymer Science)

at

Stellenbosch University

Supervisor: Prof. Bert Klumperman
Co-supervisor: Dr. Rueben Pfukwa

Department of Chemistry and Polymer Science

Faculty of Science

March 2015

Declaration

By submitting this thesis/dissertation electronically, I declare that the entirety of the work contained therein is my own, original work, that I am the sole author thereof (save to the extent explicitly otherwise stated), that reproduction and publication thereof by Stellenbosch University will not infringe any third party rights and that I have not previously in its entirety or in part submitted it for obtaining any qualification.

Ingrid Heyns   Date: March 2015

Abstract

Recently, the incorporation of renewable resources as a substitute to fossil fuels in the synthesis of polymers/materials has attracted a vast amount of interest, particularly for the green advantages offered.

This study describes the synthesis, polymerization and characterization of 3-methylene-2-pyrrolidone-based (3M2P) monomers, with 3M2P being a naturally occurring lactam moiety.

Two different chemical syntheses of the monomer, 3M2P, were attempted, with the first approach involving the Wittig reaction for the formation of the *exo*-cyclic methylene group. The second approach involved the dehydration of 3-(hydroxymethyl)-2-pyrrolidone. Preference was given to the Wittig approach during the study conducted, as the dehydration reaction of the second approach was unsuccessful. The purification and control over by- and side-products of the Wittig approach were optimized and confirmed by various spectroscopic techniques.

Statistical copolymerizations of 3M2P-based monomers revealed the formation of oligomers, while *in situ* ^{1}H NMR spectroscopic experiments failed to quantify the incorporation or consumption of either monomers due to a peak overlap. Conventional radical homopolymerizations of 3M2P were successful and polymers were characterized by NMR spectroscopy and size exclusion chromatography (SEC). It was discovered that the polymer, P(3M2P), has very good thermal stability with a $T_g = 285$ °C and a decomposition temperature between 400-500 °C. P(3M2P) proved to be extremely water-soluble, but it did not dissolve in most organic solvents. The thermal and solubility behaviour were ascribed to the structurally rigid lactam moiety and its strong hydrogen-bonding ability. Cytotoxicity testing revealed that P(3M2P) was completely non-toxic.

Finally, the polymerization versatility of 3M2P was evaluated *via* different living radical polymerization techniques in an attempt to create well-defined macromolecules with precision. SET-LRP and RAFT polymerizations proved to be controlled, with a $Đ < 1.5$, whilst NMP exhibited poor control. The RAFT polymerization was extended to an amphiphilic block copolymer with the first segment being polystyrene and the second segment, P(3M2P). During the chain-extension only oligomeric 3M2P species were incorporated.

Opsomming

Met die toenemende belangstelling in die gebruik van meer omgewingsvriendelike materiale en die soeke na plaasvervangers vir nie-hernieubare fossielbrandstowwe vir die sintese van polimere, is daar 'n alewige toename in die ontwikkellinge van prosesse om die bogenoemde te bevorder. 'n Benadering om die probleem te oorkom is om van hernubare hulpbronne gebruik te maak.

Gevolglik fokus hierdie studie op die sintese, polimerisasie en 'n ontleding van die karaktereienskappe van 3-metileen-2-pyrolidoon (3M2P) monomere. 3M2P is 'n laktaam gedeelte wat natuurlik voorkom.

Met die sintese van 3M2P, is twee verskillende chemiese benaderings aangepak. Voorkeur is gegee aan die benadering wat van die Wittig reaksie gebruik maak vir die vorming van die *ekso*-sikliese metileen groep, aangesien die tweede benadering, wat die dehidrasie van 3-(hydroksiemetiel)-2-pyrolidoon behels het, nie die dehidrasie van dié spesifieke reaksie teweeg kon bring nie. Die suiwering en beheer oor beide mede- en neweprodukte is geoptimaliseer, aangepas vir grootskaalse produksie en is bevestig deur verskeie spektroskopiese tegnieke.

Statistiese kopolimerisasies van die 3M2P-gebaseerde monomere, het die vorming van oligomere onthul, terwyl *in situ* ^{1}H KMR spektroskopie eksperimente versuim het om die gebruik en verbruik van enige van die monomere te definieer, a.g.v. die oorvleuling van pieke. Daarteenoor, was die meer algemene radikale homopolimerisasies van 3M2P meer suksesvol en dit was moontlik om die polimere se karaktereienskappe te definieer deur beide KMR spektroskopie and SEC. Daar is bevind dat die polimeer, P(3M2P), 'n baie bevredigende termiese stabiliteit met T_g = 285 °C en 'n ontbindingstemperatuur van tussen 400-500 °C, gehandhaaf het. Daar is verder bevind dat P(3M2P) water-oplosbaar was en weerstand tot die meeste organiese oplosmiddels gebied het. Die termiese en oplosbaarheidseienskappe is toeskryfbaar aan die strukturele-rigied laktaam en die sterk potensiaal om waterstofbindings te vorm. Sitotoksiese toetse het ook onthul dat P(3M2P) geheel en al nie-toksies is.

Laastens is die vermoë van 3M2P om polimere te vorm, geevalueer deur die gebruik van verskeie lewende radikaal polymerisasie tegnieke in pogings om wel-gedefinieerde

makromolekules met presisie te ontwikkel. SET-LRP en RAFT polimerisasies het gedui daarop dat beheer oor die reaksie behou is, met 'n $Đ < 1.5$, terwyl NMP op die verlies in beheer gedui het. Die RAFT polimerisasies is verder uitgebrei tot 'n amfifiliese blokkopolimeer, waarvan die eerste segment polistireën en die tweede segment P(3M2P), ingesluit het. Met die ketting-verlenging daarvan, is daar slegs oligomeriese 3M2P spesies geïnkorporeer.

To my parents, Brian, Annamarie and sister, Thea.

Acknowledgements

First of all, I would like to thank my supervisor, Prof. Klumperman, for your advice, guidance, innovative ideas and input during this project - it is an honour working in your research group.

To my co-supervisor, Dr. Rueben Pfukwa, I thank you for your patience, advice and for your continuous encouragement and assistance with my research techniques in-and outside the lab. I am extremely grateful for all your help.

I wish to thank the NRF for financial assistance during my project.

The following staff members of Polymer Science I thank for their assistance: Erinda Cooper, Aneli Fourie, Calvin Maart, Jim Motshweni and Deon Koen.

The following people I thank for their contributions with analysis: Elsa Malherbe and Dr Jaco Brand for always going out of their way to help me with NMR spectroscopy analysis. Drs Marietjie Stander and Hilten Fletcher for Mass Spectrometry. Divann Robertson I also kindly thank for his assistance with DSC.

I would like to thank Dr. Rehana Malgas for the hydrogenation reaction and Dr. Ben Loos for the biocompatibility tests.

I would also like to give a special thanks to Dr. Waled Hadasha and Dr. Lebohang Hlalele for their invaluable input during this project.

I thank the previous and present members of the Free Radical group: Rueben, Johnel, Elrika, Jane, Welmarie, Siyasanga, Lehani, Nicole, Mpho, Njabu, Judith, William, Paul, Lebohang, Sandile, Waled, Anna, Sthembile, Khotso, Alex, Nusrat, Cecilia, Precious, Andri, Barry, Inge and Renier for their contributions, friendships and all the beers. Special thanks to Johnel, for all the encouragement during the late nights spent writing up our theses.

Inge, Paul and Lebohang are thanked for their donations of living polymerization reagents - I really appreciate it.

My friends and family are acknowledged for their support and encouraging words throughout this project.

Lastly, to my parents and sister, Thea – thank you for always believing in me, you are my pillar of support! I love you!

Table of Contents

List of Figures

xiii

List of Schemes

List of tables

List of Abbreviations

3M2P	3-methylene-2-pyrrolidone
3M2P-OH	N-(hydroxymethyl)-3-methylene-2-pyrrolidone
ATRP	atom transfer radical polymerization
DCC	N,N'-dicyclohexylcarbodiimide
DMEM	Dulbecco's modified eagle medium
DMF	dimethylformamide
DMSO	dimethyl sulfoxide
DSC	differential scanning calorimetry
HFIP	1,1,1,3,3,3-hexafluoro-2-propanol
LRP	living radical polymerization
Me_6TREN	tris[2-(dimethylamino) ethyl]amine
NMP	nitroxide mediated polymerization
NMR	nuclear magnetic resonance
P(3M2P)	poly(3-methylene-2-pyrrolidone)
PEG	polyethylene glycol
PS	polystyrene
PVP	polyvinylpyrrolidone
RAFT	reversible-addition fragmentation chain-transfer
ROP	ring-opening polymerization
SEC	size exclusion chromatography
SET-LRP	single electron transfer
TGA	thermogravimetric analysis
THF	tetrahydrofuran
TPP/PPh_3	triphenylphosphine
$TPPO/O=PPh_3$	triphenylphosphine oxide
UV	ultra violet

Chapter 1: Prologue

1.1 Introduction

Currently most commodity polymers are produced from fossil fuels and the dependence on these natural resources raised many concerns with regard to the sustainability of processes that involve these resources. There are two main concerns that need to be addressed. Firstly, the rate at which the fossil fuels are being depleted create a need to develop alternatives for synthesizing polymers. Secondly, combustion of fossil fuels has various negative effects on the environment such as pollution, extinction of wild life, greenhouse gasses, *etc*.[1]

One of the approaches to finding a greener alternative and minimizing or eliminating the effects of fossil fuels, is switching to renewable resources.[2] Sugars are the most common compound harvested from a wide variety of resources, and can be used as building blocks for creating polymers of which poly(lactic acid) is a well-known example.[3]

Another example of a compound harvested from a natural resource to create polymers is tulipalin A, a compound present in certain species of tulips, *Tulipa Gesneriana L.* (Figure 1.1) and has previously been studied for its biological[4] and monomer properties. This lactone with a *exo*-methylene group is currently utilized as a monomer and extensive research has been done on the polymerization of this monomer and the interesting characteristics of poly(tulipalin A). The properties of poly(tulipalin A) have been compared to its petroleum-based ring-open analogue, poly(methyl methacrylate).[5]
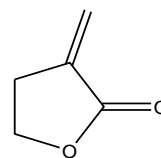
Figure 1.1: *Tulipa Gesneriana L*. **and tulipalin A.**

1.2 Objectives

The objective of this study was to chemically synthesize a biosynthetically accessible monomer, 3-methylene-2-pyrrolidone (3M2P) with the aim of synthesizing potentially renewable 3M2P-based (co)polymers. We aimed to utilize spectroscopic and chromatographic techniques to determine the molecular weights of the polymers. We anticipated that various thermal analyses, as well as solubility and cytotoxicity behaviour would be adequate for the characterizations and give an indication of possible applications of the polymer. Furthermore, living radical polymerization techniques and sophisticated architectures such as block copolymers would prove whether the 3M2P polymerizations could be controlled and ultimately establish the versatility of 3M2P.

1.3 Thesis layout

The thesis comprises six chapters:

In Chapter 1, a brief insight in the importance of finding alternatives to petroleum-based materials is provided. The objectives of the study are demonstrated.

Chapter 2 gives a literature review discussing the demand for renewable alternatives to fossil fuel-based materials, in particular, polymers that originate from renewable resources. Naturally occurring lactones and lactams incorporated into polymers and examples thereof, are presented.

In Chapter 3, two approaches to the chemical synthesis of the monomer (3M2P) are presented. The purification protocol and control over by- and side-products are demonstrated for the optimized and up-scaled synthesis route.

In Chapter 4, the conventional radical polymerization of 3M2P and a full characterization of the polymer are described.

In Chapter 5, various living radical polymerization techniques are adopted to polymerize 3M2P in an attempt to control the molar mass distribution and end-groups of P(3M2P).

Finally, Chapter 6 concludes with a summary and difficulties encountered during the entire study, with additional suggestions for future work.

1.4 References

(1) McCarthy, J. J. *Science* **2009**, *326*, 1646.

(2) Coates, G. W.; Hillmyer, M. A. *Macromolecules* **2009**, *42*, 7987.

(3) Benninga, H. In *A History of Lactic Acid Making: a Chapter in the History of Biotechnology*; Springer, 1990.

(4) Rosowsky, A.; Papathanasopoulos, N.; Lazarus, H.; Foley, G. E.; Modest, E. J. *J. Med. Chem.* **1974**, *17*, 672.

(5) Akkapeddi, M. K. *Macromolecules* **1979**, *12*, 546.

Chapter 2: Historical and theoretical background

2.1 Introduction

The aquatic and land resources that absorb and recycle carbon dioxide (CO_2) are not able to rejuvenate the accumulating CO_2 currently created by anthropogenic activities. CO_2, the main greenhouse gas, adversely effects our atmosphere by means of various types of irreversible pollutions, causing climate change, sea-level rising, extinction of wild life, *etc*.[1]

Measurements of the atmospheric CO_2 concentration were first carried out at an observatory in Mauna Loa, Hawaii. Data has been collected since 1957, and is depicted in Figure 2.1 as the so-called "Keeling curve" where the ratio of ^{13}C to ^{12}C is measured by NMR spectroscopy.[2] From this plot, it is clear that the concentration of CO_2 in the atmosphere has been increasing dramatically. Currently the "Keeling" status is above 400 ppm, which has never been observed at this level before.[1]
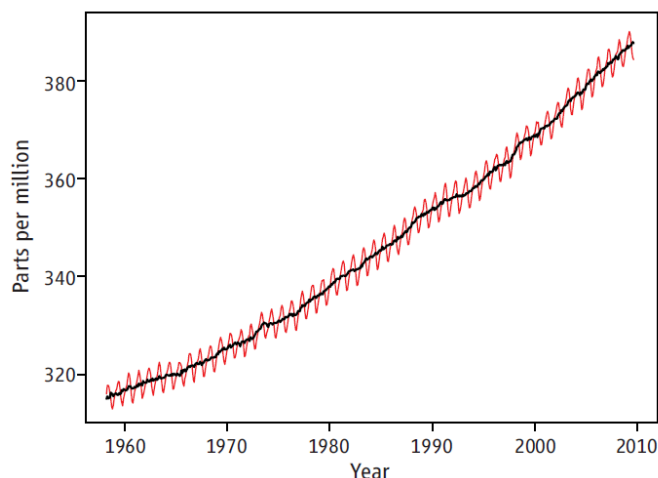
Figure 2.1: Keeling curve for 1957 - 2010 (monthly mean). The red curved line indicates the seasonal changes.[1]

Fossil fuels are utilized as an energy source and currently most hydrocarbon chemicals, such as olefins, originate from them. It is imperative to find alternatives to fossil fuels to mitigate their depletion, and the increased CO_2 levels resulting from combustion. Different strategies are being implemented, with the most important being to find a "greener" alternative to exploiting fossil

fuels as a source of energy and carbon-based chemicals.[3] An evolving approach is to eliminate the emission of CO_2, by chemists designing novel, economical and green materials, originating or biosynthesized from renewable resources. This involves the biotechnological design and synthesis of bio-monomers and polymerization thereof, towards the development of biopolymers/bio-derived materials with comparable properties to those of the petroleum-derived commodity materials.[4] Other options involve biochemical modification *via* for instance, microbial fermentation, of already available natural polymers.[5,6] The field of study is often referred to as green chemistry,[3,7] where sustainability is designed and originates on the molecular level.[8]

The importance of green chemistry practices has increased since the United States Pollution Prevention Act of 1990.[9] Chemists in this field follow a set of principles, also known as the *12 principles of green chemistry*.[7,8,10]

2.1.1 Green Chemistry

The aspect of producing green polymers from renewable resources has expanded tremendously over the last two decades.[4]The 12 principles of green chemistry can be simplified to aspects such as: waste prevention, degradable materials, less/no hazardous materials, reducing derivatives, catalyzed reactions, non-toxic solvents, implementing renewable materials and design of energy efficient processes with the potential of up-scaling *etc*.[10] Although every aspect of the 12 principles is important in practice, it is not realistic to meet all the requirements at one go.

2.1.2 Polymers from renewable resources

Biopolymers is the broad term for naturally occurring polymers and polymers originating from renewable raw materials, where the latter are often referred to as "bio-based polymers".[11]

A distinction between biodegradability of bio-based polymers and natural occurring polymers should be acknowledged. Natural microorganisms (fungi, bacteria *etc*.) degrade biopolymers into water, carbon dioxide and non-toxic byproducts. Natural occurring polymers such as polysaccharides are biodegradable. However, certain polymers derived from renewable resources are not biodegradable *per se*, and the biodegradability is reliant on the specific chemical structure.[12]

Most commercially available products derived from renewable resources are currently based on polylactic acid (PLA), which is a biodegradable polymer. PLA is derived from dextrose, glucose, maltose, sucrose, lactose (sugars) and starch; harvested from agricultural feedstocks such as rice, corn, potato, cane, cheese whey *etc*. and fermented into lactic acid,[13] and subsequently heated to yield the cyclic monomer, lactide. PLA can either be polymerized by step-growth polymerization, where two lactic acid molecules will condense or by the ring-opening polymerization (ROP) of the lactide.[14] Companies such as Cargill Dow LCC developed Natureworks™ and Ingeo™, a biodegradable and compostable bioplastic and a fiber, respectively, made of PLA.[15] Similarly, BASF developed Ecoflex®, a biodegradable aliphatic-aromatic polyester synthesized or blended with raw materials, and Ecovio®, which is a blend of Ecoflex® and PLA.[16] PLA is an aliphatic polyester and degradation will follow upon hydrolysis of the ester bond, into non-toxic compounds within six months to two years.[17] Vinyl polymers such as polystyrene and polyethylene may degrade over a period of 500 to 1000 years.[18] Their non-biodegradability is due to the hydrocarbon backbone of the polymers.[12]

Polyamides, polyesters, polyurethanes, polycarbonates and epoxy resins are all step-growth polymers originating from petroleum-based materials. Step-growth polymers condense/react at functional groups on the monomers. Similarly, monomers obtained from agricultural feedstocks; starch, fatty acids, cellulose, monosaccharides, lactic acid and amino acids are also polymerized at the functional groups *via* step-growth.[12,19]

Biodegradable polymers are not always preferred above non-degradable polymers. An impediment of commercially available biodegradable polymers is that they are not strong enough and in certain applications, polymers with specific properties are required such as; toughness, heat-resistance, solvent-and moisture resistance, *etc*. These physical properties are easily met by most all-carbon polymers, which are produced from vinyl monomers, derived from fossil fuels. Creating biopolymers from vinyl plant-based monomers circumvents the polluting effects of fossil fuels and leans towards sustainability.

In order for the bio-based polymers to compete with the existing, more affordable petroleum-based polymers, the polymers need to be designed with similar/superior physical properties, besides the green advantages that they offer.[20] For instance, the biotechnological manipulation of the polymeric backbone by introducing specific functional groups *via* functional group

methathesis polymerization (FGM) or elevating the biopolymers' thermal behaviour (melting and glass transition temperature) by incorporating aromatic compounds such as vanillin, isolated from naturally occurring, lignin.[21] Polycarbonates[22] and polyoxalates[23] are directly polymerized by FGM from a diol, dimethoxymethane, dimethyl carbonate or dimethyloxalate. Similarly, polyacetals are polymerized *via* FGM polymerization. The acetal functional group incorporated in the polymeric backbone will enable the polymer to degrade upon contact with water.

The improvement of petroleum-based commodity polymers by copolymerizing with bio-based monomers has also been investigated. An example is the copolymerization of styrene with 2-vinylfurnan (originating from non-edible vegetable oils) *via* Atom Transfer Radical Polymerization (ATRP) resulting in a polymer with an increased degradation temperature relative to atactic polystyrene.[20]

The demand to develop biopolymers, in particular tough biopolymers from vinyl plant-based monomers is of increasing importance.

2.2 Lactones and lactams

Certain species of plants produce various different lactone and lactam (**1**, **2**) moieties, that form part of more complex structures.[24] The double bond conjugated with the carbonyl group gives these molecules the ability to alkylate thiol groups in cells and terminate cellular processes. By acting as a Michael acceptor, these molecules commonly exhibit anti-cancerous properties, by reacting with mercapto groups present in enzymes and proteins in the cells, and thereby retarding their function.[25]
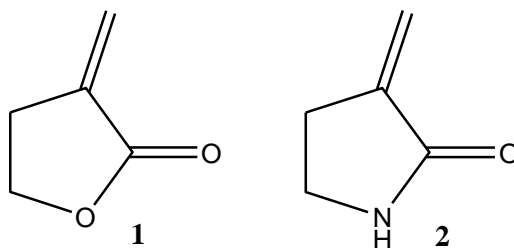
Figure 2.2: Unsubstituted, saturated α-methylene-γ-lactone (1), and α-methylene-γ–lactam (2).

The exo-methylene double bond also allows the possibility for chain growth polymerization, where unsaturated monomer units add to an active site (radical or ion). This ability to undergo

chain growth polymerizations is very unique, since the majority of bio-based polymers are produced *via* step growth polymerization.

High molecular weight polymers *via* step growth polymerizations are only obtained at very high conversions (>98 %) and rely on the availability of complementary functional groups. Therefore, the technique has a strict intolerance for functional groups from impurities that could participate.[12,26]

Unsaturated monomers undergo chain growth polymerization, via radical or ionic mechanisms. With the advent of living radical polymerization (LRP) techniques, polymers with predetermined molecular weights, well defined end groups and low molecular weight dispersities, are now readily accessible.[27] Additionally, sophisticated architectures such as block copolymers, star polymers, molecular brushes,[28] and cyclic polymers, can be obtained by LRP techniques. Examples of LRP methods include reversible addition-fragmentation chain transfer (RAFT), nitroxide mediated radical polymerization (NMP) and atom transfer radical polymerization (ATRP).[29]

2.2.1 α-Methylene-γ-lactones

The α-methylene-γ-lactones are wide spread in nature; they are abundant in plants of the *Asteraceae* or *Compositae* family. There are three categories of naturally occurring compounds with the α-methylene-γ-lactone moiety, classified according to the cyclic and acyclic carbon chains substituted on the lactone ring. These include sesquiterpenes, which consist of 15 carbon terpenoids,[30-32] the cyclic 20 carbon terpenoids[31,32] and thirdly, the non-terpenoids.[32]

Natural α-methylene-γ-lactones have important medicinal properties, they are anti-bacterial, anti-inflammatory, anti-fungal,[30] cytotoxic and they are also anti-cancerous.[33] Synthetic analogues, designed with specific biological activity have been of increasing interest.[31]
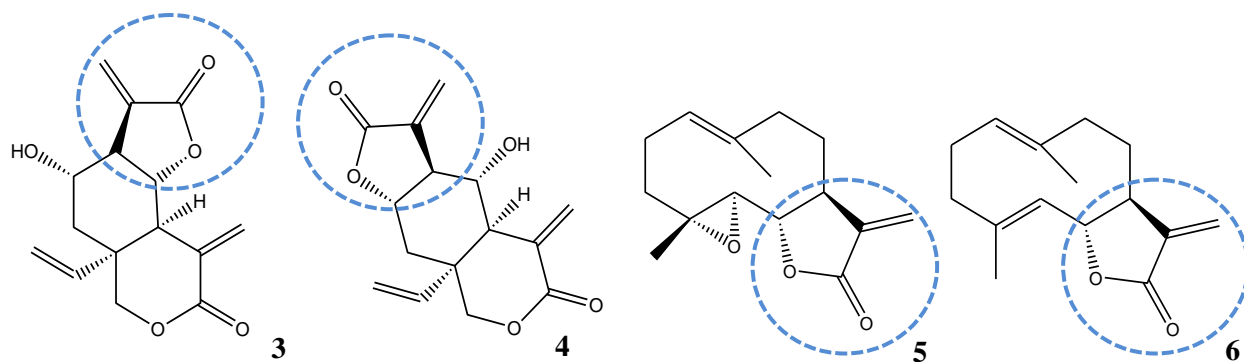
Figure 2.3: Examples of naturally occuring α-methylene-γ-lactones; vernolepin (3), vernomenin (4), parthenolide (5) and costunolide (6).

The parent compound, α-methylene-γ-lactone depicted as the encircled moieties in Figure 2.3, usually forms part of more complex compounds. However, the moiety itself, known as tulipalin A, occurs naturally and has various applications in medicinal and polymeric industries.

2.2.1.1 Tulipalin A

Tulipalin A (**1**), the unsubstituted, unsaturated α-methylene-γ-lactone, is also known as securolide, tulipaline A, LMSV-6 and 3-methylideneoxolan-2-one.

Tulipalin A is present in tulips, *Tulipa Gesneriana L.*[34] and protects the tulip against fungal infection.[30] Tulipalin A presents the same biological activity as the previously discussed naturally occuring α-methylene-γ-lactones,[31] however causes contact dermatitis.[35]

Tulipalin A is the hydrolyzed version of tuliposide A, the glucoside in the plant, and will be discussed in conjunction with the biosynthetic pathway of tulipalin A. Tuliposides A and B are present throughout the tulip's tissue and are the main tuliposides.[36]

2.2.1.2 Biosynthesis of tulipalin A

Chemical synthetic routes towards tulipalin A suffer from unwanted by-products, low yields and costly reactants.[30] The direct extraction of tulipalin A from the tulip petals is uneconomical, for example, 100 g of tulip petals yields only 40,2 mg tulipalin A (0.04 %).[37] The conversion of tuliposide A to tulipalin A *via* an enzymatic pathway, however, leads to higher yields, under milder conditions. The tuliposide-converting enzyme hydrolyzes the glucoside (**8**) to the corresponding lactone (**1**). Tuliposide A (**8**) is the glucoside of tulipalin A (**1**). Kato *et al.* have

developed an enzyme-mediated pathway to convert the tuliposide A and B to the lactone analogues, tulipalin A and B. Additionally, successful separation *via* extraction made the pathway specific for either analogue A or B.[36]

One of the biosyntheses of tulipalin A, depicted in Scheme 2.1, involves the condensation of acetyl coenzyme A with pyruvate and an additional reduction to yield the ring-open precursor of tulipalin A (**1**), γ-hydroxy-α-methylene-butanoic acid (**7**).[38]
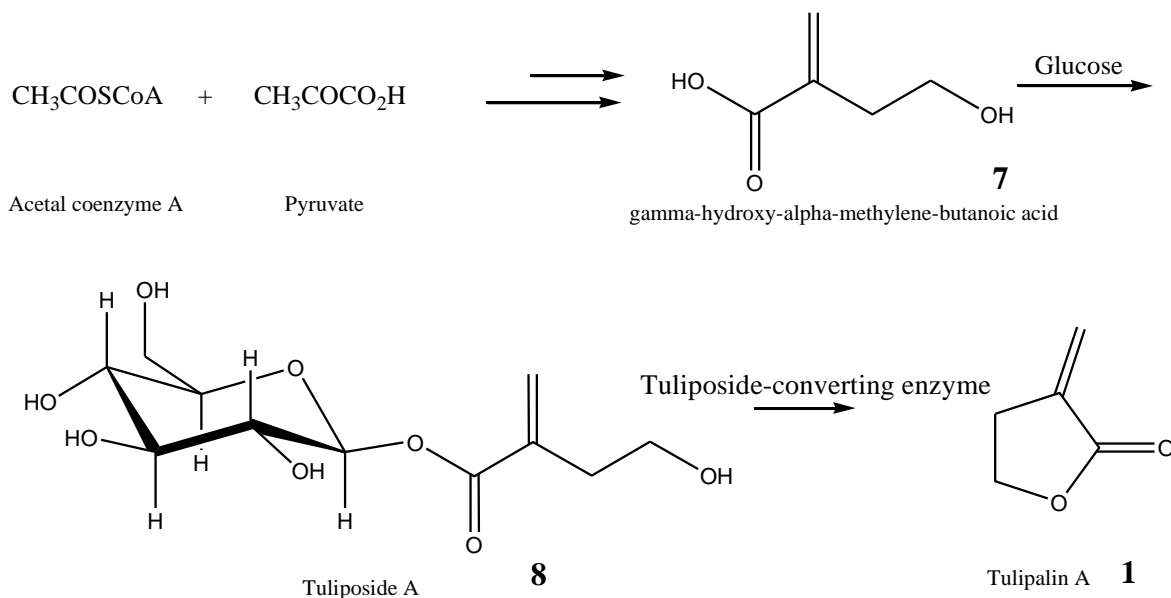
Scheme 2.1: Biosynthesis of tulipalin A.

2.2.1.3 Polymerization of tulipalin A

The *exo*-methylene double bond of tulipalin A allows the possibility of the synthesis of biopolymers *via* chain-growth polymerization.[39] Plant-derived unsaturated monomers can be described as styrenic, olefinic or acrylic, depending on the similarity to that of the petroleum-derived monomer. Tulipalin A (**1**) resembles the ring-closed version of methyl methacrylate, MMA (**9**). Thus, the radical polymerizability of tulipalin A and MMA are expected to be similar. Tulipalin A, however, has a greater reactivity,[34] a characteristic attributed to the ring-strain[40] from the fixed *s-cis* configuration.[41]

10
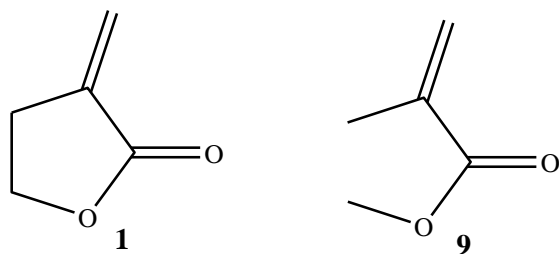
Figure 2.4: Structures of tulipalin A and MMA.

Polymerization kinetics for two monomers with similar structures to that of MMA and tulipalin A have also been reported. These monomers (Figure 2.5) have additional methyl groups at the β- and γ-positions (**10, 11**), respectively, which contribute to their properties. In particular, polymers of the γ-methyl-substituted tulipalin A had a higher glass transition temperature of 227 ˚C when compared to 195 °C of P(tulipalin A).[34]
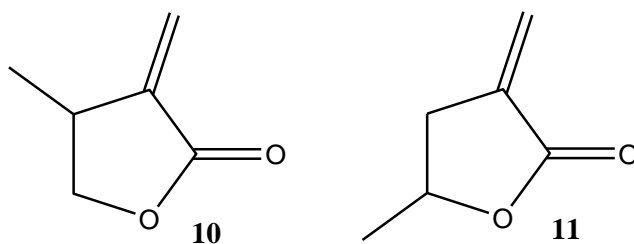
Figure 2.5: Methyl-derivatives of tulipalin A, β-and γ-methyl substituted tulipalin A.

P(tulipalin A) from conventional free radical polymerization has interesting physical properties, which could make it suitable for certain applications, for example the amorphous P(tulipalin A) has a high glass transition temperature (T_g) of 195 ˚C and thermal stability up to 320 ˚C. Compared to atactic PMMA, which has a T_g of 105 ˚C,[34] P(tulipalin A) is more desirable in applications, such as thermoplastic and coatings industry. In addition, P(tulipalin A) is also transparent, therefore it can be used in applications where optical transparency is required,[30] and its structural rigidity makes it highly solvent-resistant.[34]

Although P(tulipalin A) has superior properties to PMMA, it suffers from poor ductility/brittleness which limits its use in tough films. An approach to overcome this challenge is by tethering polymers *via* a covalent bond to a surface/substrate. It has shown to improve tribological properties of materials, such as a reduced friction coefficient between interacting

surfaces.[42] Higaki *et al.* tethered P(tulipalin A) polymers from a silica surface *via* ATRP (Scheme 2.2),[43] resulting in self-assetulipalin Aing molecular brushes with improved ductility.[44]
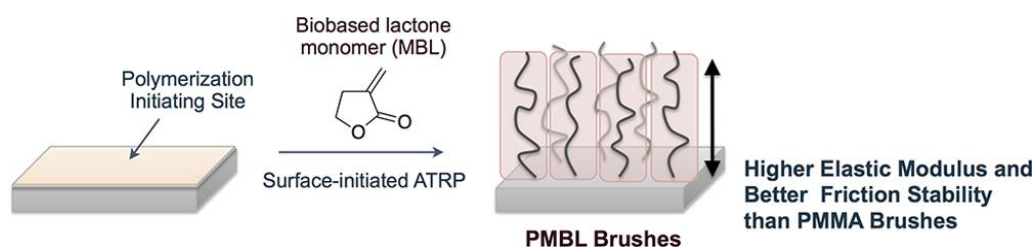
Scheme 2.2: P(tulipalin A) brushes grafted from silica surface.[43]

The first ATRP homopolymerization of tulipalin A was reported in 2008, furthermore di-and-triblocks were prepared by chain extending PMMA and poly(butyl acrylate) (PBA) blocks with tulipalin A.[45]

Co-polymerizations of tulipalin A and biobased menthide have been reported.[46] (-)-Menthide is chemically synthesized *via* a Baeyer-Villiger reaction from (-)-menthone, the ketone analogue of (-)-menthol.[47] A macroinitiator was synthesized by a ring-opening transesterification polymerization of (-)-menthide with diethylene glycol as initiator,[48] where after tulipalin A was added *via* ATRP to yield a triblock plant-based copolymer **12**, with enhanced thermoplastic properties to the homopolymer of (-)-menthide.[46]

12
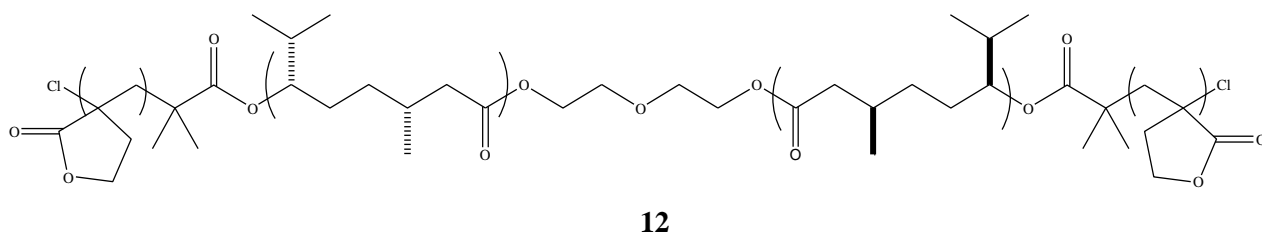
Figure 2.6: Triblock copolymer of menthide and tulipalin A.

To improve the thermal stability and poor injection moldability of polylactides, in particular poly (DL-lactide) (PDLLA), graft copolymers have been synthesized with tulipalin A. Macromonomers of PDLLA, functionalised with 2-hydroxyethyl methacrylate chain-ends, were synthesized (**13**) *via* ROP, and subsequently copolymerized with tulipalin A (**1**) to yield **14**.[49]
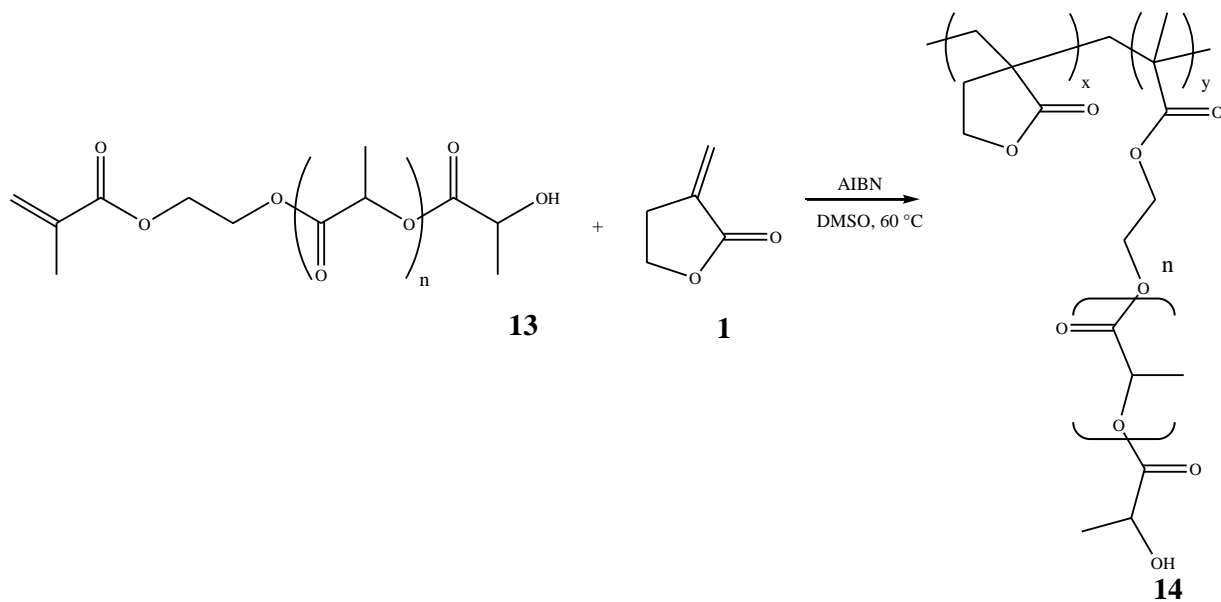
Scheme 2.3: PDLLA macromonomer and tulipalin A graft copolymer.

High molecular weight polymers were obtained by copolymerizing tulipalin A (**1**) with 2-methylene-1,3-dioxepane (MDO) **15** *via* thermal initiation. The polymers (**16**) obtained were thermally stable and hydrolytically degradable on account of the ester linkages.[50]
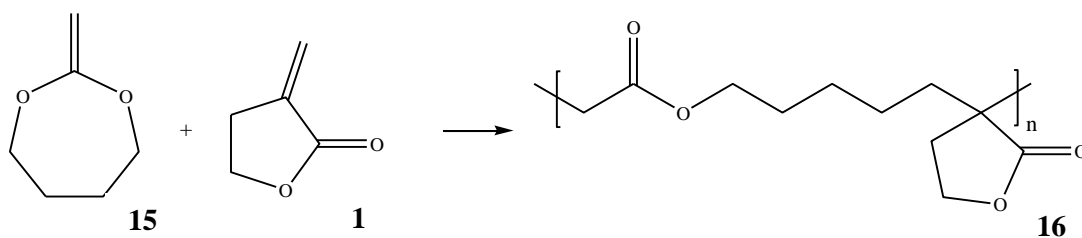
Scheme 2.4: Copolymerization of MDO and tulipalin A.

2.2.2 α-Methylene-γ-lactams

α-Alkylidene-γ-lactams, in particular the α-methylene-γ-lactams, are studied mainly for their important biological applications as antiviral[51], cytotoxic, anti-tumor, anti-bacterial, anti-inflammation and anti-fungal compounds. The derivatives of α-methylene-γ-lactams are less cytotoxic than the corresponding α-methylene-γ-lactones, making the lactam compounds of increasing interest,[52-55] in particular as anti-cancerous agents.[56,57]

α-Methylene-γ-lactams are much less abundant in nature when compared to the α-methylene-γ-lactones. The α-methylene-γ-lactam moiety has been observed in pukeleimid E (**17**) a compound

found in *Lyngbya Majuscula*, a certain species of cyanobacteria.[58] Additionally, two other compounds; anatin (**18**) and isoanatin (**19**) were discovered in the leaves of *Cynometra*, a West-African tree.[59] The γ-lactam moiety is else known as 2-pyrrolidone.
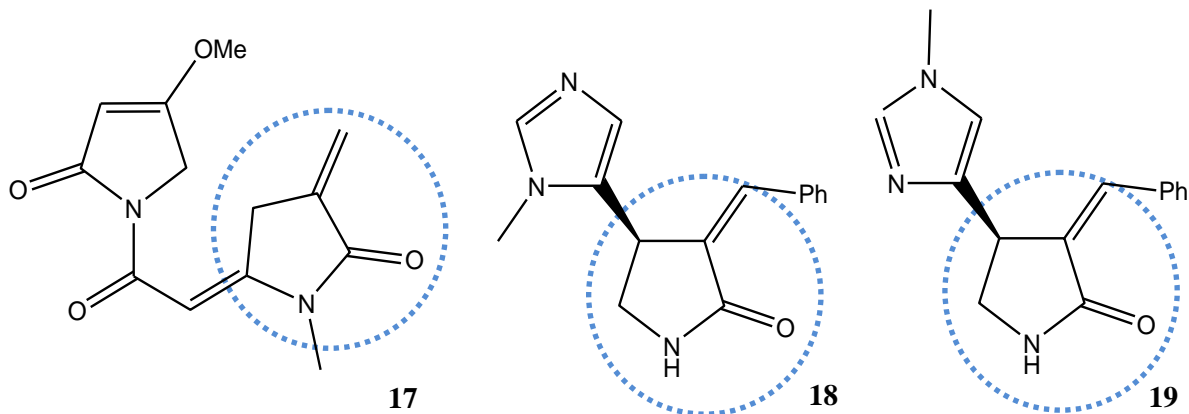
Figure 2.7: Naturally-occurring substituted α-methylene-γ-lactams: pukeleimid E (17), anantin (18) and isoanantin (19).

2.2.2.1 Chemical synthesis of substituted *exo*-cyclic α-alkylidene-γ-lactams

When a compound of interest is discovered, it is usually first chemically synthesized to fully investigate and establish its properties. Afterwards when full interest is established, the biosynthetic synthesis is carried out.

Naturally occurring α-methylene-γ-lactams are substituted (Figure 2.7). The majority of reported chemical syntheses for α-methylene-γ-lactams lead to the formation of *N*-, β-, γ-substituted and α-alkylidene lactams (Figure 2.8), with the exception of two reported methods of synthesizing α-methylene-γ-lactam itself.[60,61] A brief illustration of the chemical syntheses towards α-alkylidene lactams is shown Figure 2.8. The main disadvantages with these chemical syntheses are the formation of the unwanted *endo*-cyclic lactams (Figure 2.8).

Where R = Me, Et, Ph, NO_2, cyclic species, *etc*.
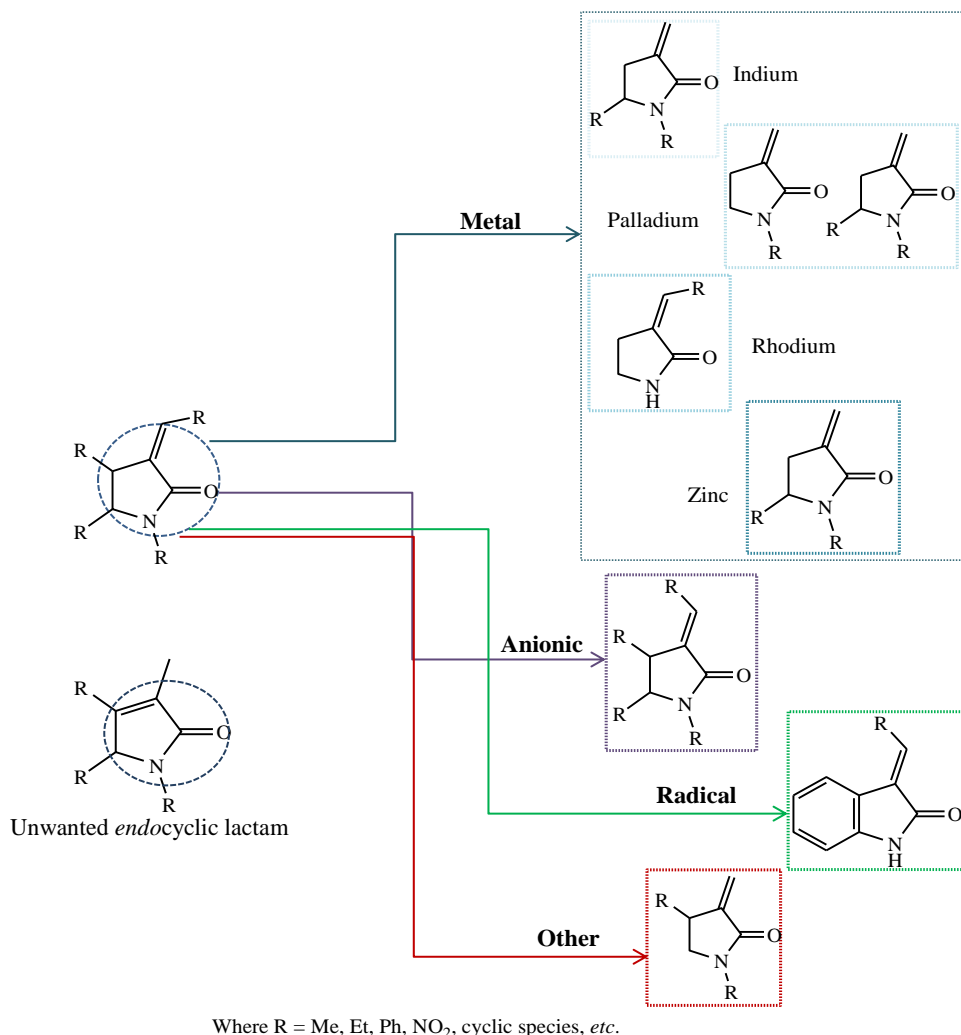
Figure 2.8: Chemical routes to substituted *exo*-cyclic α-alkylidene-γ-lactams.

The indium-catalyzed reaction relies on the substitution of the bromine on acrylic acid with indium, after which the metal complex reacts with the various aldimines to give way to the various *N* and γ-substituted α-methylene-γ-lactams. The limitation of this particular promoted reaction is the formation of unwanted *endo*-cyclic γ-lactams.[62]

A palladium-catalyzed carbonylation reaction of vinyl halides with secondary amines or alcohols led to the formation of *N*-substituted α-methylene-γ-lactams.[63] Intramolecular cyclization of homoallylic chloroformamides with palladium as a catalyst gives *N* and γ-substituted α-methylene-γ-lactams.[64] Both palladium-catalyzed methods suffer of unwanted formation of *endo*-cyclic double bonds in combination with the *exo*-cyclic version.[63,64]

Carbonylation reactions of β-aminoalkynes with hydrogen and carbon monoxide in the presence of a rhodium catalyst yield α-alkylidene-2-pyrrolidone. The unwanted hydroformylation product is also formed, which is an endocyclic α-alkyl-2-piperidone.[65]

Ethyl α-(bromomethyl)acrylate and various nitriles were reacted *via* the Reformatsky reaction with zinc as a catalyst, leading to γ-substituted α-methylene-γ-lactams.[66,67] Similarly, organozinc reagents react with chiral imines.[68,69]

N-, β-, γ-substituted α-alkylidene-γ-lactams are synthesized by the intramolecular carbanion addition of various different acetylene amides, which under certain conditions will ring-close.[70]

Ortho-aryl radicals of oxindoles were added to the α-position of the lactam to yield α,β-unsaturated oxindoles with and exo-methylene group.[71]

A nitrogen-analogue of sarkomycin, a compound with antibiotic and antitumor properties[72] was synthesized by reacting a diene (anthracene adduct) with a primary amine to yield a *N*-, β-substituted α-methylene-γ-lactam.[73]

2.2.2.2 Polymerization of lactams

Lactams can undergo ring-opening polymerizations. The rate of polymerization is influenced by the ring-size, type of substituents on the ring, and the type of initiation.[74] Hydrolytic polymerization of ε-caprolactam to produce nylon 6, is a well-known example of the ROP of a lactam.[75]

N- and γ-methyl substituted α-methylene-γ-lactams also undergo radical polymerization, similarly to the methyl-derivatives of tulipalin A; 5-methyl-3-methylene-2-pyrrolidone, or γ-methyl-α-methylene-γ-lactam, (**20**) was homopolymerized and copolymerized with MMA and styrene, respectively and the reactivity ratios were established.[76] In addition, the homopolymer of **20** was refluxed with hydrochloric acid to ring-open the lactam and form the corresponding polyelectrolyte **21**.[76] The ring-opening of lactam homopolymers is widespread in literature,[76,77] and the reactions yield poly(aminocarboxylic acids) with various applications. Generally, charged polymers have the ability to complex with metal ions *via* the amino or carboxylic acid moieties.[78]

The ring-closed version of *N,N*-disubstituted methacrylamide, α-methylene-*N*-methylpyrrolidone (**22**) has also been successfully homopolymerized *via* radical polymerization. Compound **22** is a structural isomer of *N*-vinylpyrrolidone (NVP).[76]

The highly reactive monomer, α-methylene-*N*-methylpyrrolidone (**22**) readily copolymerizes with a variety of monomers. Its homopolymer is water-soluble,[79] and water-soluble polymers have applications in various stages of production in oil and gas wells,[80] and additionally in paint, detergents *etc*.[81]
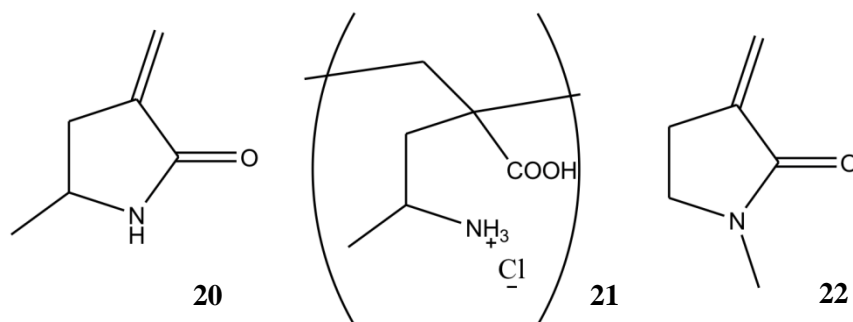
Figure 2.9: 5-Methyl-3-methylene-2-pyrrolidone, corresponding polyelectrolyte and α-methylene-*N*-methylpyrrolidone.

Five-membered lactams were incorporated onto styrene (**23** and **24**) and polymerized, yielding a styrenic backbone with lactam functionalities. A final ring-opening of the lactam with hydrochloric acid was performed, to yield poly(aminocarboxylic acid) side chains with a hydrophobic polystyrene backbone (Figure 2.10).[77]

23   **24**
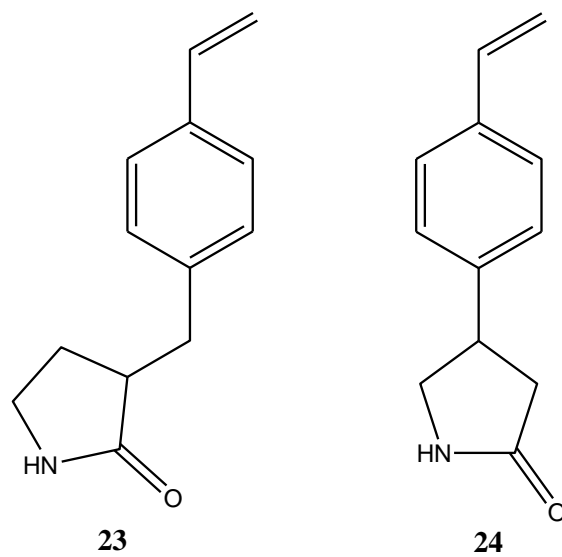
Figure 2.10: The γ-lactam-substituted styrenes; 4-(2-oxo-3-methylene-pyrrolidinyl)styrene (23) and 4-(*p*-styryl)-2-pyrrolidone (24).

2.3 Our approach

The work detailed in this chapter mainly considered the vinyl lactone, tulipalin A and P(tulipalin A), with a brief introduction to lactams. We postulated that the corresponding lactam will polymerize in a similar fashion, due to structural similarities. The chemical synthesis of the monomer, 3M2P (**2**), *i.e.* a ring-closed version of methyl methacrylamide **25** (MMAA), will be the subject of the following chapter.

To the best of our knowledge, the polymerization of 3M2P has not yet been reported. Since the monomer (**2**) can be biosynthetically accessible, polymerization thereof is towards the development of biopolymers and thus an alternative to that of the commodity petroleum-based materials. In subsequent chapters, the conventional radical polymerization and characterization will be demonstrated and finally different LRP techniques and sophisticated architectures will be pursued.
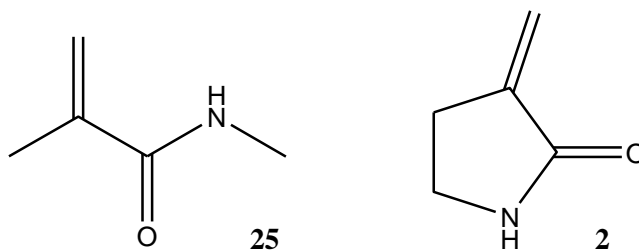
Figure 2.11: MMAA and 3M2P.

2.4 References

(1)   McCarthy, J. J. *Science* **2009**, *326*, 1646.

(2)   Keeling, C.; Whorf, T.; Wahlen, M.; Plicht, J. v. d. *Nature* **1995**, *375*, 666.

(3)   Horváth, I. T.; Anastas, P. T. *Chem. Rev.* **2007**, *107*, 2167.

(4)   Coates, G. W.; Hillmyer, M. A. *Macromolecules* **2009**, *42*, 7987.

(5)   Mülhaupt, R. *Macromol. Chem. Phys.* **2013**, *214*, 159.

(6)   Yu, L.; Dean, K.; Li, L. *Prog. Polym. Sci.* **2006**, *31*, 576.

(7)   Warner, J. C.; Cannon, A. S.; Dye, K. M. *Environ. Impact Asses.* **2004**, *24*, 775.

(8)   Anastas, P.; Eghbali, N. *Chem. Soc. Rev.* **2010**, *39*, 301.

(9)   In *Public Law* 1990; U.S. United Congress.

(10)   Anastas, P. T.; Warner, J. C. *Green Chemistry: Theory and Practice*; Oxford University Press: Oxford, 1998.

(11)   Noordover, B. A. Ph.D. thesis, Eindhoven University of Technology **2007**.

(12)   Mecking, S. *Angew. Chem. Int. Ed.* **2004**, *43*, 1078.

(13)   Benninga, H. *A History of Lactic Acid Making: A Chapter in the History of Biotechnology*; Springer, 1990.

(14)   Platel, R. H.; Hodgson, L. M.; Williams, C. K. *Polym. Rev.* **2008**, *48*, 11.

(15)   Vink, E. T. H.; Rábago, K. R.; Glassner, D. A.; Springs, B.; O'Connor, R. P.; Kolstad, J.; Gruber, P. R. *Macromol. Biosci.* **2004**, *4*, 551.

(16)   Siegenthaler, K.; Künkel, A.; Skupin, G.; Yamamoto, M. In *Synthetic Biodegradable Polymers*; Springer: 2012, p 91.

(17)   Sinclair, R. *J. Macromol. Sci., Part A: Pure Appl. Chem.* **1996**, *33*, 585.

(18)   Garlotta, D. *J. Polym. Environ.* **2001**, *9*, 63.

(19)   Seniha Güner, F.; Yağcı, Y.; Tuncer Erciyes, A. *Prog. Polym. Sci.* **2006**, *31*, 633.

(20)   Ortega Sánchez, S.; Marra, F.; Dibenedetto, A.; Aresta, M.; Grassi, A. *Macromolecules* **2014**.

(21)   Miller, S. A. *ACS Macro Lett.* **2013**, *2*, 550.

(22)   Park, J. H.; Jeon, J. Y.; Lee, J. J.; Jang, Y.; Varghese, J. K.; Lee, B. Y. *Macromolecules* **2013**, *46*, 3301.

(23)   Garcia, J. Master's thesis, University of Florida, **2012**.

(24) Vasilieva, Y. A.; Scales, C. W.; Thomas, D. B.; Ezell, R. G.; Lowe, A. B.; Ayres, N.; McCormick, C. L. *J. Polym. Sci., Part A: Polym. Chem.* **2005**, *43*, 3141.

(25) Pati, H. N.; Das, U.; Sharma, R. K.; Dimmock, J. R. *Mini-Rev. Med. Chem.* **2007**, *7*, 131.

(26) Kaplan, D. L. *Introduction to Biopolymers from Renewable Resources*; Springer, 1998.

(27) Coates, G. W.; Hillmyer, M. A. *Macromolecules* **2009**, *42*, 7987.

(28) Hadasha, W.; Mothunya, M.; Akeroyd, N.; Klumperman, B. *Aust. J. Chem.* **2011**, *64*, 1100.

(29) Webster, O. W. *Science* **1991**, *251*, 887.

(30) Damude, H. G.; Flint, D.; Prabhu, V.; Wang, H.; Google Patents: 2002.

(31) Janecka, A.; Wyrębska, A.; Gach, K.; Fichna, J.; Janecki, T. *Drug Discovery Today* **2012**, *17*, 561.

(32) Kitson, R. R. A.; Millemaggi, A.; Taylor, R. J. K. *Angew. Chem. Int. Ed.* **2009**, *48*, 9426.

(33) Rosowsky, A.; Papathanasopoulos, N.; Lazarus, H.; Foley, G. E.; Modest, E. J. *J. Med. Chem.* **1974**, *17*, 672.

(34) Akkapeddi, M. K. *Macromolecules* **1979**, *12*, 546.

(35) Tavares, B.; Loureiro, G.; Pereira, C.; Chieira, C. *Allergol. Immunopath.* **2006**, *34*, 73.

(36) Kato, Y.; Yoshida, H.; Shoji, K.; Sato, Y.; Nakajima, N.; Ogita, S. *Tetrahedron Lett.* **2009**, *50*, 4751.

(37) Smolinske, S. C. *Toxicity of Houseplants*; CRC Press, 1990.

(38) Hutchinson, C.; Leete, E. *J. Chem. Soc. Chem. Comm.* **1970**, 1189.

(39) Seema, A.; Qiao, J.; Samarendra, M. In *Biobased Monomers, Polymers, and Materials*; American Chemical Society: 2012; Vol. 1105, p 197.

(40) Pickett, J.; Ye, Q.; Steiger, D. Tulipalin Copolymers. U.S. Patent 7,932,336, **2011**.

(41) Stansbury, J.; Antonucci, J. *Dent. Mater.* **1992**, *8*, 270.

(42) Yamamoto, S.; Ejaz, M.; Tsujii, Y.; Fukuda, T. *Macromolecules* **2000**, *33*, 5608.

(43) Higaki, Y.; Okazaki, R.; Takahara, A. *ACS Macro Lett.* **2012**, *1*, 1124.

(44) Klein, J.; Kumacheva, E.; Mahalu, D.; Perahia, D.; Fetters, L. J. *Nature* **1994**, *370*, 634.

(45) Mosnáček, J.; Matyjaszewski, K. *Polym. Prepr.* **2008**, *49*, 26.

(46) Shin, J.; Lee, Y.; Tolman, W. B.; Hillmyer, M. A. *Biomacromolecules* **2012**, *13*, 3833.

(47) Zhang, D.; Hillmyer, M. A.; Tolman, W. B. *Biomacromolecules* **2005**, *6*, 2091.

(48) Jiang, X.; Vamvakaki, M.; Narain, R. *Macromolecules* **2010**, *43*, 3228.

(49) Lee, C. W.; Nakamura, S.; Kimura, Y. *J. Polym. Sci., Part A: Polym. Chem.* **2012**, *50*, 1111.

(50) Agarwal, S.; Kumar, R. *Macromol. Chem. Phys.* **2011**, *212*, 603.

(51) Johnson, T. O.; Hua, Y.; Luu, H. T.; Brown, E. L.; Chan, F.; Chu, S. S.; Dragovich, P. S.; Eastman, B. W.; Ferre, R. A.; Fuhrman, S. A.; Hendrickson, T. F.; Maldonado, F. C.; Matthews, D. A.; Meador, J. W.; Patick, A. K.; Reich, S. H.; Skalitzky, D. J.; Worland, S. T.; Yang, M.; Zalman, L. S. *J. Med. Chem.* **2002**, *45*, 2016.

(52) Belaud, C.; Roussakis, C.; Letourneux, Y.; Alami, N. E.; Villieras, J. *Synth. Comm.* **1985**, *15*, 1233.

(53) Albrecht, A.; Albrecht, Ł.; Różalski, M.; Krajewska, U.; Janecka, A.; Studzian, K.; Janecki, T. *New J. Chem.* **2010**, *34*, 750.

(54) Murata, K.; Kaneko, S.; Kitazume, T. *Bioorg. Med. Chem. Lett.* **1993**, *3*, 2685.

(55) Qiao, L.; Wang, S.; George, C.; Lewin, N. E.; Blumberg, P. M.; Kozikowski, A. P. *J. Am. Chem. Soc.* **1998**, *120*, 6629.

(56) Hoffmann, H. M. R.; Rabe, J. *Angew. Chem. Int. Ed. Engl.* **1985**, *24*, 94.

(57) Kornet, M. J. *J. Pharm. Sci.* **1979**, *68*, 350.

(58) Cardellina Ii, J. H.; Moore, R. E. *Tetrahedron Lett.* **1979**, *20*, 2007.

(59) Naito, T.; Honda, Y.; Miyata, O.; Ninomiya, I. *Chem. Pharm. Bull.* **1993**, *41*, 217.

(60) Klutchko, S.; Hoefle, M. L.; Smith, R. D.; Essenburg, A. D.; Parker, R. B.; Nemeth, V. L.; Ryan, M.; Dugan, D. H.; Kaplan, H. R. *J. Med. Chem.* **1981**, *24*, 104.

(61) Fotiadu, F.; Pardigon, O.; Buono, G.; Le Corre, M.; Hercouët, A. *Tetrahedron Lett.* **1999**, *40*, 867.

(62) Choudhury, P. K.; Foubelo, F.; Yus, M. *J. Org. Chem.* **1999**, *64*, 3376.

(63) Mori, M.; Washioka, Y.; Urayama, T.; Yoshiura, K.; Chiba, K.; Ban, Y. *J. Org. Chem.* **1983**, *48*, 4058.

(64) Henin, F.; Muzart, J.; Pete, J.-P. *Tetrahedron Lett.* **1986**, *27*, 6339.

(65) Campi, E. M.; Chong, J. M.; Jackson, W. R.; Van Der Schoot, M. *Tetrahedron* **1994**, *50*, 2533.

(66) El Alami, N.; Belaud, C.; Villieras, J. *J. Organomet. Chem.* **1987**, *319*, 303.

(67) Alami, N. E.; Belaud, C.; Villiéras, J. *J. Organomet. Chem.* **1988**, *348*, 1.

(68) Dembélé, Y. A.; Belaud, C.; Villiéras, J. *Tetrahedron: Asymmetry* **1992**, *3*, 511.

(69) Nyzam, V.; Belaud, C.; Zammattio, F.; Villieras, J. *Tetrahedron: Asymmetry* **1996**, *7*, 1835.

(70) Patra, R.; Maiti, S. B.; Chatterjee, A.; Chakravarty, A. K. *Tetrahedron Lett.* **1991**, *32*, 1363.

(71) Bowman, W. R.; Heaney, H.; Jordan, B. M. *Tetrahedron Lett.* **1988**, *29*, 6657.

(72) Kodpinid, M.; Siwapinyoyos, T.; Thebtaranonth, Y. *J. Amer. Chem. Soc.* **1984**, *106*, 4862.

(73) Tarnchompoo, B.; Thebtaranonth, C.; Thebtaranonth, Y. *Tetrahedron Lett.* **1987**, *28*, 6675.

(74) Odian, G. G.; Odian, G. *Principles of Polymerization*; Wiley-Interscience New York, 2004; Vol. 3.

(75) Reimschuessel, H. K. *J. Polym. Sci.: Macromol. Rev.* **1977**, *12*, 65.

(76) Van Beylen, M.; Samyn, C. *Makromol. Chem.* **1990**, *191*, 2485.

(77) Samyn, C.; Smets, G. *J. Polym. Sci.: Polym. Chem. Ed* **1982**, *20*, 987.

(78) Smets, G.; Samyn, C. In *Optically Active Polymers*; Springer: 1979, 331.

(79) Ueda, M.; Takahashi, M.; Suzuki, T.; Imai, Y.; Pittman, C. U. *J. Polym. Sci. Polym.: Chem. Ed.* **1983**, *21*, 1139.

(80) Chatterji, J.; Borchardt, J. *J. Petrol. Technol.* **1981**, *33*, 2.

(81) Swift, G. *Polym. Degrad. Stab.* **1994**, *45*, 215.

Chapter 3: Monomer synthesis

3.1 Introduction

Two important facets were considered upon preparation of the unsubstituted, unsaturated parent compound, α-methylene-γ-lactam known otherwise as 3-methylene-2-pyrrolidone (3M2P). Firstly, the chemical route should be specific to the formation of the *exo*-methylene group on the α-position of the lactam, without the formation of any *endo*-cyclic species. The end-application of synthesizing the monomer (3M2P) was to create a novel polymer and the *exo*-methylene will be the site of radical-formation while maintaining the rigid lactam-ring integrity, during radical polymerizations. Secondly, the chemical route should be limited in side-products, *i.e.* substitution on the β-, γ- and *N*-positions, as the specific interest was on the naturally occurring 3M2P moiety.[1,2] The chemical syntheses of substituted α-alkylidene-γ-lactams were reviewed in Chapter 2.

The synthesis of 3M2P has been reported twice in literature.[3,4] The first approach towards the synthesis of 3M2P was carried out in 1981 by Klutchko *et al*. and involved the dehydration of 3-(hydroxymethyl)-2-pyrrolidone, yielding the *exo*-methylene group, without any side-products.[3]

In 1999, Fotiadu *et al*. reported a new, efficient synthetic route towards 3M2P,[4] which involved the Wittig reaction and circumvented high pressure catalytic hydrogenation reactions and working with hazardous azides, as previously performed by Klutchko *et al*. During this study, the *exo*-double bond and the corresponding cisoïd configuration were essential, as 3M2P was studied as a dienophile with cyclopentadiene as a diene, in the Diels-Alder reaction. However, the Wittig route produced an *N*-hydroxymethyl-substituted 3M2P side-product, however the formation of the side-product could be controlled.

The Wittig reaction furthermore produces no *endo*-cyclic C=C species, as the double bond is only formed at the site of the former C-O bond and no double bond isomerization can occur.[5] Similarly, tulipalin A (lactone analogue) has been prepared *via* a Wittig reaction.[6]

3.2 Results and discussion

The main objective during the synthesis of 3M2P was to obtain the monomer in sufficient yields, in order to convert to polymer at a later stage (Chapters 4 and 5). In this work, the Wittig route[4] is the predominant approach. Additionally, the alternative synthesis route[3] was also attempted.

3.2.1 Wittig approach

The synthesis of monomers **6** and **7** is shown in Scheme 3.1. Firstly, 3-aminopropanol was reacted with ethyl chloroformate to yield ethyl *N*-(3-hydroxypropyl) carbamate (**1**).[7] Following an optimized substitution reaction with PBr$_3$, the bromo-carbamate **2** was obtained. Subsequently, the phosphonium salt **3** was obtained in very good yields upon addition of PPh$_3$.[4]
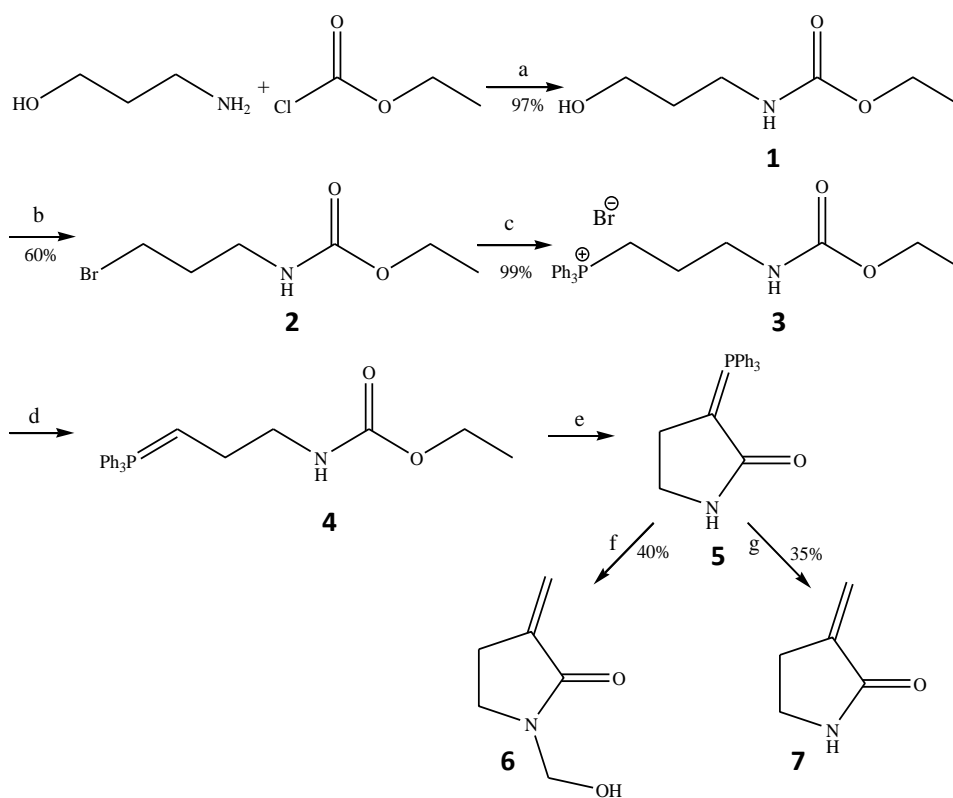
Scheme 3.1: Wittig route towards 3M2P (7) and 3M2P-OH (6). a) K$_2$CO$_3$, Water, 0 °C. b) PBr$_3$, toluene, r.t. to reflux. c) PPh$_3$, Acetonitrile, reflux. d) t-BuOK, toluene, r.t. e) 50 °C. f) Paraformaldehyde (3 equivalents), 50 °C to r.t. g) Paraformaldehyde (1 equivalent), 50 °C to r.t.

After an azeotropic distillation of compound **3** and addition of potassium *tert*-butoxide at 50 °C, ylide **4** was obtained, which subsequently gives the secondary ylide **5** through a ring-closing reaction. Finally, the addition of paraformaldehyde, under an inert atmosphere, yielded the condensation product, monomer **7**, with monomer **6** as a side-product. The amount of side-product in the reaction is dependent on the amount of paraformaldehyde added.[4] For example, when an excess of paraformaldehyde was added, only monomer **6** formed. The quantities of paraformaldehyde to the ratio of monomers **6** and **7** are shown in Table 3.1, where monomer **6** is *N*-(hydroxymethyl)-3-methylene-2-pyrrolidone (3M2P-OH) and monomer **7** is 3M2P.

Table 3.1: Different quantities of paraformaldehyde and resulting ratio of 3M2P to 3M2P-OH

Paraformaldehyde (mmol)[a] : Phosphonium salt (mmol)	3M2P : 3M2P-OH
3.3 : 1	0 : 1
1.1 : 1	8 : 1
0.4 : 1	1 : 0

- [a] Calculated by using the monomer of paraformaldehyde with a molecular weight of 30.03 g/mol.

As a by-product of the Wittig reaction, triphenylphosphine oxide (TPPO) formed as shown in Scheme 3.2. Separation of the monomers from this by-product will be discussed in detail at a later stage.

In Scheme 3.2 the cyclization mechanism of ylide **4** to give the ylene **5** is shown by a nucleophilic attack towards the carbamate carbon atom, with ethanol as by-product. Subsequently, the carbanion of ylene **5** and paraformaldehyde undergo a condensation reaction (Wittig) to give either monomer **6** or **7**, or a mixture.
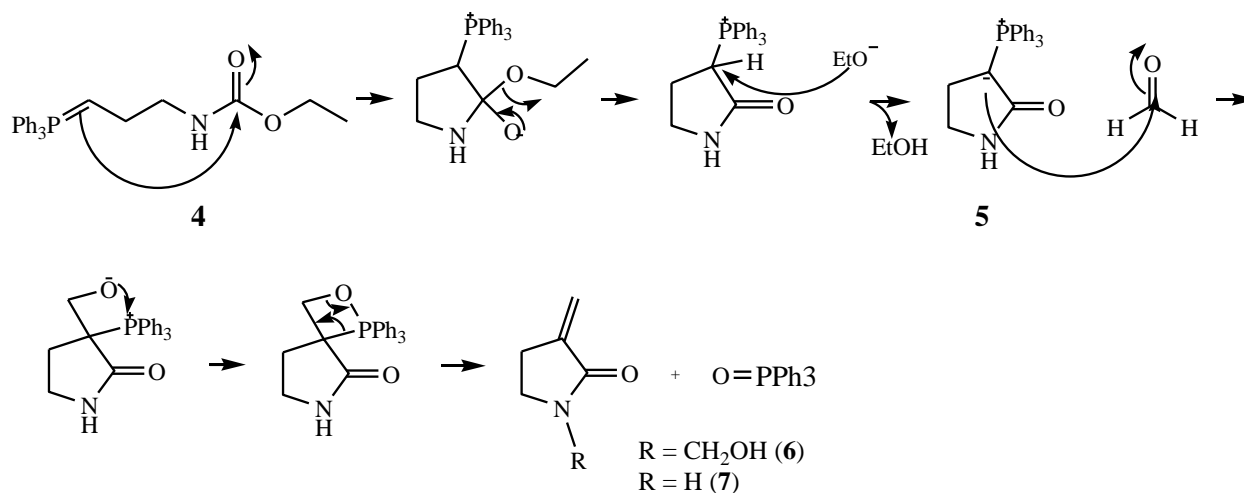
Scheme 3.2: Wittig mechanism towards 3M2P and 3M2P-OH.

Jouglet *et al*. reported on the direct *N*-hydroxymethylation of amides and lactams, when paraformaldehyde did not form part of the synthetic route towards the specific compounds. Base catalysis, ultrasound activation energy (sonication) and an aqueous formaldehyde solution or paraformaldehyde introduced the *N*-hydroxymethyl group on the nitrogen atom of the amide/lactam.[8] The removal of the introduced *N*-hydroxymethyl group was also investigated. Upon heating (200 °C) and under vacuum the *N*-hydroxymethyl group was removed with good yields (70-80 %).[9]

Monomer **6** or 3M2P-OH was only partially soluble in chloroform and water. It was proposed that inter- and intramolecular complexation of 3M2P-OH prevented complete solubility. In Figure 3.1 the dashed line indicates possible intramolecular interaction, whereas the curly lines indicate intermolecular sites of complexation, which will influence the solubility.
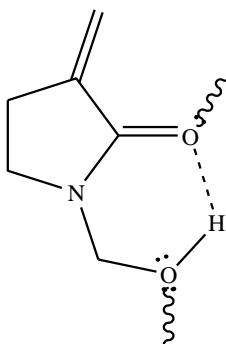
Figure 3.1: Proposed intra- and intermolecular complexation of 3M2P-OH.

3.2.2 Purification of the monomers

Difficulties were encountered with the separation of the by-product, TPPO, from the target monomer. It was contemplated that the NH-group of 3M2P formed strong hydrogen-bonds with TPPO, making separation difficult. Different techniques were investigated:

Numerous solvent systems, on silica and alumina were attempted, with all attempts unsuccessful in removing TPPO.

Kugelrohr distillation was also considered as it is dependent on applying gradient heat and vacuum to separate compounds according to boiling points. The distillation successfully separated 3M2P and 3M2P-OH from TPPO; however yields were extremely low (6-10 %) and the majority of the reaction mixture auto-polymerized upon applying high temperature and vacuum. An alternative method was required to isolate the monomer in more acceptable yields.

In further attempts to remove TPPO, Merrifield resin was considered. Merrifield resin is a chloromethylated polystyrene that removes TPP and TPPO upon addition of sodium iodide as shown in Scheme 3.2. The resin can be rejuvenated or synthesized[10] and has been shown to remove 2 mmol of phosphine per gram of resin at 25 °C.[11]
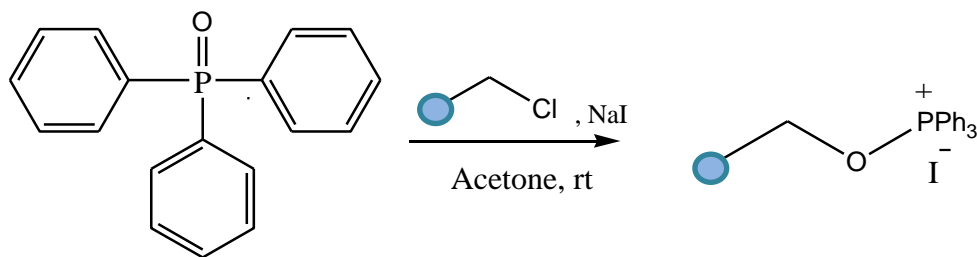
Scheme 3.3: Merrifield resin.

Despite using the standardized conditions, an excess of the resin and higher temperatures as described in Table 3.2, TPPO could not be removed by this method.

Table 3.2: Reaction conditions for removing TPPO with Merrifield resin

Resin (mg) : TPPO (mmol)	Temperature (°C)
140 : 0.28	25
280 : 0.28	25
140 : 0.28	40
140 : 0.28	50

A method was developed for separating 3M2P and 3M2P-OH from TPPO, with moderately good yields (35-40%). The method relied on recrystallizing the crude, filtered reaction mixture where after the recrystallized mixture was dissolved in warm chloroform and monomers extracted into water.

3.2.3 NMR spectroscopic analysis

The gradient Heteronuclear Single Quantum Coherence (gHSQC) NMR spectrum couples carbon atoms with the according protons ($^1J_{C\text{-}H}$) for one-bond correlation, with the ^{13}C NMR spectrum on the y-axis and the ^{1}H NMR spectrum on the x-axis.

The gHSQC NMR spectrum of monomers 3M2P-OH (**6**) and 3M2P (**7**), in a 1:1 ratio that was quantified by the ^{1}H NMR spectrum (x-axis), is shown in Figure 3.2. From the ^{13}C NMR spectrum, depicted as the y-axis in Figure 3.2, duplicates are observed for each carbon, except carbon (signal 8), which correlated with 2 methylene protons α to the hydroxyl group of 3M2P-OH. Additionally, only signal 4, contributed by the amide proton from 3M2P, and CDCl$_3$ were present in the aromatic region, indicating the successful removal of the by-product, TPPO.
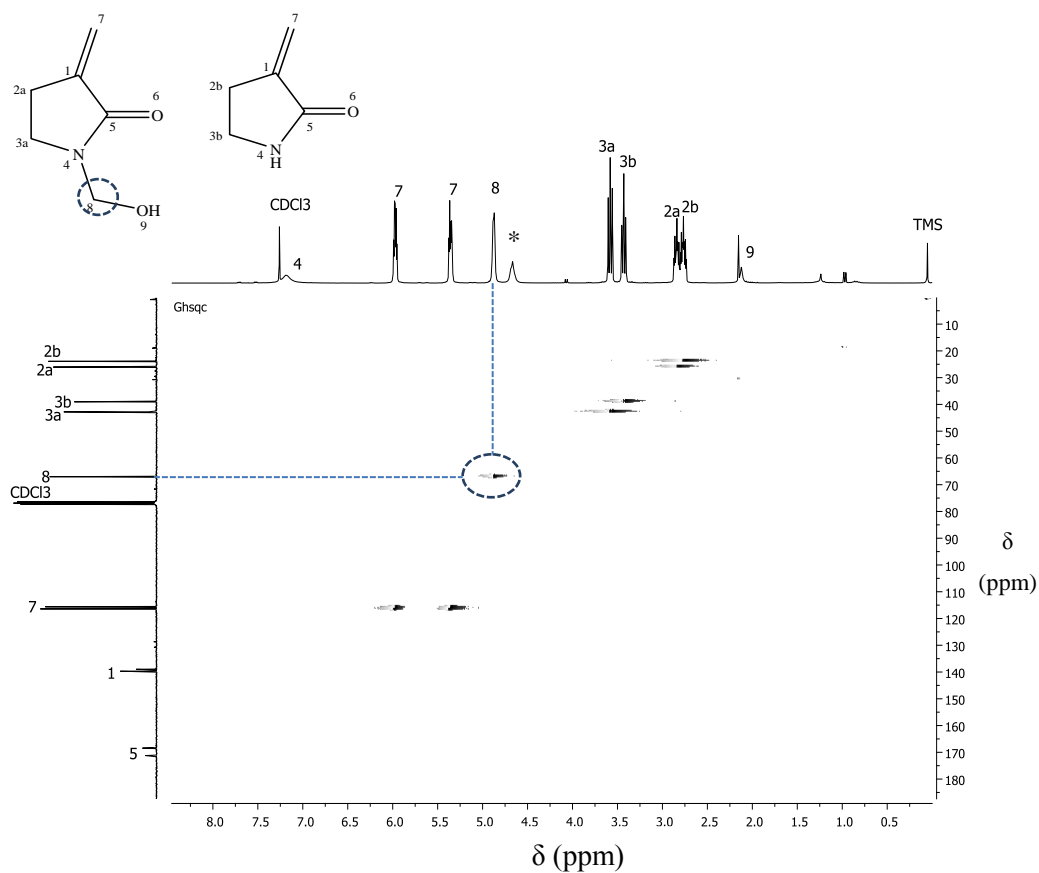
Figure 3.2: gHSQC NMR spectrum of 3M2P and 3M2P-OH in a 1:1 ratio in CDCl₃.

The ^{1}H NMR spectra of 3M2P and 3M2P-OH in DMSO-d_6 are shown in Figure 3.3, respectively. The signals 7 and 3 are shifted slightly upfield for the more shielded 3M2P than 3M2P-OH.
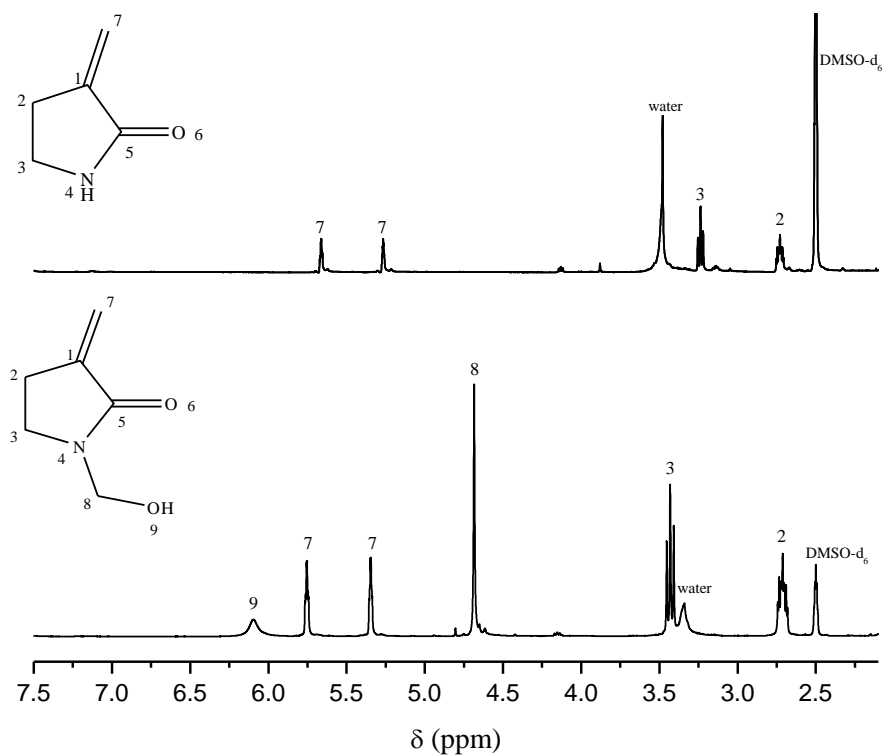
Figure 3.3: ^{1}H NMR spectra of 3M2P and 3M2P-OH, respectively in DMSO-d$_6$.

Figure 3.4 shows the COSY NMR spectrum of 3M2P, where the solid lines indicate solvents and a reagent, *t*-BuOK. The dashed lines indicate the H-H coupling, up to the ^{4}J coupling constant, as indicated by the coupling of signal 7 to 2 that is ascribed to the double bond allowing better through-bond coupling. Additionally, ^{3}J coupling was observed for signal 2 to 3.
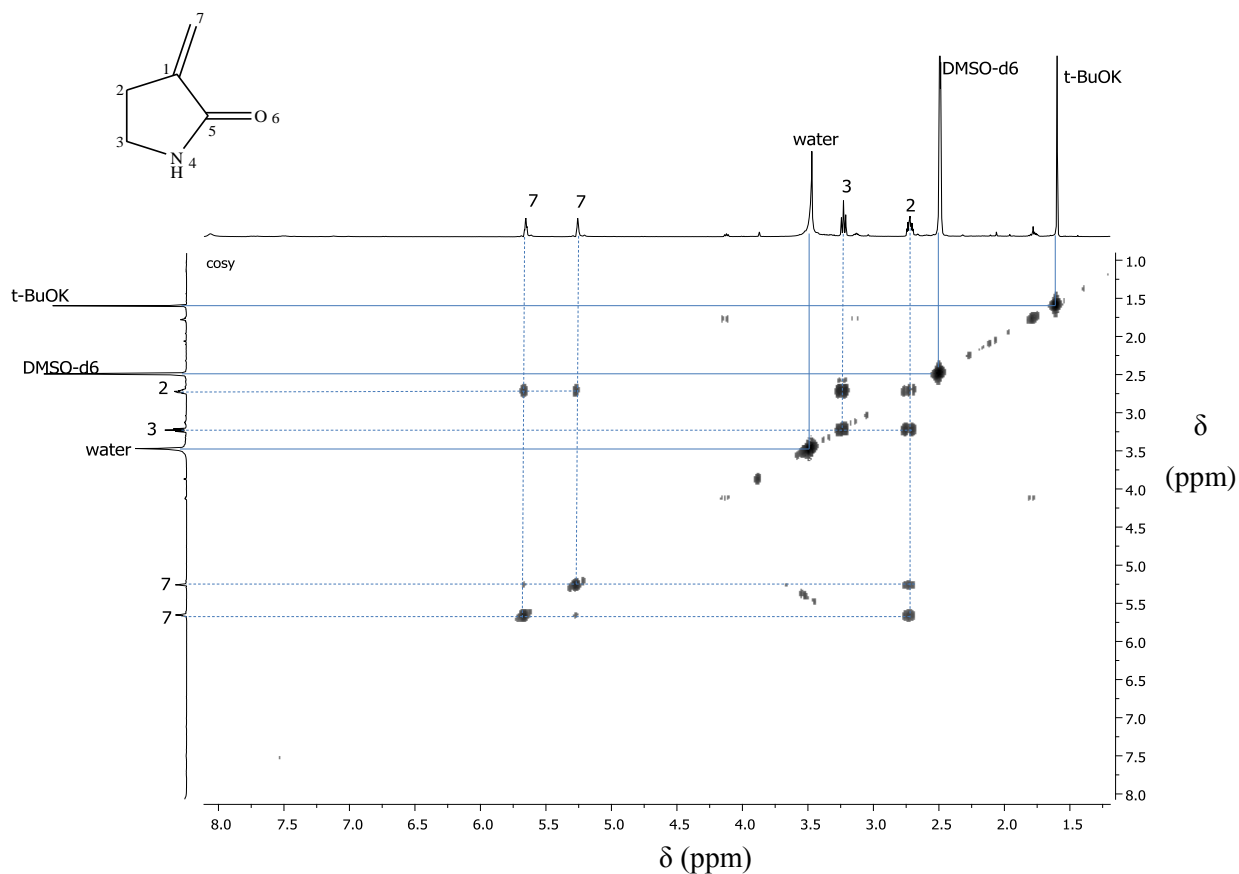
Figure 3.4: COSY NMR spectrum of 3M2P in DMSO-d$_6$.

3.2.4 Alternative monomer synthesis approach

During the purification difficulties of the first approach (Wittig route), an alternative approach was attempted, simultaneously (Scheme 3.4). The alternative synthesis approach mainly involved the dehydration of 3-(hydroxymethyl)-2-pyrrolidone to yield 3M2P.

A cyclopropyl group was introduced to diethyl malonate with 1,2-dibromoethane *via* a substitution reaction with tetrabutylammonium bromide as a catalyst to form compound **8**.[12] Sodium azide opened the cyclopropyl ring in the subsequent reaction, in the presence of triethylamine hydrochloride, affording the azide compound **9**. The azide was converted to the pyrrolidone ester **10** *via* catalytic hydrogenation with palladium on carbon catalyst, which yielded the nucleophilic amine required for lactam formation.[13] The pyrrolidone ester was further reduced with calcium borohydride to yield the pyrrolidone alcohol **11**. A further dehydration of the alcohol in order to form 3M2P (**7**) was attempted, however unsuccessful.[3]
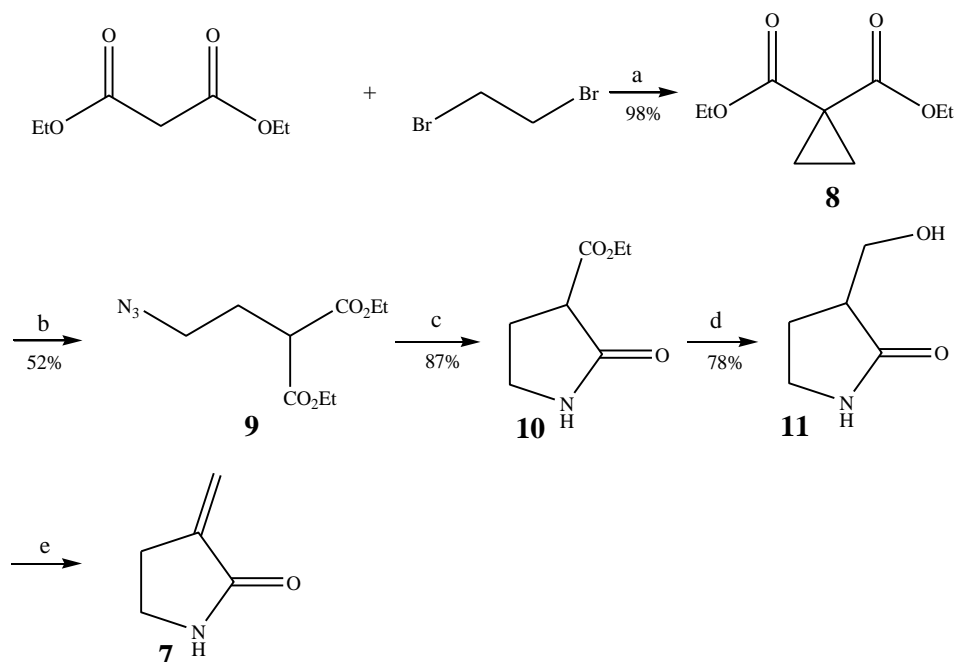
Scheme 3.4: Alternative synthesis towards 3M2P. a) K_2CO_3, Bu_4NBr, DMF, r.t.; b) NaN_3, $Et_3N.HCl$, NMP, 100 °C; c) H_2, 10% Pd/C, EtOH; d) $CaCl_2$, $NaBH_4$, MeOH, 0 °C→5 °C→r.t.; e) CuI, DCC, Chlorobenzene, 125 °C to reflux.

Although the alternative route had better yields throughout, the dehydration reaction of the pyrrolidone alcohol towards 3M2P could not be optimized because of time constraints. Therefore, only the Wittig route was further utilized.

3.3 Conclusion

The monomers, 3M2P-OH (**6**) and 3M2P (**7**) were successfully synthesized and a purification protocol for the removal of TPPO was developed, dependent on the good water-solubility of the monomers. The quantities of paraformaldehyde and corresponding ratios of 3M2P to 3M2P-OH were established, leading to the synthesis of a mixture of the two monomers, which was quantified by ^{1}H NMR spectroscopy and further characterized by g-HSQC NMR spectroscopy. Separate synthesis of either 3M2P or 3M2P-OH was also successfully controlled by the amount of paraformaldehyde and characterized by ^{1}H and ^{13}C NMR spectroscopy. The monomer of interest, 3M2P, was fully characterized by NMR spectroscopy experiments, such as; ^{1}H, ^{13}C and COSY NMR spectroscopy and additional evidence is provided in the following experimental section.

33

3.4 Experimental

3.4.1 General details

The following chemicals were utilized: Methyl chloroformate (Aldrich, 99 %), ethyl chloroformate (Aldrich, 97 %), potassium carbonate (Fluka, 99 %), 3-amino-1-propanol (Aldrich, 99 %), phosphorus tribromide (Aldrich, 99 %), triphenylphosphine (Acros, 99 %), PPh_3 was recrystallized from anhydrous acetone.[14] Potassium *tert*-butoxide (Aldrich, 98 %), paraformaldehyde (Aldrich, 95 %), Merrifield′s peptide resin 200-400 mesh, 3.5-4.5 mmol/g Cl-loading, 1 % cross-linked (Sigma), tetrabutylammonium bromide (Fluka, 97 %), diethyl malonate (Aldrich, 98 %), 1,2-dibromoethane (Merck, 99 %), ammonium chloride (Merck, 99 %), sodium azide (Merck, 98 %), triethylamine hydrochloride (Aldrich, 99 %), 10 % Pd/C (Aldrich, dry support), anhydrous calcium chloride (Merck, 98 %), sodium borohydride (Fluka, 99 %). Solvents; methanol, toluene, 1-methyl-2-pyrrolidone, chlorobenzene and acetonitrile were purchased from Sigma Aldrich and used without further purification. TLC plates (0.20 mm Silica gel 60, with fluorescent indicator UV254) and Silica gel 60(0.063 - 0.2 mm/70 - 230 mesh) were purchased from Machery-Nagel.

^1H, ^{13}C, COSY and gHSQC NMR spectra were obtained with a Varian VXR-Unity (300 MHz) spectrometer, unless stated otherwise. Majority of the compounds were dissolved in $CDCl_3$ or DMSO-d_6 with trimethylsilane (TMS) as an internal reference. Abbreviations for NMR data: s = singlet; bs = broad singlet; d = doublet; t = triplet; q = quartet; p = pentet; dd = doublet of doublets; dt = doublet of triples; m = multiplet. NMR solvents: $CDCl_3$-d_1 (Aldrich, 99.9 %), DMSO-d_6 (MagniSolv, 99.9 %), Acetone-d_6 (MagniSolv, 99.9 %) and D_2O-d_2 (MagniSolv, 99.9 %). Gas Chromatography Mass Spectrometry (GC-MS) was obtained with an Agilent 6890N GC with CTC CombiPAL Autosampler and Agilent 5975B MS. The column used was ZB 7HG-G027-11 with a ZB-Semivolatiles Guardian column (30 m, 0.25 mm ID, 0.25 µm film thickness). Mass Spectrometry (MS) and Liquid Chromatography Mass Spectrometry (LC-MS) was obtained with a Waters Synapt G2 with Electron Spray Ionization (ESI) in the positive mode. The column used was Waters UPLC C18, 2.1x100 mm.

3.4.2 Synthetic procedures

3.4.2.1 Preparation of Ethyl *N*-(3-hydroxypropyl) carbamate (1):
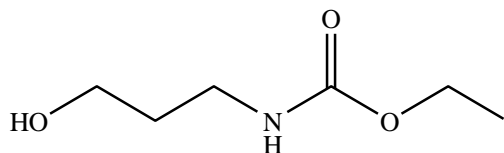
This compound was prepared from an adapted literature procedure.[7] 3-Aminopropanol (9.0 g, 119.82 mmol) was dissolved in 30 mL water. Potassium carbonate (26.55 g, 192.11 mmol) in 30 mL water was added to the reaction mixture. Ethyl chloroformate (19.56 g, 180.24 mmol) was added dropwise over 2 h, while the reaction was kept at 0 °C. The reaction mixture was allowed to stir for an additional 2 h, where after it was filtered and extracted with three portions of DCM (3 × 40 mL). The organic layer extracts were dried over Na_2SO_4 and the solvent was removed under reduced pressure to yield a colourless oil (17.1 g, 97 %). ^1H NMR (300 MHz, $CDCl_3$) δ 5.11 (bs, 1H, -N$\underline{H}$), 4.08 (q, J = 7.1 Hz, 2H, -O-C$\underline{H}_2$), 3.64 (t, J = 5.7 Hz, 2H, -C$\underline{H}_2$-OH), 3.29 (q, J = 6.1 Hz, 2H, -C$\underline{H}_2$-NH), 2.79 (bs, 1H, -O$\underline{H}$), 1.70 (p, 6.0 Hz, 2H, -CH$_2$-C$\underline{H}_2$-CH$_2$), 1.21 (t, J = 7.1 Hz, 3H, -C$\underline{H}_3$). ^{13}C NMR (300 MHz, $CDCl_3$) δ: 156.92, 61.09, 39.49, 32.75, 30.91, 14.83. MS (ESI): m/z = 148.1 (calculated: 148.17 for $[M + H]^+$), 170.1 (calculated: 170.16 for $[M + Na]^+$).

3.4.2.2 Preparation of Ethyl *N*-(3-bromopropyl) carbamate (2):
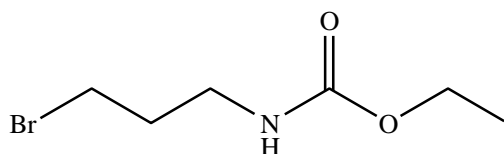
A solution of PBr_3 (11.3 mL, 119.1 mmol) in anhydrous toluene (40 mL) was added to a solution of ethyl *N*-(3-hydroxypropyl) carbamate (13.5 g, 104.8 mmol) in anhydrous toluene (140 mL) over 2 h at room temperature. Precautions were taken for the highly air and moisture sensitive PBr_3. The reaction mixture was allowed to stir for a further 2 h, whereafter it was refluxed for 25 min. The mixture was washed with water (3 × 80 mL) and was saturated with NaCl. The water phase was extracted with DCM (3 × 50 mL). The DCM and toluene phases were dried over $MgSO_4$ and solvents were removed under reduced pressure. Majority of the product was in the

toluene phase as a yellow liquid (11.5 g, 60 %). ^{1}H NMR (300 MHz, CDCl$_3$) δ 4.94 (bs, 1H, -N$\underline{H}$), 4.14 (q, J = 7.1 Hz, 2H, -O-C$\underline{H}_2$), 3.47 (t, J = 6.5 Hz, 2H, -Br-C$\underline{H}_2$), 3.36 (q, J = 6.4 Hz, 2H, -C$\underline{H}_2$-NH), 2.10 (p, J = 6.5 Hz, 2H, -CH$_2$-C$\underline{H}_2$-CH$_2$), 1.27 (t, J = 7.1 Hz, 3H, -C$\underline{H}_3$). ^{13}C NMR (300 MHz, CDCl$_3$) δ: 156.68, 60.87, 39.28, 32.56, 30.71, 14.62. MS (ESI): m/z = 210.0 (calculated: 210.07 for [M]$^+$), 212.0 (calculated: 212.07 for [M]$^+$).

3.4.2.3 Preparation of Ethyl *N*-(3-bromo triphenylphosphoniumpropyl) carbamate (3):
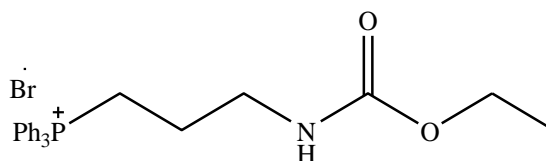
To a solution of ethyl *N*-(3-bromopropyl) carbamate (13.5 g, 64.1 mmol) in acetonitrile (80 mL), recrystallized PPh$_3$ (17.6 g, 67.2 mmol) was added and refluxed at 100 °C for 24 h. After cooling, the mixture was precipitated in ethyl acetate (200 mL), filtered and dried, to afford the product as a white solid (29.9 g, 99 %). ^{1}H NMR (300 MHz, CDCl$_3$) δ: 7.79-7.62 (m, 15H, -P-Ar-$\underline{H}$), 6.97 (bs, 1H, -CH$_2$-N$\underline{H}$), 4.11 (q, J = 7.1 Hz, 2H, -O-C$\underline{H}_2$), 3.44 (t, J = 6.4 Hz 2H, -C$\underline{H}_2$-NH), 1.89-1.77 (m, 2H, -CH$_2$-C$\underline{H}_2$-CH$_2$), 1.23 (t, J = 7.2 Hz, 3H, -C$\underline{H}_3$), 1.17 (t, J = 7.1 Hz, 2H, -P-C$\underline{H}_2$). ^{31}P NMR (300 MHz, CDCl$_3$) δ: 25.18. MS (ESI): m/z = 392.0 (calculated: 392.27 for [M]$^+$).

3.4.2.4 Preparation of *N*-(hydroxymethyl) 3-methylene 2-pyrrolidone (6):
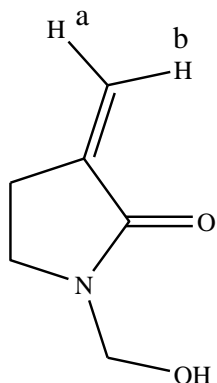
A solution of ethyl *N*-(3-bromo triphenylphosphoniumpropyl) carbamate (3.2 g, 6.9 mmol) in anhydrous toluene (30 mL) was dried by an azeotropic distillation for 3 h. The solution was

cooled to room temperature, whereafter a base, *t*-BuOK (0.8 g, 7.2 mmol) was added. The solution turned bright orange and was stirred for a further 1 h at 50 °C. Paraformaldehyde (0.7 g) was added to the reaction mixture at this temperature and the reaction was allowed to proceed for a further 30 min. The reaction mixture was purged with argon upon the addition of the base and paraformaldehyde. The crude reaction mixture was filtered, concentrated and recrystallized with ethyl acetate. The recrystallized compound was dissolved in chloroform and extracted with water. The water was removed under reduced pressure to yield a sticky solid (0.3 g, 40 %). ^{1}H NMR (300 MHz, CDCl$_3$) δ: 5.98 (t, J = 2.9 Hz, 1H, =C$\underline{H}_b$), 5.38 (t, J = 2.5 Hz, 1H, =C$\underline{H}_a$), 4.87 (s, 2H, -NH-C$\underline{H}_2$-OH), 3.60 (t, J = 6.8 Hz, 2H, -C$\underline{H}_2$-N), 2.80-2.73 (m, 2H, -C$\underline{H}_2$-C=). ^{13}C NMR (300 MHz, CDCl$_3$) δ: 168.36, 140.02, 116.77, 67.23, 43.14, 24.02. GC-MS: *m/z* = 128.1 (calculated: 127.14 for [M]$^+$).

3.2.4.5 Preparation of 3-Methylene-2-pyrrolidone (7):
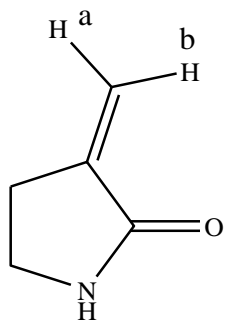
A solution of ethyl *N*-(3-bromo triphenylphosphoniumpropyl) carbamate (3.2 g, 6.9 mmol) in anhydrous toluene (30 mL) was dried by an azeotropic distillation for 3 h. The solution was cooled to room temperature, whereafter a base, *t*-BuOK (0.8 g, 7.2 mmol), was added, under an argon atmosphere. The solution turned bright orange, and was stirred for a further 1 h at 50 °C. Paraformaldehyde (0.05 g, 1.7 mmol) was added to the reaction mixture at this temperature, under an argon atmosphere. Afterwards the reaction was stirred for a further 30 min. The crude reaction mixture was filtered, concentrated and recrystallized with ethyl acetate. The recrystallized compound was dissolved in warm chloroform and extracted with water. The water was removed under reduced pressure to yield a colourless crystal (0.23 g, 35 %). ^{1}H NMR (300 MHz, DMSO-d$_6$) δ: 8.05 (bs, 1H, -N$\underline{H}$), 5.67 (td, J = 2.9, 1.3 Hz, 1H, =C$\underline{H}_b$), 5.26-5.24 (m, 1H, =C$\underline{H}_a$), 3.25 (t, J = 6.6 Hz, 2H, -C$\underline{H}_2$-NH), 2.75-2.71 (m, 2H, -C$\underline{H}_2$-C=). ^{13}C NMR (300 MHz,

DMSO-d$_6$) δ: 175.45, 141.62, 114.47, 38.90, 26.32. MS (ESI): m/z = 98.06 (calculated: 98.11 for [M + H]$^+$), 115.96 (calculated: 115.15 for [M + NH$_4$]$^+$). R$_f$ in ethyl acetate = 0.423.

3.2.4.6 Preparation of Diethyl cyclopropane-1,1-dicarboxylate (8):
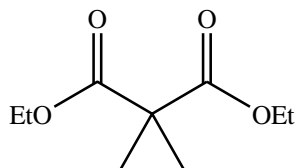
This compound was prepared as described in literature.[12] Tetrabutylammonium bromide (0.8 g, 0.25 mmol), K$_2$CO$_3$ (17.1 g, 125 mmol) and 1,2-dibromoethane (12.2 g, 65 mmol) were added to a solution of diethyl malonate (8.0 g, 50 mmol) in NMP (10 mL), at room temperature. The reaction mixture was stirred for 12 h, whereafter the mixture was diluted with ethyl acetate and washed with ammonium chloride solution (1.9 M). The organic layer was dried with anhydrous MgSO$_4$ and the solvent was removed *in vacuo* yielding the product (98%). ^{1}H NMR (300 MHz, CDCl$_3$) δ: 4.21 (q, J = 7.1 Hz, 4H, -O-C$\underline{H}_2$), 1.42 (s, 4H, -C$\underline{H}_2$), 1.31-1.26 (t, J = 6.8 Hz, 6H, -C$\underline{H}_3$). ^{13}C NMR (300 MHz, CDCl$_3$) δ: 169.66, 166.48, 61.36, 61.26, 29.51, 16.14, 16.10, 13.97. MS (ESI): m/z = 187.1 (calculated: 187.2 for [M + H]$^+$), 209.08 (calculated: 209.21 for [M + Na]$^+$).

3.2.4.7 Preparation of Diethyl 2-azidoethylmalonate (9):
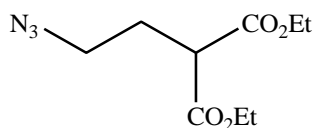
The procedure was adapted from literature.[13] To a 100 mL round bottom flask were added diethyl 1,1-cyclopropanedicarboxylate (8.3 g, 44.7 mmol), sodium azide (5.8 g, 89.5 mmol) and triethylamine hydrochloride (12.3 g, 89.5 mmol) in NMP (40 mL), the solution was heated for 18 h at 100 °C. After the mixture returned to room temperature, it was diluted with diethyl ether (180 mL) and washed with water (7 × 85 mL) as well as a saturated ammonium chloride solution (7 × 85 mL). The organic layer was dried over MgSO$_4$ and the solvent was removed under reduced pressure, yielding the product as an orange oil (52 %). ^{1}H NMR (300 MHz, DMSO-d6) δ: 4.13 (q, J = 7.1 Hz, 4H, -O-C$\underline{H}_2$), 3.57 (t, J = 7.3 Hz, 1H, -C$\underline{H}$), 3.42 (t, J = 6.8 Hz, 2H, -C$\underline{H}_2$-

CH), 2.05 (q, J = 6.8 Hz, 2H, -N$_3$-C$\underline{H}_2$), 1.21 (t, J = 7.1 Hz, 6H, -C$\underline{H}_3$). ^{13}C NMR (300 MHz, DMSO-d$_6$) δ: 168.94, 61.60, 49.24, 48.94, 28.08, 14.31. MS (ESI): *m/z* = 252.1 (calculated: 252.23 for [M + Na]$^+$).

3.2.4.8 Preparation of Ethyl 2-oxo-3-pyrrolidonecarboxylate (10):[13]
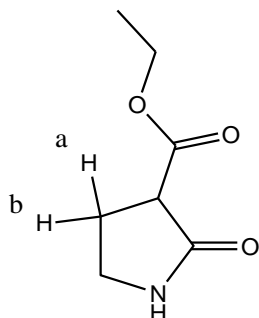
A solution of diethyl 2-azidoethylmalonate (1.9 g, 14.3 mmol) in anhydrous ethanol (40 mL) was hydrogenated over a 10 % Pd/C (166 mg) catalyst for 2 h at room temperature. The reaction mixture was filtered through Celite *545* and washed with anhydrous ethanol (60 mL). The solvent was removed under reduced pressure to yield a yellow-white crystal as the product. Recrystallization from ethyl acetate : hexane (3 : 1) afforded the pure product (87 %). ^{1}H NMR (300 MHz, CDCl$_3$) δ: 6.20 (bs, 1H, -N$\underline{H}$), 4.29 (q, J = 7.1 Hz, 2H, -O-C$\underline{H}_2$), 3.57-3.50 (m, 1H, -C$\underline{H}$), 3.448 (q, J = 7.1 Hz, 2H, -C$\underline{H}_2$-NH), 2.61-2.49 (m, 1H, -C$\underline{H}_{2(a)}$-CH), 2.45-2.33 (m, 1H, -C$\underline{H}_{2(b)}$-CH), 1.35 (t, J = 7.2 Hz, 3H, -C$\underline{H}_3$). ^{13}C NMR (300 MHz, CDCl$_3$) δ: 169.94, 166.53, 61.66, 47.60, 40.72, 25.08, 14.15.MS (ESI): *m/z* = 158.08 (calculated: 158.18 for [M + H]$^+$), 180.06 (calculated: 180.17 for [M + Na]$^+$).

3.2.4.9 Preparation of 3-(Hydroxymethyl)-2-pyrrolidone (11):[3]
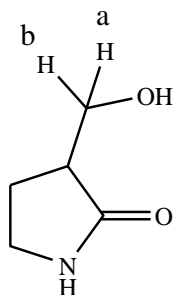
At 0 °C, a solution of ethyl 2-oxo-3-pyrrolidonecarboxylate (0.5 g, 3.2 mmol), calcium chloride (0.4 g, 3.2 mmol) in anhydrous methanol (8 mL) and sodium borohydride (0.1 g, 3.2 mmol) was added. The solution was stirred for 2 h, keeping the temperature between 0-5 °C, whereafter the reaction mixture was allowed to warm to room temperature, and stirred overnight. The mixture was filtered, the residue was washed with anhydrous methanol (3 mL) and the filtrate was concentrated. Diethyl ether (15 mL) was added and decanted, leaving a solid. Diethyl ether washing and decantation was repeated twice. The solids were washed with water (6 mL) and filtered, washing the solids further with water (5 mL). The aqueous layer was washed with DCM (3 × 5 mL). The solvents were removed under reduced pressure with the product was in the aqueous layer as white crystals (78 %). ^{1}H NMR (300 MHz, CDCl$_3$) δ: 6.03 (bs, 1H, -N$\underline{H}$), 3.84 (dd, J = 11.0, 4.8 Hz, 1H, -C$\underline{H}_{2(b)}$-OH), 3.70 (dd, J = 11.0, 7.2 Hz, 1H, -C$\underline{H}_{2(a)}$-OH), 3.36-3.28 (m, 2H, -C$\underline{H}_2$-NH), 2.61-2.51 (m, 1H, -C$\underline{H}$-), 1.96-1.83 (m, 2H, -C$\underline{H}_2$-CH), 1.26 (t, J = 7.1 Hz, 1H, -O$\underline{H}$). ^{13}C NMR (300 MHz, CDCl$_3$) δ: 180.14, 62.56, 42.53, 40.76, 23.76. MS (ESI): m/z = 116.07 (calculated: 116.14 for [M + H]$^+$), 138.05 (calculated: 138.13 for [M + Na]$^+$).

3.5 References

(1)   Cardellina Ii, J. H.; Moore, R. E. *Tetrahedron Lett.* **1979**, *20*, 2007.

(2)   Naito, T.; Honda, Y.; Miyata, O.; Ninomiya, I. *Chem. Pharm. Bull.* **1993**, *41*, 217.

(3)   Klutchko, S.; Hoefle, M. L.; Smith, R. D.; Essenburg, A. D.; Parker, R. B.; Nemeth, V. L.; Ryan, M.; Dugan, D. H.; Kaplan, H. R. *J. Med. Chem.* **1981**, *24*, 104.

(4)   Fotiadu, F.; Pardigon, O.; Buono, G.; Le Corre, M.; Hercouët, A. *Tetrahedron Lett.* **1999**, *40*, 867.

(5)   Schlosser, M. *Topics in Stereochemistry,* Wiley Online Library, 1970.

(6)   Grieco, P. A.; Pogonowski, C. S. *J. Org. Chem.* **1974**, *39*, 1958.

(7)   Xu, G.; Micklatcher, M.; Silvestri, M. A.; Hartman, T. L.; Burrier, J.; Osterling, M. C.; Wargo, H.; Turpin, J. A.; Buckheit, R. W.; Cushman, M. *J. Med. Chem.* **2001**, *44*, 4092.

(8)   Jouglet, B.; Oumoch, S.; Rousseau, G. *Synth. Comm.* **1995**, *25*, 3869.

(9)   Jouglet, B.; Rousseau, G. *Tetrahedron Lett.* **1993**, *34*, 2307.

(10)   Carre, E. L.; Lewis, N.; Ribas, C.; Wells, A. *Org. Process Res. Dev.* **2000**, *4*, 606.

(11)   Lipshutz, B. H.; Blomgren, P. A. *Org. Lett.* **2001**, *3*, 1869.

(12)   Chang, X.-W.; Han, Q.-C.; Jiao, Z.-G.; Weng, L.-H.; Zhang, D.-W. *Tetrahedron* **2010**, *66*, 9733.

(13)   Lindstrom, K. J.; Crooks, S. L. *Synth. Comm.* **1990**, *20*, 2335.

(14)   Gao, J.; Wang, Z.; Xu, D.; Zhang, R. *J. Chem. Eng. Data* **2007**, *52*, 189.

Chapter 4: Conventional radical (co)polymerizations of 3-methylene-2-pyrrolidone-based monomers

4.1 Introduction

An essential aspect towards reducing CO_2 emission, toxic materials and the dependence on fossil fuel resources, is the development of new non-toxic materials. Renewable feedstocks are implemented to produce bio-based materials, assisting in the global efforts of minimizing the polluting effects of fossil fuels. Besides tulipalin A, and the radical chain growth polymerizations thereof (see Chapter 2), examples (depicted in Figure 4.1) of other monomers from renewable feedstocks include lactide (**1**) from plant sugars that undergo ring-opening polymerization (ROP),[1] δ-decalactone (**2**)[2] and substituted ε-caprolactones (**3**) derived from fatty acids and mint (oil), respectively, which both undergo ROP as well. 3-Methylenecyclopentene (**4**), which originates from turpentine, can undergo chain-growth polymerization by cationic, anionic and radical polymerization mechanisms.[3,4]
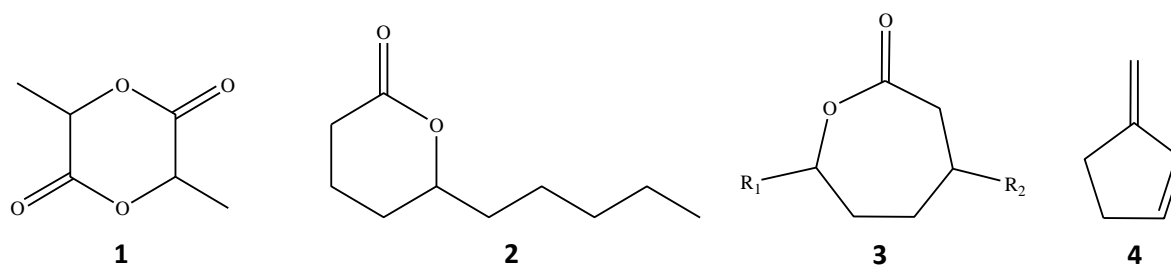
Figure 4.1: Examples of renewable monomers.

Currently, the majority of known renewable monomers either undergo ROP or step growth polymerizations (see Chapter 2). However, a few exceptions that undergo chain growth polymerizations include myrcene,[5] β-pinene,[6] α-phellandrene[7] and 3-methylenecyclopentene (**4**).[3] Additionally, various alkyl (meth) acrylates originating from fatty acids,[8] rosin[9] and vanillin methacrylate from lignin,[10] also undergo chain growth polymerizations.

Although ROP is a type of chain growth process, living radical polymerizations have a larger versatility in terms of monomer compatibility compared to processes such as ROP, ring-opening metathesis (ROMP) and group-transfer-polymerizations. Also, with polymerizations such as

ROP, the polymer backbone contains acetals, amides, esters *etc*. groups, that sacrifice the stability of the polymer.

Conventional free radical polymerization has important applications and a vast majority of commercially available synthetic polymers such as polystyrene and poly(methyl methacrylate) are produced *via* this chain-growth mechanism. The conventional radical polymerization process can be applied to various vinylic monomers, even in the presence of impurities and water. A wide variety of solvents, reaction conditions and temperatures can be used, making this a very versatile process.[11]

3-Methylene-2-pyrrolidone (3M2P) is a vinylic compound and structurally similar to tulipalin A. It was proposed that 3M2P should undergo chain growth polymerizations, in particular conventional radical polymerizations, creating polymers with an all-carbon backbone.

The conventional radical polymerization mechanism consists of three elementary steps: initiation, propagation and termination. Propagation involves the process where the polymer chain grows, *i.e.* addition of monomer to the growing chain. However, the radicals formed via photochemical or thermal homolysis of the initiator are very reactive and can either grow or terminate. Thus, polymers with various chain lengths are formed and the molecular weight distribution obtained is broad (dispersities $Đ \geq 1.5$).[11]

4.2 Results and discussion

4.2.1 Polymer synthesis

In this section, the conventional radical copolymerization of 3M2P and 3M2P-OH, and the conventional radical homopolymerization of 3M2P are demonstrated. The monomer, 3M2P-OH did not homopolymerize due to poor solubility (see Chapter 3).

4.2.1.1 Copolymerizations

Prior to establishing the separate synthesis of 3M2P and 3M2P-OH or separation thereof, the co-monomers were obtained in different ratios and polymerized as is.

The ratios of 3M2P to 3M2P-OH were quantified by ^{1}H NMR spectroscopy, as shown in Figure 3.3 in Chapter 3, with the more shielded 3M2P methylene peaks shifted upfield with respect to 3M2P-OH, and were used to the determine the ratio.
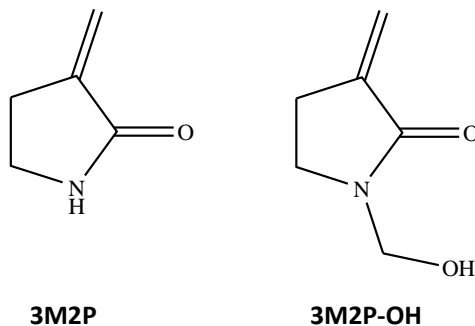
Figure 4.2: The two monomers, 3M2P and 3M2P-OH.

The co-monomers, depicted in Figure 4.2 were soluble in the majority of organic solvents, as well as water-soluble.
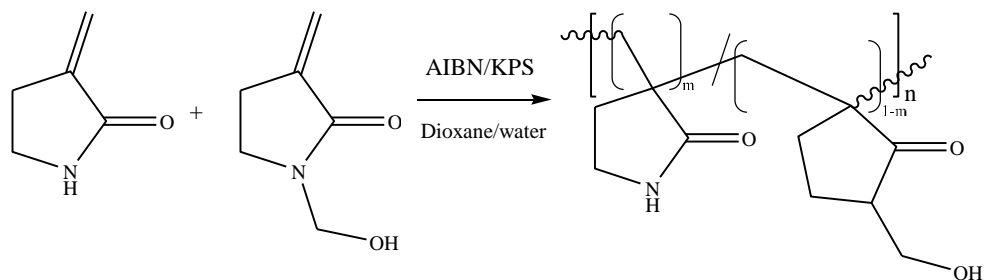
Scheme 4.1: Statistical copolymerization of 3M2P and 3M2P-OH.

Scheme 4.1 indicates the copolymerization of 3M2P and 3M2P-OH. Copolymerizations were carried out using water and dioxane as solvents. The thermal initiators, azobisisobutyronitrile (AIBN) and water-soluble potassium persulfate (KPS) were used at an elevated temperature of 75 °C. All copolymerizations were carried out under an inert atmosphere. Copolymerization molecular weights and dispersities are shown in Table 4.1.

Table 4.1: Copolymerization conditions for 3M2P and 3M2P-OH

Sample	3M2P:3M2P-OH	Initiator	Rxn temp. (°C)	M_n^a	M_w^a	$Đ^b$
1	1.5:1	AIBN[c]	75	715	1 932	2.70
2	2:1	KPS[d]	75	218	655	2.33

- [a] Number average and weight average molecular weights, respectively, in g/mol, determined by aqueous SEC. Detailed SEC conditions in the experimental Section 4.4.
- [b] $Đ = \dfrac{M_w}{M_n}$
- [c] Polymerization solvent was dioxane.
- [d] Polymerization solvent was water.

Co-monomer mixtures with similar chemical compositions (Table 4.1) were copolymerized, producing oligomeric species with high dispersities, $Đ > 1.5$ typical of conventional radical polymerizations.[11] Oligomeric species failed to precipitate in various solvents such as methanol, isopropanol and acetone and these were removed under reduced pressure.

In addition, copolymerizations with *in situ* ^{1}H NMR spectroscopy were performed in order to obtain a better understanding of the formation of the short oligomeric chains, *e.g.* chain transfer to the 3M2P-OH monomer or if 3M2P-OH in fact is incorporated into the chain. Numerous ^{1}H NMR spectroscopy experiments were inconclusive in confirming the incorporation or consumption of 3M2P-OH due to a broad peak overlapping with both co-monomers' methylene peaks.

4.2.1.2 Homopolymerization of 3M2P

Upon the discovery of the separate synthesis of 3M2P, the quest was extended to obtaining high molecular weight homopolymers of 3M2P, as initially intended.

The conventional radical homopolymerization of 3M2P (depicted in Scheme 4.2) was carried out using optimized conditions reported for conventional radical homopolymerization of tulipalin A, described by Akkapeddi *et al*.[12]
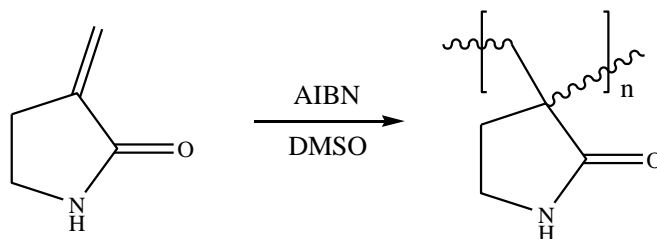
Scheme 4.2: Homopolymerization of 3M2P.

Initially, obstacles were encountered obtaining high molecular weight P(3M2P). The lower molecular weight homopolymer species did not precipitate in methanol, isopropanol or acetone, similar to the copolymers of 3M2P and 3M2P-OH.

Upon polymerization in DMSO at lower initiator concentration, high molecular weight P(3M2P) was obtained and precipitated easily into acetone. Polymerization conditions are given in Table 4.2.

Table 4.2: Homopolymerization conditions

Sample	α^a (%)	Rxn time (h)	Rxn temp.($^\circ$C)	M_n^b	M_w^b	$Đ^c$
3	82	24	60	67 177	156 281	2.33
4	83	16	75	52 335	97 137	1.86

- [a] Gravimetrical conversion.
- [b] Number average and weight average molecular weights determined by 1,1,1,3,3,3-hexafluoro-2-propanol (HFIP) SEC. Detailed SEC conditions are provided in the experimental Section 4.4.
- [c] $Đ = \dfrac{M_w}{M_n}$

From Table 4.2, sample **3** and **4** have molar mass dispersities of $Đ > 1.5$, typical of conventional radical polymerizations.[11] Optimized polymerization conditions yielded very good conversions of > 80 %, and high molecular weights were measured *via* SEC in HFIP.

Routine analyses of P(3M2P) were carried out with ^{1}H NMR spectroscopy that consisted of presaturation experiments, suppressing water peaks carried over from the monomer synthesis. ^{1}H NMR spectroscopy was carried out in D_2O, since the polymer is extremely water-soluble. Typical ^{1}H NMR spectra for 3M2P **A** (monomer), P(3M2P) **B** and P(3M2P) with integrations **C** are shown Figure 4.3.

The spectra depicted in Figure 4.3 show that the methylene peaks from 3M2P monomer **A** (signal 7a and 7b) disappear in the polymer **B**. Additionally the broadening of peaks in **B** are indicative of polymer formation. The γ-CH_2 (signal 4) protons of the lactam-ring in **B** were observed at ~3.4-3.3 ppm, contributed by 2 protons in **C** and were assigned more downfield due to deshielding from the neighbouring NH-group. The β-CH_2 (signal 3) protons and the backbone CH_2 (signal 1) protons were overlapped and were contributed by 4 protons, in the region of ~2.4-1.3 ppm, as shown in **C**.
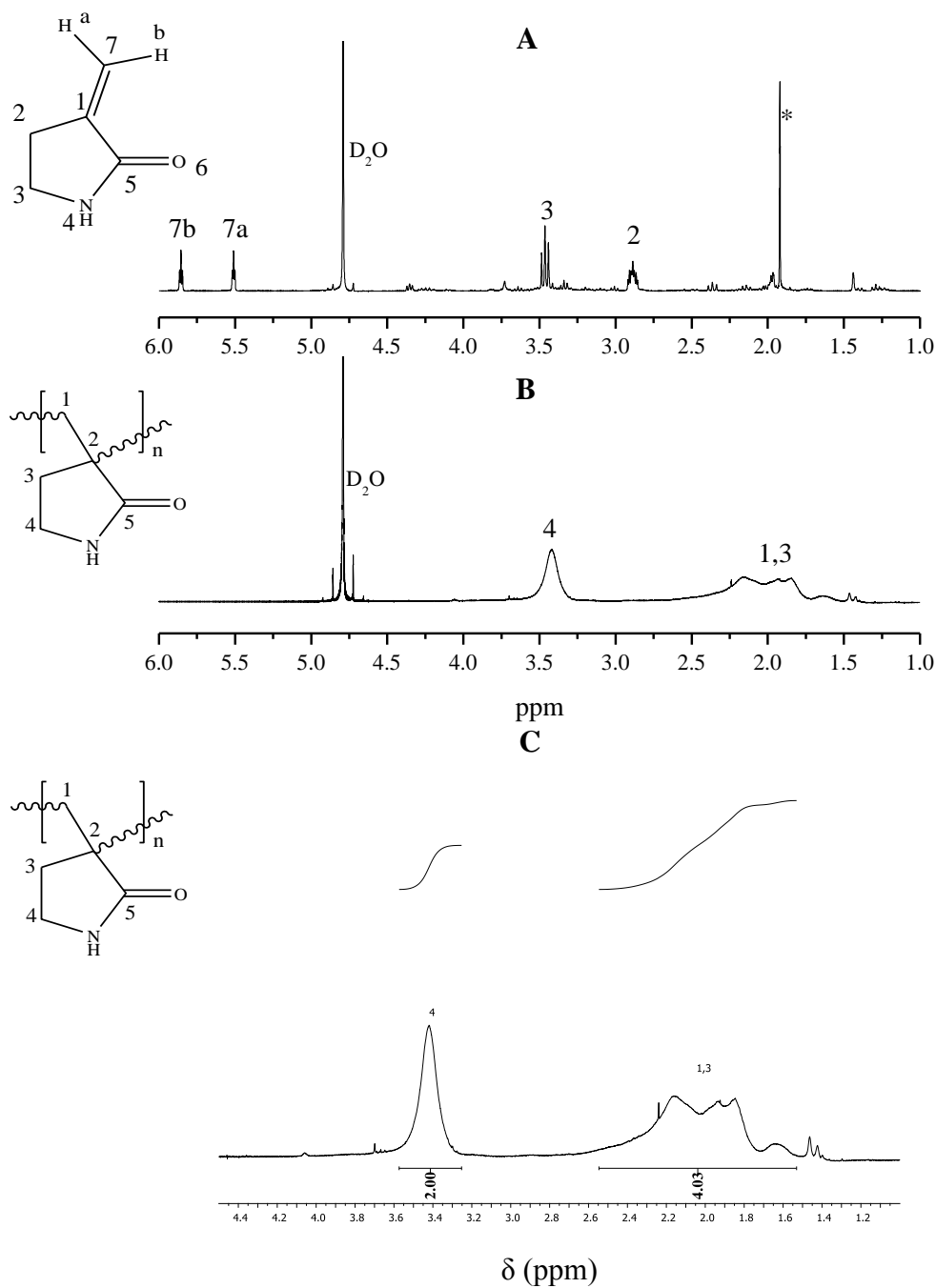
Figure 4.3: Presaturation ^{1}H NMR spectra in D$_2$O of A) 3M2P monomer, B) P(3M2P) and C) P(3M2P) with integration.

The ^{13}C NMR spectrum of P(3M2P) was recorded in D$_2$O as solvent, shown in Figure 4.4, with residual DMSO carried over from the polymerization. Signal 5 was assigned to the carbonyl carbon, in agreement with the downfield shift. The α-carbon (signal 2) was observed at ~46 ppm, which is in good agreement with that of the α-carbon of poly(tulipalin A) at ~46-47 ppm.[12] The

β-carbon (3) was shifted most upfield, similar to that in poly(tulipalin A) and the backbone carbon (signal 1) was observed at ~39 ppm.
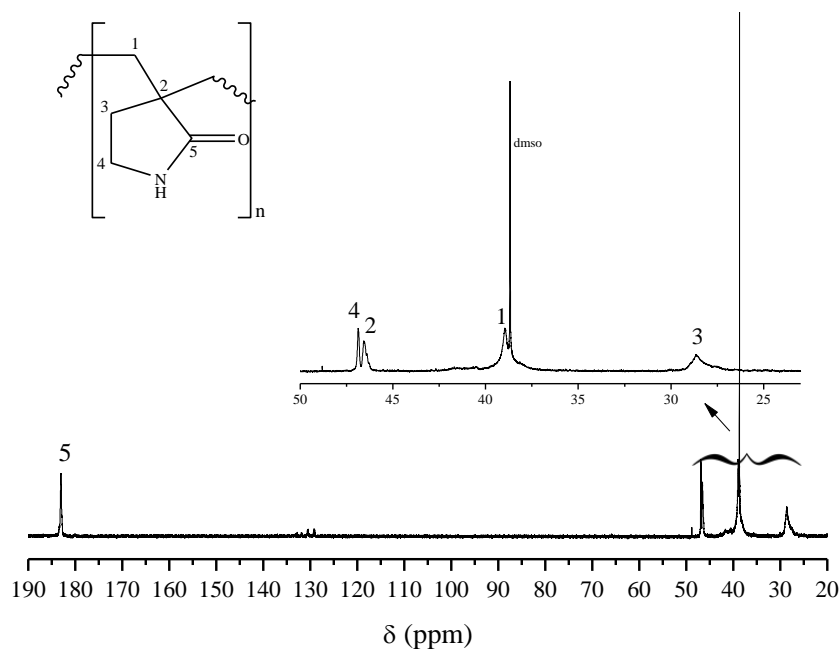
Figure 4.4: ^{13}C NMR spectroscopy of P(3M2P) in D$_2$O.

The conventional homopolymerization of 3M2P with AIBN as initiator, resulted in 99.9 % monomer consumption in the 10 hours of reaction time, as depicted in Figure 4.4. In situ ^{1}H NMR spectroscopy was used to monitor the concentration of the depleting monomer peaks. The majority of monomer consumption occurred within the first 200 min of the reaction.
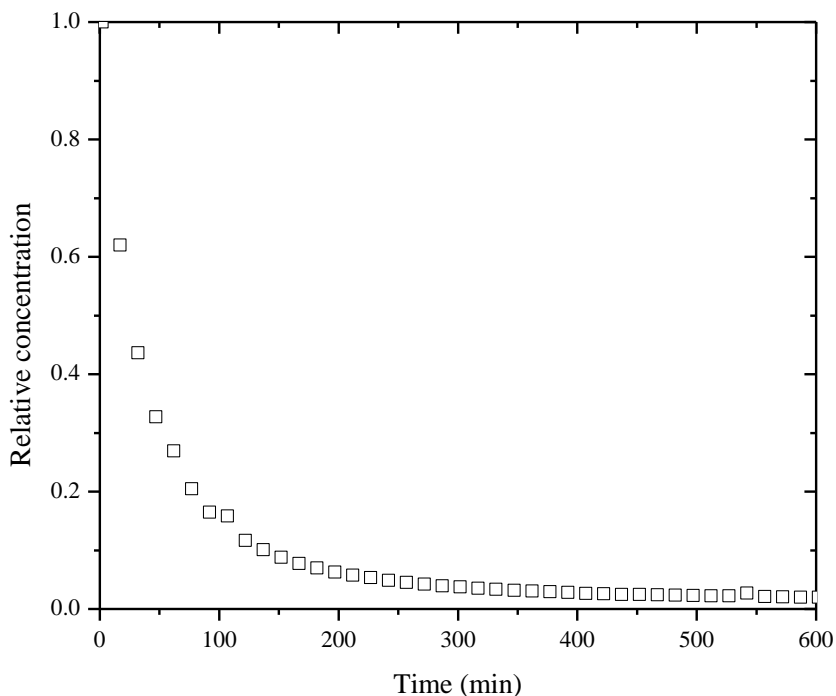
Figure 4.5: The relative concentration of 3M2P monomer of conventional homopolymerization at 75 °C monitored by *in-situ* **¹H NMR run for 10 h.**

4.2.2 Polymer properties

To obtain a better impression of the new P(3M2P) and the possible applications thereof, different properties were investigated.

4.2.2.1 Thermal analysis

Thermal properties such as degradation and stability temperatures were investigated, to obtain a better understanding of the thermal behaviour of P(3M2P). In addition, the thermo-responsive behaviour of the polymer was tested.

Differential scanning calorimetry (DSC) thermograms give thermal properties such as the glass transition temperature (T_g), as well as the melting and crystallization temperatures. DSC measures the change in heat flow of the sample compared to a reference sample, with a predetermined temperature program,[13] and a glass transition is shown for P(3M2P) in Figure 4.6, indicating a T_g of ~ 285 °C, where the glass transition temperature gives the temperature of transition from a glassy to a rubbery state of a material. The ring-open version of P(3M2P),

50

poly(*N*-methyl methacrylamide) also has a high T_g of 255 °C but lower than P(3M2P). Whereas poly(tulipalin A) has a T_g of 195 °C.[12] Both the lactam and lactone polymers present high glass transition temperatures, indicative of the lactone and lactam ring's structural rigidity. The higher T_g of P(3M2P) could be described to stronger hydrogen bonding of the amide than the ester in poly(tulipalin A). Furthermore, no melting peak was observed in the heating cycle as well as no crystallization peak in the cooling cycle and it was concluded that P(3M2P) was an amorphous polymer, similar to poly(tulipalin A).[12]
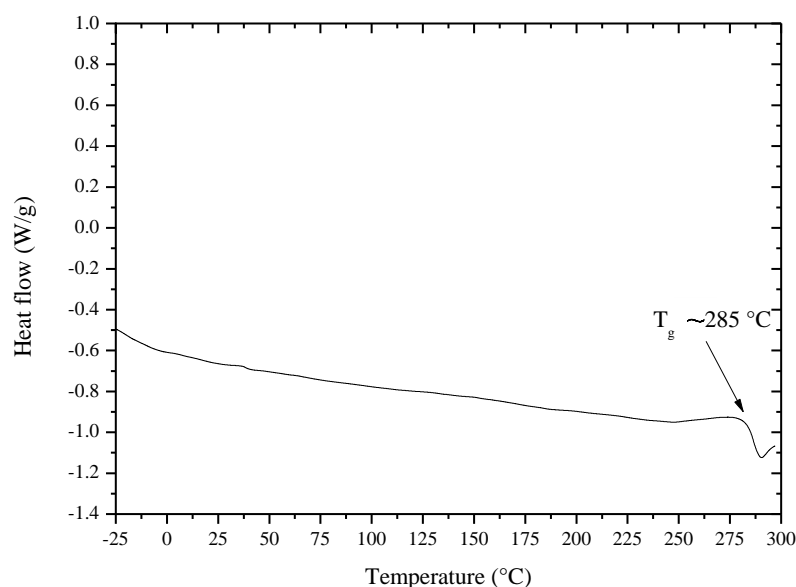
Figure 4.6: DSC thermogram of second heating cycle of P(3M2P).

Additionally, thermogravimetric analysis (TGA) on P(3M2P) was performed to give an indication of the polymer's thermal stability. The weight change of a material is measured as a function of temperature and gives the main thermal decomposition temperature of a material.[14]

The percentage weight loss versus temperature and corresponding weight derivative (blue) for P(3M2P) is shown in Figure 4.7. The thermogram was obtained under a nitrogen atmosphere, to prevent oxidation, with a wide temperature range of 20-900 °C. The weight derivative (blue curve) in Fig.4.7 gives a maximum weight loss rate at approximately 400 °C, indicating thermal stability up to this temperature, with the main thermal decomposition occurring between 400-500

51

°C. The onset of ~20 % weight loss prior to 110 °C is attributed to water loss, due to the hygroscopic nature of P(3M2P).
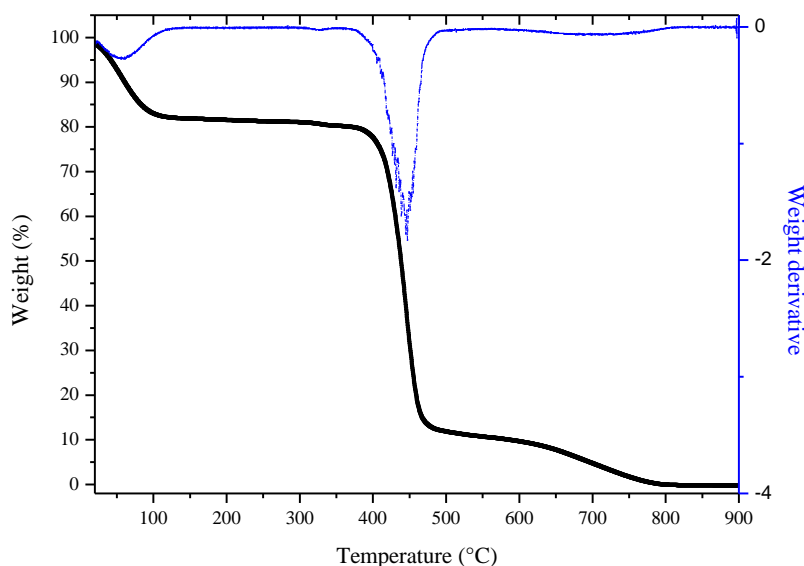
Figure 4.7: TGA thermogram and corresponding weight derivative of the decomposition of P(3M2P).

Recently, stimuli-responsive polymers have gained importance in the field of drug-delivery, tissue-engineering *etc*. In addition, the stimuli-responsive behaviour of P(3M2P), in particular the thermo-responsive behaviour was tested for a lower and upper critical solution temperature (LCST and UCST). A polymer with a LCST exhibits a hydrophilic to hydrophobic transition at the cloud point temperature, with the transition being reversible. For example, polymers with a LCST like poly(*N*-isopropylacrylamide) are miscible (hydrophilic) in the solution below the cloud point temperature of 32 °C and immiscible (hydrophobic) above the cloud point temperature.[15]

P(3M2P) was dissolved in water and UV at three different wavelengths (300, 400 and 500 nm) were recorded upon varying temperatures. The temperature program consisted of a heating (25-80 °C) and cooling (80-25 °C) cycles, while the percentage transmittance of the aqueous solution was measured. However, the percentage transmittance remained unchanged over both temperature cycles and thus no LCST or UCST was observed under these conditions.

4.2.2.2 Solubility behaviour

The solubility and solvent-resistance of a polymer determines and alters the applications thereof. An investigation of P(3M2P)'s solubility was performed in a wide variety of solvents. Overall it had poor solubility in most organic solvents, however was completely water-soluble, as indicated in Table 4.3 below.

Table 4.3: Solubility of P(3M2P) in various solvents

Solvent	Solubility	Solvent	Solubility
Acetone	Is	Ethanol	Is
Acetonitrile	Is	Ethyl acetate	Is
Anisole	Is	Hexafluoro-2-propanol	S
Benzene	Is	Isopropanol	Is
Butanone	Is	Methanol	Is
Chloroform	Is	Nitromethane	Is
Dichloromethane	Is	N-methyl-2-pyrrolidone	Is
Diethyl ether	Is	Pentane	Is
Dimethyl sulfoxide	Ps	Pyridine	Is
Dimethylacetamide	Is	Tetrahydrofuran	Is
Dimethylformamide	Is	Toluene	Is
Dioxane	Is	Water	S

- S - soluble.
- Is - insoluble.
- Ps - partially soluble upon heating and sonication.

It was proposed that the solvent-resistance of P(3M2P) could be ascribed to the structural rigidity of the lactam ring as well as strong hydrogen bonding. Similarly, the lactone-analogue, poly(tulipalin A), also exhibits resistance to the majority of organic solvents, except DMF and DMSO.[12] Interestingly, the polymer was exceptionally water-soluble, associating it with various applications, for example in different stages of production in oil and gas wells,[16] paints, water treatment plants, detergents *etc*.[17] Other water-soluble polymers include poly(vinyl alcohol), poly(acrylic acid), poly(ethylene glycol), poly(*N*-vinylpyrrolidone) and polyacrylamide.[17]

Water-soluble, biocompatible polymers also have important applications in pharmaceuticals. Drugs, in particular certain anti-cancer drugs, are poorly water-soluble and precipitate and degrade in the bloodstream upon intravenous administration.[18,19] Therefore, polymeric drug-delivery systems are designed as carriers of these hydrophobic drugs.[20] Liposomes,[21] polymer-drug conjugates,[22] micelles[23] and vesicles[24] are polymeric drug-delivery systems that aid in the solubility of the hydrophobic drugs; they are typically designed to target certain biological sites and control the drug-release. Amphiphilic drug-delivery systems consisting of block copolymers have a hydrophobic segment and hydrophilic segment that assists with the solubility and delivery of the drug in the bloodstream. Examples of hydrophilic blocks include water-soluble, biocompatible polymers such as poly(*N*-vinyl pyrrolidone) (PVP), poly(acrylamide) and poly(ethylene glycol) (PEG).[25] Bailly *et al*. reported on a drug delivery system, where an amphiphilic block copolymer was synthesized and self-assetulipalin Aed into a vesicle as a vehicle for hydrophobic drugs. The hydrophilic segment consisted of a PVP block and the hydrophobic segment of poly(vinyl acetate).[26]

4.2.2.3 Cytotoxicity testing

The water-solubility of P(3M2P) makes it an attractive polymer especially when applications are extended to the biomedical field as abovementioned. However, biomedical polymers require interaction with cells without any undesirable effects and thus should be non-toxic to biological systems.[27] Investigation of the biocompatibility of P(3M2P) towards cells gives this new polymer a broader scope of possible applications.

Biocompatibility is dependent on various aspects such as chemical properties, cytotoxicity, mutagenic and allergenic effects *etc*. Biocompatibility testing is divided in three categories; primary (level I), secondary (level II) and preclinical (level III). Level I can either be performed *in vitro* or *in vivo*.[28] Cytotoxicity testing is generally performed on primary cultures or permanent cell lines.[27]

In vitro cytotoxicity studies of P(3M2P) were performed against cultured GT1-7 (hypothalamic mouse cell lines) in Dulbecco's modified eagle medium (DMEM) with 1 % penicillin/ streptomycin and 10 % fetal calf serum (FCS). Three different concentrations of P(3M2P) were added to the cell medium and the polymer dissolved rapidly, where after the cell-polymer

solutions were incubated for 4 hours at 37 °C. Subsequently, the samples were stained with the fluorescent markers Hoechst 33342 dye and propidium iodide. The fluorescent markers are either permeable or impermeable to the cell membrane, dependent on the cell viability.

The positively charged Hoechst 33342 dye (blue) binds to the minor grooves in the DNA double helix and is also permeable to healthy cell membranes.[29] It is mainly used to stain cell structures for cell morphology studies. It can however also indicate apoptotic cell death.[30] Propidium iodide (red) binds and stains DNA molecules and is impermeable to healthy cell membranes. Propidium iodide is used as a counterstain to Hoechst 33342 dye as it is permeable to the membrane of dead cells and indicates necrotic cell death.

In Figure 4.8, fluorescence and light transmission micrographs of the polymer-cell solutions are stained with Hoechst 33342 dye (column **A**), propidium iodide (column **B**) and an overlay of Hoechst 33342 dye and propidium iodide (column **C**). The control micrographs show that the cell membranes were permeable to the blue Hoechst 33342 dye (**A**) as expected and that the cells were healthy as no propidium iodide (red) stain penetrated the cell membrane in **B** and **C**. The micrographs of the polymer-cell solutions with concentrations of 1 mg/mL and 1 µg/mL of P(3M2P) present in the solution, showed similar behaviour as the control, where Hoechst 33342 dye stained the cell with no propidium iodide penetrating the cell membrane, indicating that the cells were in fact still healthy, with no indication of cell death. On the contrary, the positive control cells were treated with ethanol, intending to visualize cell death. From Figure 4.8 the positive control micrographs show definitive propidium iodide penetrating the cell membrane with the red stain in **B**, indicative of cell death. The overlay micrograph (**C**) of the positive control shows a pink colour, as a result of the overlay of the red and blue stains.

In vitro experiments demonstrated that P(3M2P) showed no cytotoxicity, confirming the biocompatibility of the polymer. This aspect broadens the scope of possible applications of P(3M2P) and can be compared to other biocompatible, water-soluble, non-ionic polymers such as PVP, PEG, poly(acrylamide), *etc*.[25]
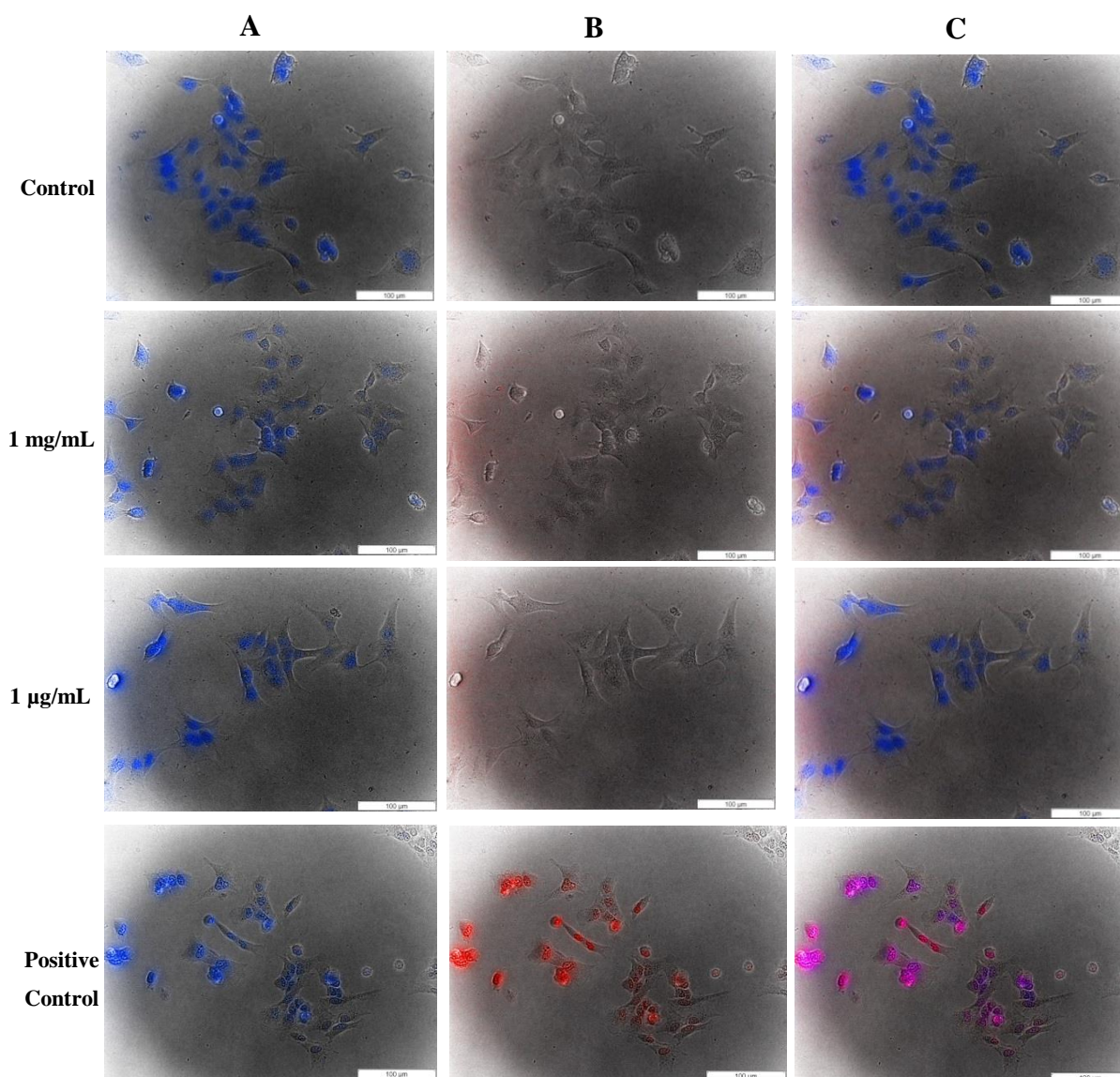
Figure 4.8: Fluorescence and light transmission micrographs where A) is the cells dyed with Hoechst 33342 dye, samples B) is the cells with propidium iodide and C) is an overlay of A and B. Scale bar: 100μm.

4.3 Conclusion

Novel water-soluble co-oligomers of 3M2P and 3M2P-OH co-monomers were developed *via* conventional radical polymerization. The homopolymer, P(3M2P) was also successfully synthesized *via* conventional radical polymerization. P(3M2P) was analyzed by SEC and molecular weights and dispersities were determined, in line with typical conventional radical polymerizations. Additionally, properties of P(3M2P) were investigated and revealed very good thermal stability with a $T_g \sim 285$ °C and main thermal decomposition temperature of 400 °C. P(3M2P)'s thermo-responsive behaviour was tested, however no LCST or UCST was observed.

P(3M2P) was resistant to the majority of organic solvents, with water and HFIP as exceptions. The high thermal stability and solvent-resistance of P(3M2P) was ascribed to the structural rigid lactam ring, accompanied by strong hydrogen bonding and was compared to that of the lactone-analogue and the ring-open version, poly(*N*-methyl methacrylamide). Finally, *in vitro* cytotoxicity testing confirmed the biocompatibility of P(3M2P). The water-solubility and biocompatibility of P(3M2P) makes it a suitable polymer for a variety of biomedical applications, which should be investigated further in the future.

4.4 Experimental

4.4.1 General details

All chemicals and solvents were reagent-grade and purchased from commercial sources. Distilled water was used. AIBN was recrystallized from anhydrous methanol and KPS from cold water. All polymerizations were carried out under an inert atmosphere. SnakeSkin® dialysis tubing with a MW cut-off of 3 500 was purchased from Thermoscientific.

^{1}H and ^{13}C NMR spectra were obtained with a Varian VXR-Unity (300 MHz) spectrometer, unless stated otherwise. Majority of the compounds were dissolved in D_2O and spectra were obtained by presaturation experiments. *In situ* ^{1}H NMR experiments were monitored with a Varian VXR-Unity (400 MHz) at elevated temperatures. ACD Labs (version 12.0) was used for data processing. Molar masses and dispersities of the co-polymers were obtained by aqueous SEC. The instrument was an Agilent 1260 fitted with a guard column in series with three columns (10 µm × 300 mm) with the following pore sizes; 30 Å, 1000 Å (2 × PSS Suprema) columns, with an Agilent 1260 Quad pump and refractive index detector. The flow rate was 1.00 mL/min and the injection volume, 100 µL. Distilled water and HPLC-grade methanol was used as solvent (water/methanol, 70:30). The column oven temperature was 35 °C. The calculated molar masses were relative to poly(ethylene glycol) (PEG) standards with low dispersities, obtained from Polymer Laboratories. Molar masses and dispersities of the homopolymer, poly(3M2P) were obtained by HFIP SEC. The SEC instrument was equipped with a Waters 1515 Isocratic HPLC pump, a Waters 2414 refractive index detector, a Waters 2707 autosampler, PSS PFG guard column and two PFG-linear-XL (7 µm, 8 × 300 mm) columns in series. The HFIP contained lithium chloride (2 g/L), the flow rate was 0.8 mL/min and the injection volume was

57

75 µL. The calculated molar masses were relative to poly(methyl methacrylate) (PMMA) standards with low dispersities, obtained from Polymer Laboratories. Mass Spectrometry (MS) and Liquid Chromatography Mass Spectrometry (LC-MS) were performed on a Waters Synapt G2 with Electron Spray Ionization (ESI) in the positive mode. The column used was Waters UPLC C18, 2.1x100mm. UV-vis spectra were obtained using Specord® 210 Plus (heating and cooling rate = 5 °C/min). Thermal analysis studies were obtained by DSC with a TA Instruments Q100 calorimeter calibrated with an indium standard under N_2 atmosphere. Cooling and heating rates were fixed at 10 °C/min and were obtained from -60 to 300 °C. Thermal analysis (TGA) samples were analysed using a Perkin Elmer TGA 7, under an inert nitrogen atmosphere to prevent oxidation. The heating rate was 20 °C per minute up to 900 °C. Micrographs image acquisition was performed on an Olympus Cell system attached to an IX81 inverted fluorescence microscope equipped with an F-view-II cooled CCD camera (Soft Imaging Systems) using a Xenon-Arc burner (Olympus Biosystems GmbH) as light source.

4.4.2 Synthetic procedures

4.4.2.1 General polymerizations of poly(3M2P) and poly(3M2P)-co-(3M2P-OH)

Copolymerizations were carried out in a 5 mL pear flask, where different ratios of 3M2P to 3M2P-OH were dissolved in 0.5-0.8 mL dioxane or water. The initiator (AIBN or KPS) was added in 50:1 ([M]:[I]) ratio, where after the reaction mixture was degassed with Argon for 45 min, whilst stirring. The pear flask was placed in an oil bath at 75 °C for 24 h. When the polymerization was complete, the solvent was removed under reduced pressure to yield oligomers.

Homopolymerizations were carried out in a 5 mL pear flask, where 3M2P (100 mg, 1.03 mmol) and AIBN, in a ratio of 100:1 were added. Homopolymerizations were carried out in DMSO as solvent and under an inert atmosphere. Reaction temperatures are specified in Table 4.2. When the polymerization had reached completion, the mixture was precipitated slowly into acetone, filtered and yielded a white powder. For specified analyses, P(3M2P) was dialyzed against water for ~5 days using SnakeSkin®, replacing the water every 12 h.

4.4.2.2 General *in-situ* homopolymerization of poly (3M2P)

In situ conventional homopolymerization of 3M2P experiments was monitored using 400 MHz ^{1}H NMR spectroscopy in DMSO-d_6 at 75 °C. DMF was added as an internal reference and appeared as a singlet at 7.95 ppm. The polymerization reaction mixture consisted of: DMSO-d_6 (0.55 g, 7.04 mmol), 3M2P (30 mg, 0.31 mmol), AIBN (1.1 mg, 0.006 mmol) and 5 µL DMF as internal reference. The reaction mixture was mixed in a J-Young type NMR tube, followed by five freeze-pump thaw cycles and lastly, the tube was filled with a N$_2$ gas. The first spectrum was obtained at 25 °C, where after the magnet cavity was heated to 75 °C and 2-3 min after re-insertion the second spectrum was obtained, subsequently spectra was taken every 15 min for 10-15 hours.

4.4.2.3 Cytotoxicity testing

Different concentrations of dialyzed P(3M2P) (1 mg/mL, 1 µg/mL and 1 ng/mL) were investigated. P(3M2P) was dissolved in Dulbecco's modified eagle medium (DMEM) containing 1 % penicillin/streptomycin and 10 % fetal calf serum and added to GT1-7 cell cultures. A control (media and cells) and a positive control (media and cells treated with ethanol) were used as references. Subsequently, the samples were incubated at 37 °C for 4 h, where after the cells were stained with fluorescent markers, Hoechst 33342 dye and propidium iodide, respectively. Fluorescence and light transmission micrographs were obtained and cell viability was determined.

4.5 References

(1) Inkinen, S.; Hakkarainen, M.; Albertsson, A.-C.; Södergård, A. *Biomacromolecules* **2011**, *12*, 523.

(2) Martello, M. T.; Burns, A.; Hillmyer, M. *ACS Macro Lett.* **2011**, *1*, 131.

(3) Kobayashi, S.; Lu, C.; Hoye, T. R.; Hillmyer, M. A. *J. Amer. Chem. Soc.* **2009**, *131*, 7960.

(4) Holmberg, A. L.; Reno, K. H.; Wool, R. P.; Epps III, T. H. *Soft Matter* **2014**, *10*, 7405.

(5) Cawse, J.; Stanford, J.; Still, R. *J. Appl. Polym. Sci.* **1986**, *31*, 1963.

(6) Satoh, K.; Sugiyama, H.; Kamigaito, M. *Green Chemistry* **2006**, *8*, 878.

(7) Satoh, K.; Lee, D. H.; Nagai, K.; Kamigaito, M. *Macromol. Rapid Commun.* **2014**, *35*, 161.

(8) Coelho, J. F.; Carvalho, E. Y.; Marques, D. S.; Popov, A. V.; Goncalves, P. M.; Gil, M. H. *Macromol. Chem. Phys.* **2007**, *208*, 1218.

(9) Wang, J.; Yao, K.; Korich, A. L.; Li, S.; Ma, S.; Ploehn, H. J.; Iovine, P. M.; Wang, C.; Chu, F.; Tang, C. *J. Polym. Sci. Part A: Polym. Chem.* **2011**, *49*, 3728.

(10) Holmberg, A. L.; Stanzione III, J. F.; Wool, R. P.; Epps III, T. H. *ACS Sustain. Chem. Eng.* **2014**, *2*, 569.

(11) Matyjaszewski, K.; Davis, T. P. *Handbook of Radical Polymerization*; Wiley Online Library, 2002.

(12) Akkapeddi, M. K. *Macromolecules* **1979**, *12*, 546.

(13) Höhne, G.; Hemminger, W.; Flammersheim, H.-J. *Differential Scanning Calorimetry*; Springer, 2003.

(14) Chan, J.; Balke, S. *Polym. Degrad. Stab.* **1997**, *57*, 135.

(15) Lee, S. G.; Pascal, T. A.; Koh, W.; Brunello, G. F.; Goddard, W. A.; Jang, S. S. *J. Phys. Chem. C* **2012**, *116*, 15974.

(16) Chatterji, J.; Borchardt, J. *J. Petrol. Technol.* **1981**, *33*, 2.

(17) Swift, G. *Polym. Degrad. Stab.* **1994**, *45*, 215.

(18) Lipinski, C. A. *Am. Pharm. Rev.* **2002**, *5*, 82.

(19) Merisko-Liversidge, E. M.; Liversidge, G. G. *J. Toxicol. Pathol.* **2008**, *36*, 43.

(20) Kwon, G. S.; Kataoka, K. *Adv. Drug Deliv. Rev.* **1995**, *16*, 295.

(21) Barenholz, Y. *Curr. Opin. Colloid Interface Sci.* **2001**, *6*, 66.

(22) Duncan, R. *Nat. Rev. Drug Discov.* **2003**, *2*, 347.

(23) Mikhail, A. S.; Allen, C. *J. Controlled Release* **2009**, *138*, 214.

(24) Choucair, A.; Lim Soo, P.; Eisenberg, A. *Langmuir* **2005**, *21*, 9308.

(25) Lukyanov, A. N.; Torchilin, V. P. *Adv. Drug Deliv. Rev.* **2004**, *56*, 1273.

(26) Bailly, N.; Thomas, M.; Klumperman, B. *Biomacromolecules* **2012**, *13*, 4109.

(27) Fischer, D.; Li, Y.; Ahlemeyer, B.; Krieglstein, J.; Kissel, T. *Biomaterials* **2003**, *24*, 1121.

(28) Anusavice, K. J.; Phillips, R. W.; Shen, C.; Rawls, H. R. *Phillips' science of dental materials*; Elsevier Health Sciences, 2012.

(29) Carrondo, M. A. d. C.; Coll, M.; Aymami, J.; Wang, A. H.; Van der Marel, G. A.; Van Boom, J. H.; Rich, A. *Biochemistry* **1989**, *28*, 7849.

(30) Foglieni, C.; Meoni, C.; Davalli, A. M. *Histochem. Cell Biol.* **2001**, *115*, 223.

Chapter 5: Towards the control of poly(3-methylene-2-pyrrolidone) macromolecular architectures

5.1 Introduction

Conventional radical polymerization is an advantageous and versatile polymerization technique and annually 100 million tons of various polymers are produced by this technique.[1] The main disadvantage however is the lack of control over the molecular weight, and thus polymers with broad molecular weight distributions (dispersity ($Đ$) > 1.5) are formed. This is ascribed to the very fast initiation and termination of the polymer chains, throughout the polymerization.[2] Furthermore, the control over the architecture of the polymeric chain is limited and sophisticated architectures such as star, block and brush morphologies are not obtainable.[1]

To gain control over the polymer architectures and molecular weights, termination and chain transfer reactions must be suppressed during the polymerization. Szwarc performed the first successful living polymerization in 1956, *i.e.* the anionic polymerization of styrene, initiated with sodium napthalenide.[3,4]

The most well-known living radical polymerization techniques include atom transfer radical polymerization (ATRP), nitroxide mediated polymerization (NMP) and reversible-addition fragmentation chain-transfer (RAFT). With ATRP and NMP, control is gained over the polymerization by reversibly capping active radicals into dormant chains, which in return is governed by the persistant radical effect (PRE) that ensures a low concentration of propagating radicals.[5] RAFT on the other hand involves a degenerative chain transfer mechanism where the rate of (reversible) chain transfer is greater than the rate of propagation.[6]

5.1.1 ATRP

Transition metal catalysed polymerizations are a versatile and mild technique to gain control over macromolecules, and the transition metals utilized include ruthenium, iron, molybdenum, osmium *etc*.[7,8] The copper-catalysed polymerizations were first reported by Matyjaszewski *et al*. and the most efficient and versatile catalysts for a broad range of monomers turn out to be copper based.[9]

In the classical ATRP, the Cu^I-ligand complex activates the dormant chain, in the form of an alkyl halide (P_n-X), forming a radical and a Cu^{II} halide complex, as shown in Scheme 5.1. The radical propagates with monomer addition and at this stage can also undergo termination. However, the Cu^{II} halide complex will intermittently reverse the reaction and deactivate propagation, in turn, forming the dormant P_n-X chain and the Cu^I species.
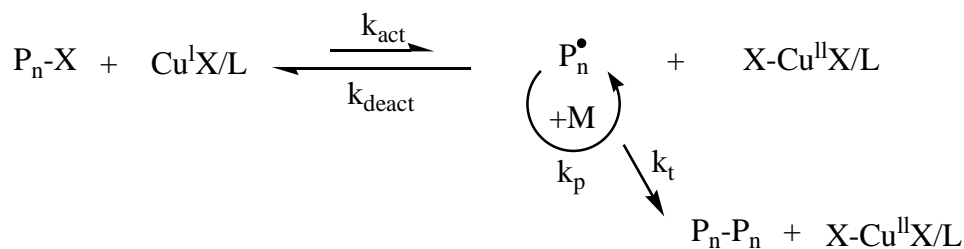
Scheme 5.1: Mechanism of classical ATRP.

Various reactions are possible with transition metals in different oxidation states and since 1997, zerovalent metals were incorporated into ATRP systems.[10] In 2006, Percec and coworkers discovered an efficient living radical polymerization system, using Cu^0 as catalyst and activator, which was called single electron transfer (SET) LRP.[11] Similar to Cu^I in classic ATRP, in SET LRP, Cu^0 acts as the main activator. Cu^0 additionally oxidizes and produces the active Cu^I species, which however instantaneously disproportionates to Cu^0 and Cu^{II}. Equilibrium between Cu^0 (activator) and $Cu^{II}X_2/L$ (deactivator) gives the balance between dormant species and active polymer chains (refer to Scheme 5.2).[1,12]
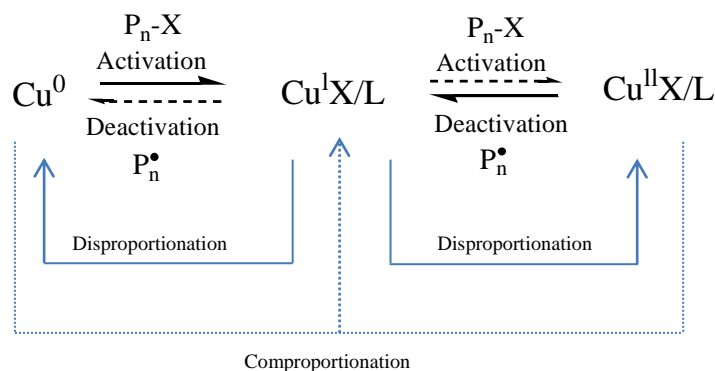
Scheme 5.2: Mechanism of SET-LRP.

The electron transfer occurs by an outer sphere electron transfer mechanism; however it can also occur by a faster, inner sphere electron transfer mechanism. In the case of the latter, it is referred

to as SARA-(supplemental activator and reducing agent) ATRP, with the Cu^I species as the main activator originating from comproportionation (see Scheme 5.2).[1,13]

The advantages of using a Cu^0 catalyst in a polymerization is that advanced architectures are possible (dendritic, hyperbranched, block copolymer *etc*.) with effortless removal of soluble copper species present only in low concentrations, differing from classic ATRP.[14] However, ARGET (activator regenerated by electron transfer)-ATRP also has very low concentrations of copper species present in the reaction mixture. ARGET-ATRP requires a reducing agent that continuously regenerates the activating Cu^I species from the formed Cu^{II} species.[15]

In literature there is on-going debate on the mechanism of SET-LRP and if it in fact follows an ATRP-type mechanism, since the main activator is Cu^0 and not Cu^I. Providing a resolution for the debate on SET-LRP and ATRP was beyond the scope of this work.

5.1.2 NMP

Similar to ATRP, NMP involves a dynamic equilibrium between a dormant alkoxyamine and transient propagating radicals, while persistent nitroxide radicals ensure control over the system. The stable nitroxide radicals react with propagating chains forming the dormant alkoxyamine terminated chain, which in turn is thermally activated, as shown in Scheme 5.3.[16]
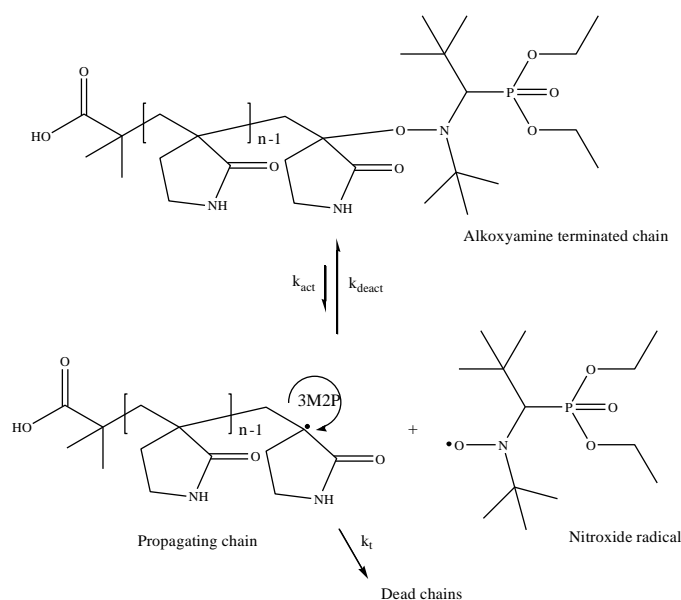
Scheme 5.3: Mechanism of the NMP of 3M2P using BlocBuilder® as the alkoxyamine.

5.1.3 RAFT

RAFT depends on a degenerative chain transfer mechanism, where the RAFT agent is the reversible deactivator. Rapid equilibrium between dormant species (macro-RAFT agent) and propagating radicals, depicted in Scheme 5.4, yields polymers with narrow molecular weight distributions ($Đ < 1.5$), where Z indicates the stabilizing-group of the RAFT-agent. In a well behaved RAFT system, the rate of chain transfer is higher than the rate of propagation and polymer chains are predominantly in the dormant state.[6,17]
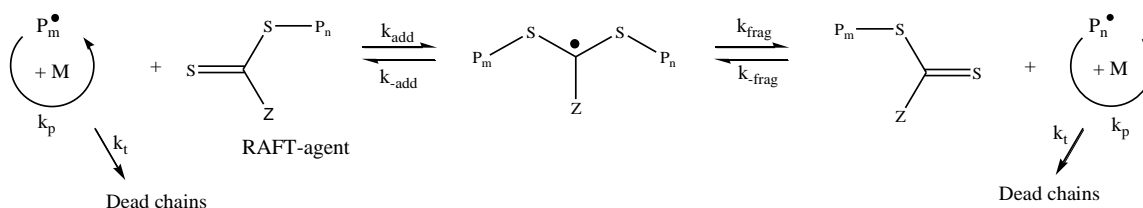
Scheme 5.4: Main equilibria of the RAFT process.

5.2 Results and discussion

In this chapter, three different LRP techniques are discussed. The rationale behind demonstrating these different techniques is that the monomer 3M2P can potentially undergo a wide variety of LRP techniques yielding a novel, water-soluble and all-carbon backbone polymer that has a greater polymerization versatility than other water-soluble polymer like PVP, PEG, polyacrylamides, *etc*.

5.2.1 SET-LRP

Attractive properties of SET-LRP, apart from the effortless removal of copper species, include the ultrafast synthesis of linear polymers with predictable molecular weights and low dispersities. These polymerizations also have mild conditions and can be carried out at room temperature and in solvents such as DMSO and water, which are generally not used in classical ATRP. The polymers and polymer mixtures obtained from SET-LRP are generally colourless. Additionally, ultrahigh molecular weight polymers can be achieved with quantitative retention of the chain-end functionalities.[14]

A typical SET-LRP polymerization mixture includes monomer, Cu^0 catalyst, ligand, initiator and solvent. Each reagent in a SET-LRP system needs to be considered thoroughly, as it influences the efficiency and overall control of the system. For the SET-LRP of 3M2P, all of the abovementioned aspects were considered.

Firstly, Cu^0 wire was utilized as a uniform copper catalyst, as it has shown better molecular weight predictions than Cu^0 powder and also a simpler experimental setup.[18] Secondly, in a successful SET-LRP all Cu^I species formed must instantaneously disproportionate to Cu^0 (activator) and Cu^{II} (deactivator) species. Polar solvents such as water and DMSO assist in the electron transfer of Cu^I species and are spontaneously disproportionated.[14,19] Both solvents were used and dissolved 3M2P very rapidly.

Thirdly, Me_6TREN (tris[2-dimethylamino)ethyl]amine) was chosen as the ligand, as Zhang *et al*. reported the rapid disproportionation of CuBr species with Me_6TREN as ligand in aqueous media.[20] Additionally, Me_6TREN was reported in successful ATRP of (meth)acrylamides,[21] which are structurally similar to the ring-closed *N*-methyl methacrylamide, 3M2P. The initiator in the SET-LRP of 3M2P was a water-soluble bromo-ester, 1,2-dihydroxypropane-3-oxy-2-bromo-2-methylpropionyl, with previous success reported on substituted acrylamides, in particular poly(*N*-isopropylacrylamide).[20] Lastly, the temperature was set at 50 °C as it was reported to enhance the disproportionation of Cu^I species.[22] The reaction conditions are depicted in Scheme 5.5.
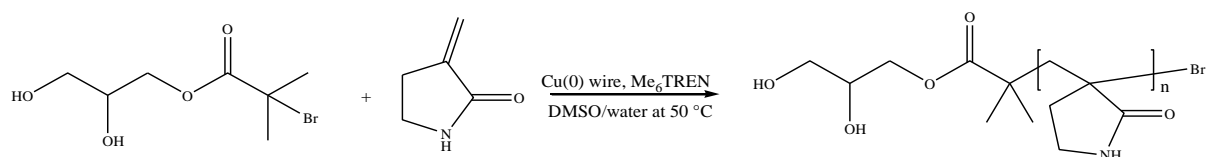
Scheme 5.5: SET-LRP of 3M2P.

The polymerization in DMSO developed a slight green colour visualized within 35 min of the polymerization that is ascribed to the formation of Cu^{II} species. As mentioned above, various conditions for the polymerization were chosen to favour disproportionation of the Cu^I species. After the polymerization mixture was filtered through a short aluminium oxide column to

remove residual soluble copper species and the solvent was removed *in vacuo*, a colourless polymer was obtained. Subsequently, the polymer was re-dissolved and precipitated into acetone, giving a white powder.

The conditions and results for the polymerization in DMSO are given in Table 5.1.

Table 5.1: Reaction conditions and results for the SET-LRP in DMSO

Sample	$[M_o]/[I_o]/[Me_6TREN]$	Solvent	Targeted M_n^a	M_n^b	M_w^b	M_n^c, NMR	$Đ^d$
1	100/1/0.5	DMSO	10 000	11 176	12 936	8 009	1.16

- [a] The target M_n was calculated as following:

$$M_n^{Targeted} = \frac{n_{M_0}}{n_{I_0}} \times M_{r(M)} + M_r(I)$$

- [b] Number average and weight average molecular weights (g/mol) determined by HFIP SEC. Detailed SEC conditions in the experimental Section 4.4.
- [c] Number average molecular from ^1H NMR calculated as:

$$M_n^{NMR} = \frac{\int Polymeric\ protons(b)/2}{\int Chain\ end\ proton(a)/1} \times M_{3M2P} + M_{initiator}$$

- [d] $Đ$ is the molar mass dispersity.

It was observed that a high molecular weight polymer was synthesized with precision, as the M_n value determined *via* SEC was comparable to the targeted M_n. The molecular weight distribution was narrow, with a low $Đ = 1.16$, indicating that the polymerization was controlled. The M_n value from ^1H NMR spectroscopy, (M_n^{NMR}) of 8 009 g/mol, was also comparable to the theoretical value. The difference between M_n^{NMR} and M_n^{SEC} is ascribed to the method of calculation, where the latter is a relative value calculated from a calibration curve determined by PMMA standards. The M_n^{NMR} value was calculated from the equation in Table 5.1, where signal b from Figure 5.1, was attributed to 2 protons from the repeating 3M2P units. This was integrated towards signal a, attributed to 1 proton from the polymer chain-end, giving the degree of polymerization (DP). To yield the M_n^{NMR}, the DP was multiplied by the molar mass of 3M2P and the chain-end from the initiator was added.
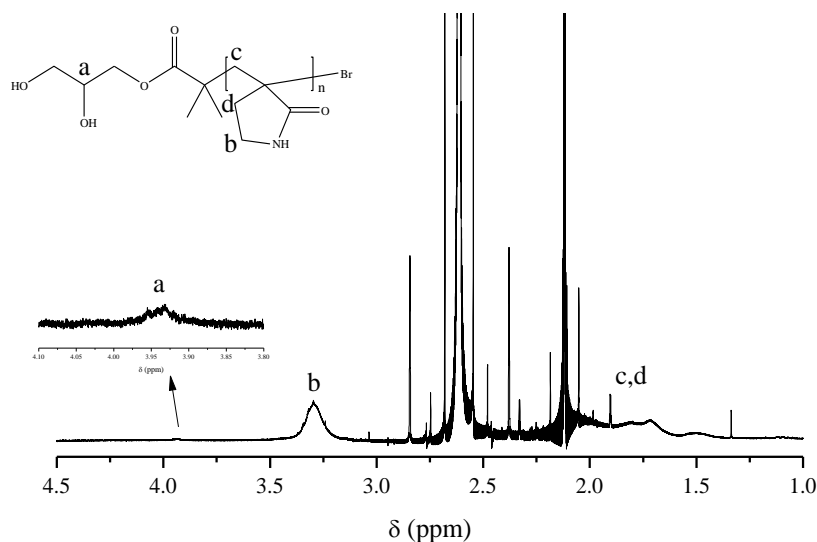
Figure 5.1: ^{1}H NMR spectrum of polymer 1 in D$_2$O.

Two aqueous polymerizations were adapted from a procedure by Percec *et al*. for the SET-LRP of *N*-(2-hydroxypropyl)methacrylamide in water.[22] Similarly to polymer **1**, the aqueous polymerization yielded colourless polymers and upon further precipitation yielded a white powder. The first polymerization having conditions as depicted in Table 5.1, gave a M_n^{NMR} = 3 568 g/mol and the second polymerization with an additional 5 % CuBr$_2$, acting as a supplemental deactivator (Cu^{II} species), yielded a polymer in the same molecular weight range with a M_n^{NMR} = 3 210 g/mol. The general trend of the aqueous polymerizations showed a lower M_n^{NMR} and overall lower conversion than the polymerization in DMSO. The M_n^{NMR} values of the aqueous polymerizations were calculated in a similar fashion as polymer **1**, however the conversions were extremely low and SEC analysis could not be performed on the samples.

The low conversions observed from the aqueous SET-LRP of 3M2P were ascribed to using bromide initiators. Percec *et al*. additionally reported either low, no conversions or ultrahigh molecular weights with low conversions when bromide initiators, instead of chloride initiators, were used during the aqueous SET-LRP of *N*-(2-hydroxypropyl)methacrylamide.[22] Furthermore, the removal of copper through the aluminium oxide column may have influenced the experimental determination of the conversion.

5.2.2 NMP

NMP can produce well-defined macromolecules, with this technique being mainly temperature-dependent (see Section 5.1.2), whereas ATRP is dependent on catalysts, initiators *etc*. The alkoxyamine, 2-methyl-2[*N*-tert-butyl-*N*-(1-diethoxyphosphoryl-2,2-dimethoxypropyl)aminoxy]propionic acid, also known as BlocBuilder®, was used as it has shown success with various acrylates and styrenic compounds.[23] The polymerization conditions are depicted in Scheme 5.6.
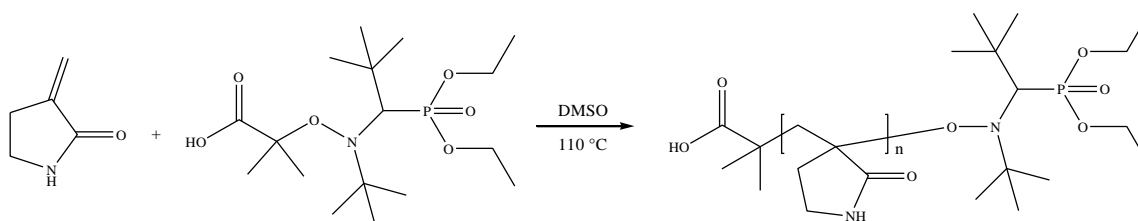
Scheme 5.6: NMP of 3M2P with BlocBuilder®.

Chain end functionalities were not visible on ^{1}H NMR spectra and could not be used to determine number average molecular weights. SEC was used to obtain number and weight average molecular weights, tabulated in Table 5.2.

Table 5.2: Reaction conditions for NMP of 3M2P

Sample	[M$_0$]/[BlocBuilder®]	Solvent	Reaction Time (h)	Reaction Temp (˚C)	Targeted M$_n$[a]	M$_n$[b]	M$_w$[b]	Đ[c]
2	100/1	DMSO	12	110	10 000	6 151	10 152	1.65

- [a] The target M$_n$ was calculated as following:

$$M_n^{Targeted} = \frac{n_{M_0}}{n_{BlocBuilder®_0}} \times M_{r(M)} + M_r(BlocBuilder®)$$

-
- [b] Number average and weight average molecular weights (g/mol) determined by HFIP SEC. Detailed SEC conditions in the experimental Section 4.4.
- [c] Đ is the molar mass dispersity.

A high molecular weight polymer was obtained with a broad molecular weight distribution of Đ = 1.65, an indication of poor control. The poor control can be ascribed to an initial rapid exothermic polymerization, which was also reported for the homopolymerizations of polymethacrylates at 80 °C. NMP is also very specific and limited in terms of monomer

compatibility, with (meth)acrylates, (meth)acrylic acids and styrenics being a few of the monomers successfully polymerized by NMP.[24]

Due to restraint of time and minute quantities of monomer yielded, the optimization of the NMP polymerization of 3M2P could not be demonstrated. However, the bond between 3M2P-alkoxyamine (BlocBuilder®) plays a significant role and if the bond is more thermally stable, polymerizations will be slowed down. In the case of 3M2P, further experiments are required to determine the compatibility of the monomer to alkoxyamine and the stability of the 3M2P-BlocBuilder® bond. If the bond were to be unstable it would create fast polymerizations leading to poor control. A solution to overcome fast and uncontrolled polymerizations may be reduction of the polymerization temperature.

5.2.3 RAFT

Although RAFT has the possibility of polymerizing a wide variety of monomers, the choice of the appropriate RAFT agent is essential. With reference to Section 5.1.3 mentioned above, predetermined molecular weight polymers with low dispersities can be prepared *via* this technique.[6]

Trithiocarbonates, with high transfer constants generally work for most monomer classes, whilst RAFT agents such as xanthates and dithiocarbamates, with low transfer constants work for less activated monomer systems. All RAFT agents consist of various Z (stabilizing)-and R (leaving)-groups. The role of the Z-group, as depicted in Figure 5.2, is to stabilize and activate the intermediate radical. The selected R-group should be a good homolytic leaving group and be capable of re-initiating chains.[25]

It was contemplated that 3M2P was stabilized by the conjugated carbonyl and similarly, styrene was stabilized by the conjugation in the aromatic ring. RAFT agents with a high transfer constant such as trithiocarbonates were proposed to successfully polymerize these stabilized monomer systems. An additional advantage of using trithiocarbonates is that they can be synthesized with two homolytic R-groups and ABA triblock polymers can easily be synthesized in this manner.[26]
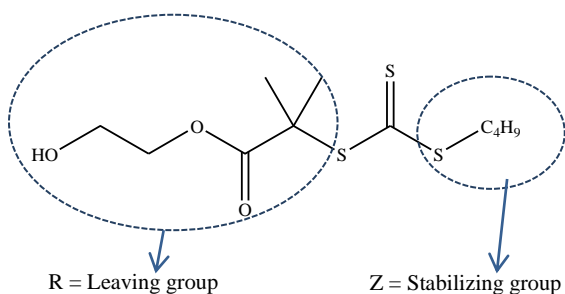
Figure 5.2: Choice of RAFT agent for polymerization of 3M2P and styrene, 2-hydroxyethyl 2-(butylthiocarbonothioylthio)-2-methylpropanoate.

The trithiocarbonate, 2-hydroxyethyl 2-(butylthiocarbonothioylthio)-2-methylpropanoate, depicted in Figure 5.2 was proposed for the polymerization of 3M2P as well as the block copolymer synthesis of styrene and 3M2P. The Z-group, a thiobutyl chain provides, a high transfer constant. Furthermore, R-groups with the structure $C(CH_3)_2COOEt$ are known for being very good homolytic leaving groups.[27] Similarly, the RAFT agent of choice is a hydroxyl-terminated $C(CH_3)_2COOEt$ analogue.

The RAFT polymerizations were carried out as shown in Scheme 5.7.
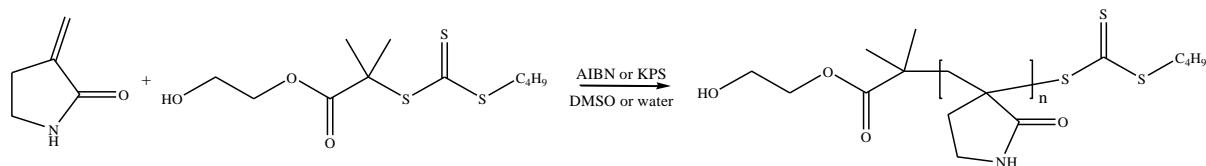
Scheme 5.7: RAFT polymerization of 3M2P.

The RAFT polymerizations carried out in an aqueous medium at 75 °C with KPS as initiator gave a white powder that was insoluble in HFIP for SEC analysis. ^{1}H NMR spectroscopy in D_2O revealed the loss of chain-end functionalities. Loss of the RAFT chain-ends can be ascribed to various side-reactions such as aminolysis, oxidation, hydrolysis, *etc*. It has been reported by McCormick *et al*. that aqueous homopolymerizations with trithiocarbonates in particular, are prone to hydrolysis and that reagents and reaction conditions must be selected in order to eliminate or minimize hydrolysis.[28] Due to the disadvantages of utilizing aqueous polymerization mediums, as mentioned above, this technique was not used to optimize and further polymerizations were carried out in DMSO.

Table 5.3: RAFT polymerizations conditions and results in DMSO

Sample	$[M_0]/[R_0]/[AIBN_0]$	Rxn Time (h)	Rxn Temp (°C)	Targeted M_n (g/mol)[a]	M_n[b]	M_w[b]	M_n[c] NMR	$Đ$[d]
3	113/0.56/0.11	40	60	20 000	16 335	20 036	4 841	1.23
4	113/0.56/0.11	36	75	20 000	14 882	20 057	13 853	1.35
5	113/2.34/0.47	50	75	5 000	9 369	12 373	4 793	1.32

- [a] The target M_n was calculated as following:

$$M_n^{Targeted} = \frac{n_{M_0}}{n_{R_0}} \times M_{r(M)} + M_r(R)$$

- [b] Number average and weight average molecular weights (g/mol) determined by HFIP SEC. Detailed SEC conditions in the experimental Section 4.4.
- [c] Number average molecular from ^{1}H NMR calculated as:

$$M_n = \frac{\int Polymeric\ protons(c)/2}{\int Chain\ end\ proton(a\ or\ b)/2} \times M_{3M2P} + M_{RAFT-agent}$$

- [d] $Đ$ is the molar mass dispersity.

Table 5.3 depicts the RAFT polymerizations in DMSO with all molar mass disperties $Đ < 1.5$, indicating narrow molecular weight distributions, typical of living radical polymerizations. In particular, polymer **3** (at 60 °C) showed a very low dispersity of 1.23; however polymer **4** (at 75 °C) had a higher dispersity of 1.35. The M_n^{SEC} was higher than the M_n^{NMR} in all cases, which can be ascribed to the method of calculation. The SEC chromatograms give a relative molecular weight compared to PMMA standards with a different hydrodynamic volume than that of P(3M2P), whereas M_n^{NMR} relies on the retained chain-end functionality.

The M_n^{NMR} was calculated using the equation in Table 5.3. Figure 5.3 depicts the ^{1}H NMR spectrum of polymer **4** in D_2O. Signals a and b from the chain-end, each signal attributed to 2 protons, were integrated and compared with signal c, attributed to 2 protons from repeating monomer units (polymeric protons).

The same conditions of **4** were used to synthesize **5**. This was done to demonstrate that lower molecular weight polymers with narrow dispersities can also be synthesized by this technique.
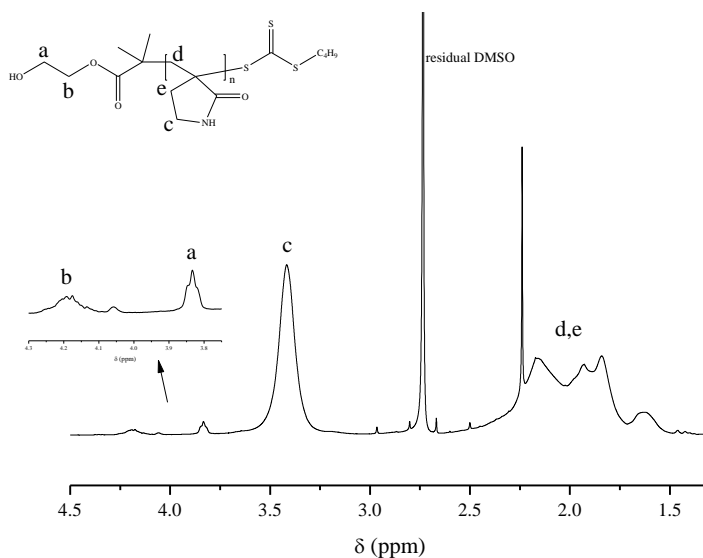
Figure 5.3: ^{1}H NMR spectrum of P(3M2P) with RAFT chain-ends in D$_2$O.

The conversion for a RAFT polymerization with conditions similar to that of polymer **4** was monitored over 20 hours, as shown in Figure 5.4 (**A**). The conversion was calculated from depleting monomer peaks with respect to a reference peak (DMF) via ^{1}H NMR spectra at different time intervals. Subsequently, the ^{1}H NMR spectroscopy samples were precipitated and SEC chromatograms obtained for each time interval. After 20 hours, the polymerization reached a conversion of 55 %, typical for the RAFT polymerizations of 3M2P. Figure 5.4 (**B**) also shows the conversion versus $M_n^{\text{Theoretical}}$ (blue graph) and M_n^{SEC} (black graph), respectively. All data points for M_n^{SEC} were not collected, as the quantities in which the samples were obtained, were too little to measure.
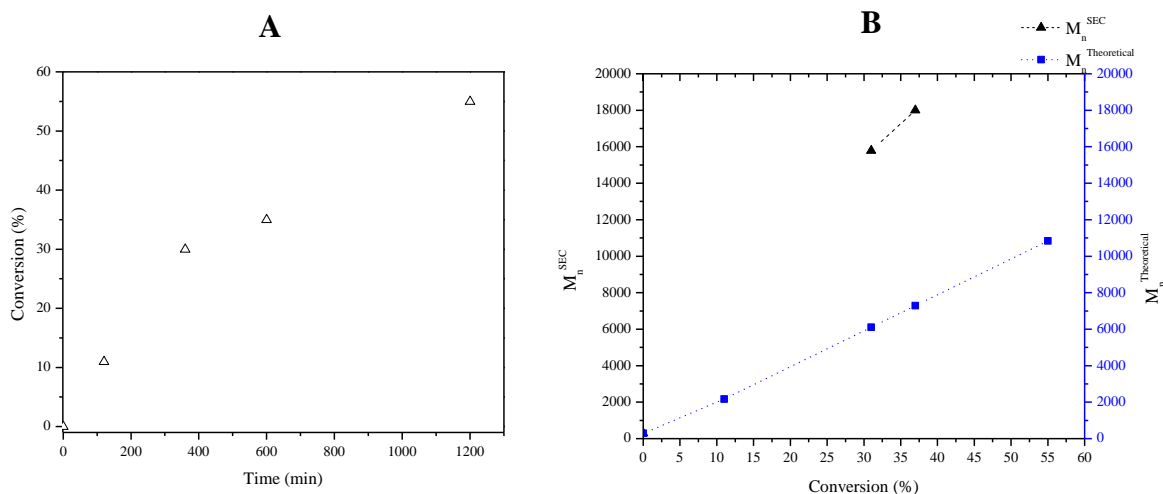
Figure 5.4: Conversion versus time and M_n^{SEC} and $M_n^{Theoretical}$ versus conversion for 20 h.

The M_n^{SEC} is higher than the $M_n^{Theoretical}$ which is attributed to the PMMA standards used as a calibration from SEC that have different hydrodynamic volumes compared to P(3M2P), giving larger molecular weights.

5.2.4 Towards block copolymers

Block copolymers have a broad spectrum of applications and are incorporated in various fields such as thermoplastic elastomers with each block contributing to the materials' thermoplastic or elastomeric properties.[29] Block copolymers also have gained increasing importance, especially in the development of micelles, vesicles, nanospheres, *etc*. for drug-delivery.[30] Other applications of block copolymers include lithography,[31] templating materials, nanocomposites,[32] *etc*.

A preliminary AB block amphiphilic copolymer was attempted with the same RAFT agent (trithiocarbonate) as the RAFT homopolymerizations of 3M2P. Initially, P(3M2P) was synthesized as the macro-initiator in DMSO and subsequently chain-extended with polystyrene (PS). However, the limited solubility of the isolated P(3M2P) macro-initiator had difficulties upon chain-extension. An approach by Qu *et al*. reported on the synthesis of an ABC triblock copolymer using a trithiocarbonate. Firstly, the AB diblock copolymer was synthesized by creating the polystyrene macro-initiator and subsequently, *N*,*N*-dimethylacrylamide was incorporated. Poly(*N*-isopropylacrylamide) was the third block incorporated in the triblock copolymer.[33] It was therefore proposed to first synthesize the hydrophobic polystyrene (PS)

segment as Qu *et al.* demonstrated, and then to chain-extend with the water-soluble P(3M2P) segment in an attempt to improve the solubility of the block copolymer, as shown in Scheme 5.8.
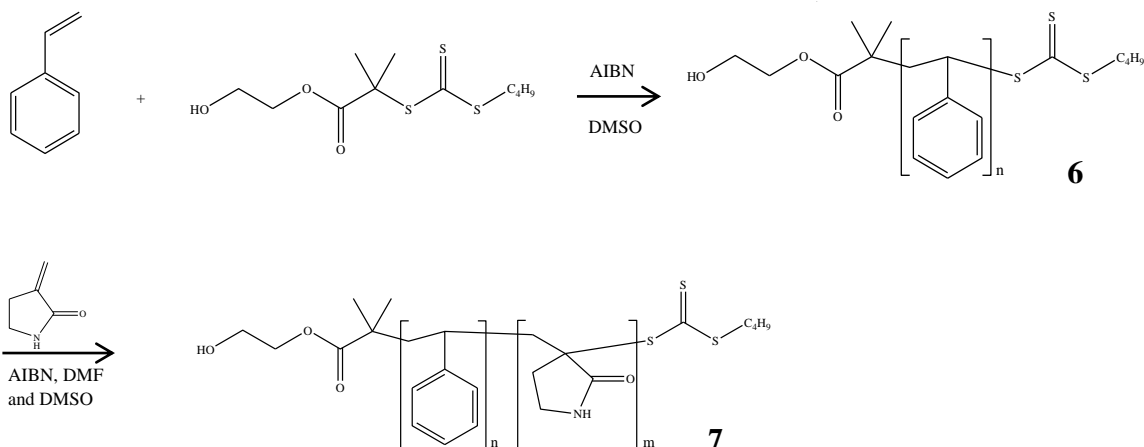
Scheme 5.8: Synthesis of PS-*b*-P(3M2P).

Table 5.4 indicates the RAFT polymerization conditions of styrene to yield macro-initiator **6**. A very low dispersity of 1.17 was obtained in dioxane. A yellowish polymer was obtained and the colour is ascribed to the RAFT chain ends.

Table 5.4: RAFT polymerization of styrene macro-initiator (6)

Sample	Solvent	Rxn Time (h)	Rxn Temp (°C)	Targeted M_n (g/mol)[a]	M_n[b]	M_w[b]	M_n[c] NMR	$Đ$[d]
6	dioxane	24	75	20 000	7 017	8 209	9 731	1.17

- [a] The target M_n was calculated as following:

$$M_n^{Theoretical} = \frac{n_{M_0}}{n_{R_0}} \times M_{r(M)} + M_r(R)$$

- [b] Number average and weight average molecular weights (g/mol) determined by THF SEC. Detailed SEC conditions in the experimental Section 5.4.
- [c] Number average molecular from ^{1}H NMR calculated as:

$$M_n = \frac{\int \text{Polymeric protons (c and d)}/2}{\int \text{Chain end proton(a and b)}/2} \times M_S + M_{RAFT-agent}$$

- [d] $Đ$ is the molar mass dispersity.

The equation from Table 5.4 was used to calculate M_n^{NMR} of **6**, from signals indicated in Figure 5.5. All other chain-end signals were overlapped and were not used to determine the molecular weight. The M_n^{NMR} and M_n^{SEC} of 9 731 and 7 017 g/mol respectively, were in fairly good agreement and this can be attributed to the low dispersity polystyrene standards used for

calibration of the SEC. THF was the eluent for all block copolymer SEC chromatograms, as the block copolymers were insoluble in HFIP.
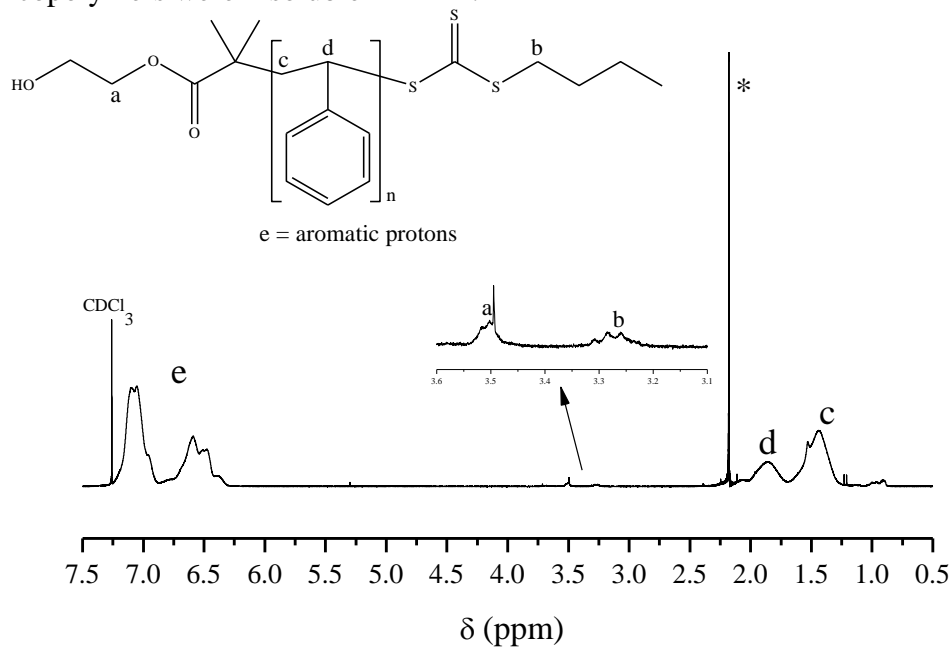
Figure 5.5: ^{1}H NMR spectroscopy of polystyrene macro-initiator in CDCl$_3$.

The ^{1}H NMR spectroscopy and SEC analysis of **6** in Table 5.4 indicate a molecular weight of approximately 10 000 g/mol. Since styrene and 3M2P have similar molecular weights of 104 and 97 g/mol respectively, a preliminary chain extension of **6** with a 5 000 g/mol P(3M2P) chain was attempted.

The block copolymerization was carried out in a DMSO:DMF solvent mixture with a ratio of 1:1. AIBN was used as initiator in small quantities at 75 °C for 24 hours. After isolation, the block copolymer **7** was a white powder. The colour change from yellow of **6** to a white powder of **7** is indicative of the loss of Z chain-ends.

From the SEC chromatogram, in Figure 5.6, the dotted line indicates the polystyrene macro-initiator, whereas the red solid line indicates the block copolymer, after chain extending the polystyrene macro-initiator with 3M2P. The block copolymer shows an increase in molecular weight of approximately 860 g/mol, indicative of ≈ 8 monomer units. Thus, the second block consisted of a short oligomeric hydrophilic 3M2P chain.

76

Figure 5.6: SEC chromatograms of PS and after chain-extending, PS-b-P(3M2P).

A presaturation ^{1}H NMR spectrum of PS-b-P(3M2P) in DMSO-d_6 at 80 °C is shown in Figure 5.7. At room temperature the block copolymer in DMSO-d_6 was a white, milky solution and at approximately 70-80 °C became a clear solution.

Figure 5.7: PS-b-P(3M2P) ^{1}H NMR spectroscopy in DMSO-d_6 at 80 °C.

77

5.3 Conclusion
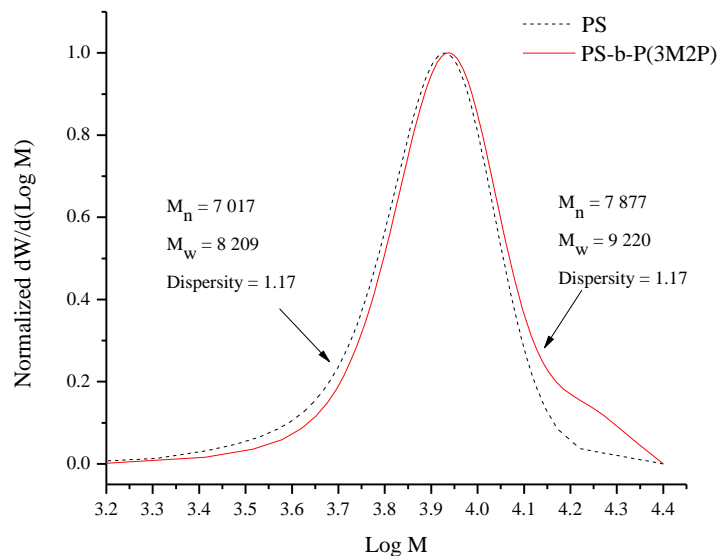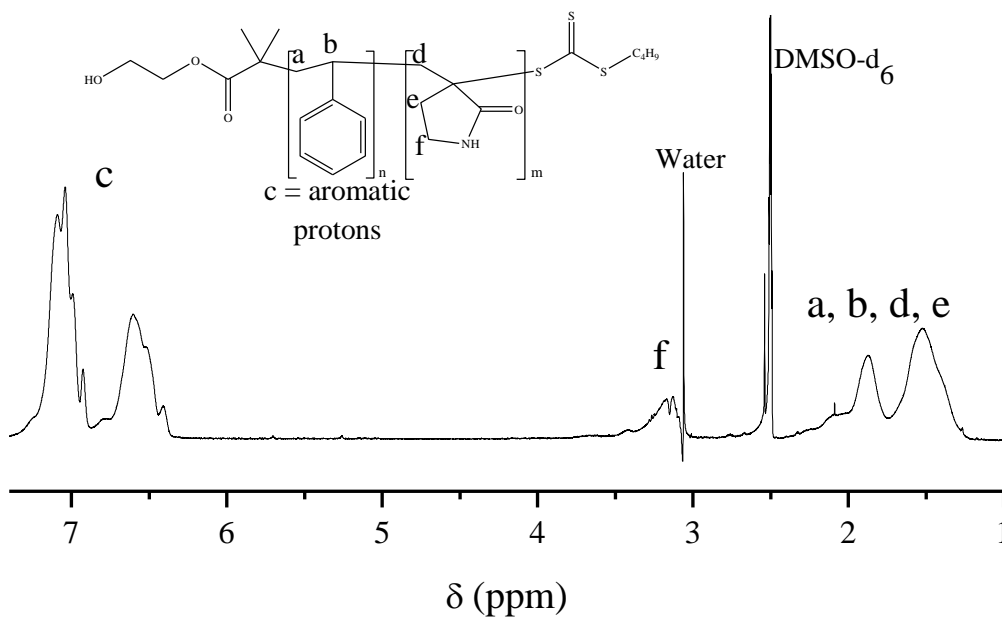
3M2P was polymerized *via* three different LRP techniques; SET-LRP, NMP and RAFT, respectively. Polymers obtained *via* SET-LRP in DMSO had the best control with dispersities of ≈ 1.16, whereas aqueous SET-LRP showed very low conversions, ascribed to the bromo-initiator utilized in water. Contrarily, NMP had poor control with high dispersities > 1.5 that is ascribed to the unstable 3M2P-BlocBuilder® bond. RAFT polymerizations in DMSO gave good dispersities and conversions, with good integrity of chain-end functionalities and were characterized by SEC and ¹H NMR spectroscopy. Both SET-LRP and RAFT polymerizations were performed in water and DMSO, of which the latter was more successful. From all the LRP techniques considered above, P(3M2P) has proven to be a promising, versatile new polymer.

In addition, a preliminary amphiphilic PS-*b*-P(3M2P) block copolymer was synthesized and the polystyrene macro-initiator was successfully chain-extended with oligomeric chains of 3M2P as indicated by SEC.

5.4 Experimental

5.4.1 General details

General information is stated in Section 3.4.1 and 4.4.1. Styrene (Sigma Aldrich, 99%) was passed through an aluminium oxide column to remove any oligomers and subsequently stored on molecular sieves (4 Å). Anhydrous DMSO (Sigma, > 99%) and distilled water were utilized as solvents.

THF SEC were performed on an Agilent 1260 Infinity series consisting of a 1260 degasser and quaternary pump, 1260 ALS auto sampler, a 1260 variable wavelength UV detector operating at wavelengths of 254 and 320 nm and a PL-ELS 1200 evaporative light scattering detector. The stationary phases consisted of three columns, PLgel 3 μm Guard (50 mm × 7.5 mm) and 2 PLgel 3 μm Mixed-E (300 mm × 7.5 mm). The flow rate was 1 mL/min with a column oven temperature of 30 ℃. The injection volume was 100 μL, with a sample concentration of 2 mg/mL in HPLC-grade THF. PSS WinGPC Unity software was used for data collection. Polystyrene standards, all with narrow dispersities were obtained from Chemetrix (Pty) Limited South Africa, Agilent Technologies.

The water-soluble initiator for SET-LRP, 1,2-dihydroxypropane-3-oxy-2-bromo-2-methylpropionyl was prepared in a two-step reaction as indicated in literature.[34] The ligand, Me₆TREN was prepared as indicated in literature.[35]

BlocBuilder® was donated by Dr Lebohang Hlalele.

5.4.2 Synthetic procedures

5.4.2.1 Synthesis of the carboxylic acid terminated trithiocarbonate

The RAFT agent utilized was 2-hydroxyethyl 2-(butylthiocarbonothioylthio)-2-methylpropanoate and was prepared in a two-step reaction, adapted from literature:[36]
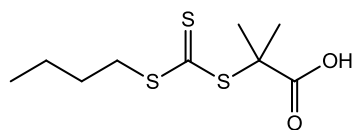
To a 500 mL round bottom flask was added potassium phosphate tribasic (16.60 g, 78.20 mmol) in 130 mL acetone and the reaction mixture was stirred for 5 h, yielding a yellow suspension. Subsequently, 1-butanethiol (8.0 mL, 74.2 mmol) was added to the reaction mixture and stirred for an hour. Carbon disulfide (9.10 mL, 151 mmol) was added dropwise and the reaction mixture was stirred for 2 h, while immersed in an ice bath. Where after 2-bromo-2-methylpropionic acid (11.70 g, 70.0 mmol) was added to the reaction mixture at room temperature whilst stirring and left stirring overnight. The solid was filtered and the filtrate concentrated. Cold 10 % HCl solution (100 mL) was added to the residue at room temperature and stirred overnight. The reaction mixture was extracted with two portions of hexane (50 mL) where after the organic phase was dried over MgSO₄, filtered and the solvent was removed under reduced pressure giving a bright yellow solid. The solid was purified by column chromatography using ethyl acetate:pentane (1:4) on silica gel. Solvents were removed *in vacuo* to yield the product, the carboxylic acid terminated trithiocarbonate (72 %). ¹H NMR (300 MHz, CDCl₃) δ: 3.29 (t, J = 7.5 Hz, 2H, -S-C$\underline{H}_2$), 1.71 (s, 6H, -S-CH-(C$\underline{H}_3$)₂), 1.64 (p, J = 8.9 Hz, 2H, -CH₂-C$\underline{H}_2$-CH₂), 1.39 (m, 2H, -CH₃-C$\underline{H}_2$-CH₂), 0.90 (t, J = 7.3 Hz, 3H, -C$\underline{H}_3$-CH₂).

5.4.2.2 Synthesis of the hydroxyl-terminated trithiocarbonate
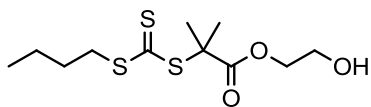
The second step was carried out to esterify the carboxylic acid terminated trithiocarbonate. The purified carboxylic acid terminated trithiocarbonate (1.50 g, 5.94 mmol) and ethylene glycol (3.60 g, 59.0 mmol) was dissolved in 75 mL THF. The reaction mixture was stirred and DCC (1.23 g, 5.94 mmol) was added to the reaction flask, which was immersed in an ice bath 5 minutes prior to the addition of DMAP (0.07 g, 0.59 mmol) whilst stirring. The ice bath was removed after 1 h and the reaction was allowed to run overnight at room temperature. Subsequently, the reaction mixture was dispersed in diethyl ether and filtered. The filtrate was washed with a 5 % sodium hydrogen carbonate solution (2×30 mL) and water (1×30 mL). Where after the organic phase was dried over $MgSO_4$, filtered and the solvent removed under reduced pressure to give a dark, orange oil. The oil was purified by column chromatography using ethyl acetate: pentane (1:4) solvent system. The hydroxyl terminated trithiocarbonate was yielded (62 %). ^{1}H NMR (300 MHz, CDCl$_3$) δ: 4.18 (m, 2H, -O-C$\underline{H}_2$), 3.74 (m, 2H, -C$\underline{H}_2$-OH), 3.29 (t, J = 7.4 Hz, 2H, -S-C$\underline{H}_2$), 1.65 (s, 6H, -CH(C$\underline{H}_3$)$_2$), 1.62 (m, 2H, -S-CH$_2$-C$\underline{H}_2$), 1.37 (m, 2H, -CH$_3$-C$\underline{H}_2$), 0.86 (t, J = 7.3 Hz, 3H, -C$\underline{H}_3$-CH$_2$).

5.4.2.3 General SET-LRP polymerization procedure of 3M2P at 50 °C:

The procedure was adapted from literature.[22] To a 25 mL Schlenk flask was added 3M2P (0.10 g, 1.03 mmol), Cu(0) wire wrapped around the stirring bar and 1,2-dihydroxypropane-3-oxy-2-bromo-2-methylpropionyl (2.47 mg, 0.10 mmol) as initiator, in 1.0 mL water or DMSO (as specified in Table 5.1). CuBr$_2$ (0.12 mg) was added as a radical deactivator in specified experiments. The reaction mixture was freeze-pump-thawed for five cycles where after the flask was filled with argon. A micro-syringe, flushed with argon thrice, was used to transfer the ligand, Me$_6$TREN (1.19 mg, 1.4 µL, 0.01 mmol), to the already deoxygenized reaction mixture. The reaction mixture was filtered through a short basic aluminium oxide column to remove copper, where after the polymer was precipitated from acetone to yield a white powder.

5.4.2.4 General NMP polymerization procedure of 3M2P at 110 °C:

The procedure was adapted from a combination of literature.[37,38] A typical polymerization consisted of 3M2P (0.11 g, 1.13 mmol) and BlocBuilder® (4.20 mg, 0.01 mmol) in 0.8 mL DMSO, with a [3M2P]:[BlocBuilder®] ratio of ~[100]:[1]. After the reaction mixture was dissolved and degassed with argon gas for 45 min, the mixture was heated to 110 °C for 12 h. After the reaction reached completion, the polymerization mixture was precipitated, slowly, into acetone and filtered, resulting in a brown powder.

5.4.2.5 General RAFT polymerization procedure of 3M2P (Target M_n = 20 000 g/mol) in DMSO:

To a 5 mL pear flask was added 3M2P (0.11 g, 1.13 mmol), RAFT agent (1.65 mg, 0.01 mmol) and AIBN (0.18 mg, 0.001 mmol), where [R]:[I] was chosen: $[n_I] = \frac{[n_R]}{5}$, in 0.8-1.0 mL DMSO. After the reaction mixture was dissolved and degassed with argon gas for 45 min, the polymerization vessel was placed in the heated oil bath (temperatures, initiators, polymerization solvents and targeted M_n with corresponding formula are specified in Table 5.3). When water was used as polymerization solvent, KPS, a water-soluble initiator was used. When the polymerization was considered complete, the polymer was precipitated from acetone and filtered, yielding a white-yellowish powder.

For the plot of conversion (from ^{1}H NMR spectroscopy) versus time (min), samples were removed from the polymerization vessel at predetermined times with an argon-vacuated syringe *via* the septum on the pear flask. To a 5 mL pear flask was added 3M2P (0.11 g, 1.13 mmol), RAFT agent (1.65 mg, 0.01 mmol), AIBN (0.18 mg, 0.001 mmol) and DMF (25 µL) as reference in 1.5 mL DMSO-d_6. The samples were directly transferred to a NMR spectroscopy tube, where after they were placed in the freezer to terminate any further radical-formation. ^{1}H NMR spectra were obtained and conversions were calculated from the depleting monomer peaks and reference (DMF) peak.

5.4.2.6 General PS-*b*-P(3M2P) polymerization procedure:

Firstly, a series of hydroxyl-end functionalized PS macro-initiators were synthesized with the RAFT agent, 2-hydroxyethyl 2-(butylthiocarbonothioylthio)-2-methylpropanoate. Styrene (1.0 g,

9.60 mmol), RAFT agent (15.0 mg, 0.05 mmol) and AIBN (1.67 mg, 0.01 mmol) were dissolved in 1 mL of 1,4-dioxane (this particular procedure was for a targeted M_n = 20 000 g/mol and additional information is specified in Table 5.4). The reaction mixture was degassed with argon gas for 45 min, whilst stirring and subsequently placed in an oil bath at 75 °C for 24h. When the polymerization was considered complete, the PS was precipitated from isopropanol, re-dissolved, precipitated (three times) to remove all unreacted monomer/oligomer and filtered to yield a yellowish powder.

Secondly, the PS macro-initiator was chain-extended with 3M2P. The macro-initiator (0.1 g, 0.01 mmol, M_n from ^{1}H NMR spectra = 9 427 g/mol), 3M2P (52.0 mg, 0.53 mmol) and AIBN (0.35 mg, 0.002 mmol) were dissolved in a 1 mL DMSO:DMF solvent mixture with a ratio of 1:1. Subsequently, the reaction mixture was degassed with argon gas for 45 min, where after the polymerization vessel was placed in a heated oil bath at 75 °C for 24 h. When the polymerization was considered complete, the polymer was precipitated into methanol and filtered to yield white powder.

5.5 References

(1) Matyjaszewski, K. *Macromolecules* **2012**, *45*, 4015.

(2) Odian, G. G.; Odian, G. *Principles of Polymerization*; Wiley-Interscience New York, 2004.

(3) Szwarc, M. *Nature* **1956***, 178*, 1168.

(4) Szwarc, M. *J. Polym. Sci., Part A: Polym. Chem.* **1998**, *36*, IX.

(5) Goto, A.; Fukuda, T. *Prog. Polym. Sci.* **2004**, *29*, 329.

(6) Barner-Kowollik, C. *Handbook of RAFT Polymerization*; John Wiley & Sons, 2008.

(7) Kato, M.; Kamigaito, M.; Sawamoto, M.; Higashimura, T. *Macromolecules* **1995**, *28*, 1721.

(8) Di Lena, F.; Matyjaszewski, K. *Prog. Polym. Sci.* **2010**, *35*, 959.

(9) Wang, J.-S.; Matyjaszewski, K. *J. Am. Chem. Soc.* **1995**, *117*, 5614.

(10) Matyjaszewski, K.; Coca, S.; Gaynor, S. G.; Wei, M.; Woodworth, B. E. *Macromolecules* **1997**, *30*, 7348.

(11) Percec, V.; Guliashvili, T.; Ladislaw, J. S.; Wistrand, A.; Stjerndahl, A.; Sienkowska, M. J.; Monteiro, M. J.; Sahoo, S. *J. Am. Chem. Soc.* **2006**, *128*, 14156.

(12) Konkolewicz, D.; Wang, Y.; Zhong, M.; Krys, P.; Isse, A. A.; Gennaro, A.; Matyjaszewski, K. *Macromolecules* **2013**, *46*, 8749.

(13) Konkolewicz, D.; Wang, Y.; Krys, P.; Zhong, M.; Isse, A. A.; Gennaro, A.; Matyjaszewski, K. *Polym. Chem.* **2014**.

(14) Rosen, B. M.; Percec, V. *Chem. Rev.* **2009**, *109*, 5069.

(15) Kwak, Y.; Matyjaszewski, K. *Polym. Int.* **2009**, *58*, 242.

(16) Matyjaszewski, K.; Davis, T. P. *Handbook of Radical Polymerization*; Wiley Online Library, 2002.

(17) Moad, G.; Rizzardo, E.; Thang, S. H. *Aust. J. Chem.* **2005**, *58*, 379.

(18) Nguyen, N. H.; Rosen, B. M.; Lligadas, G.; Percec, V. *Macromolecules* **2009**, *42*, 2379.

(19) Monge, S.; Darcos, V.; Haddleton, D. M. *J. Polym. Sci., Part A: Polym. Chem.* **2004**, *42*, 6299.

(20) Zhang, Q.; Wilson, P.; Li, Z.; McHale, R.; Godfrey, J.; Anastasaki, A.; Waldron, C.; Haddleton, D. M. *J. Polym. Sci., Part A: Polym. Chem.* **2013**, *135*, 7355.

(21) Teodorescu, M.; Matyjaszewski, K. *Macromolecules* **1999**, *32*, 4826.

(22) Nguyen, N. H.; Rodriguez-Emmenegger, C.; Brynda, E.; Sedlakova, Z.; Percec, V. *Polym. Chem.* **2013**, *4*, 2424.

(23) Gigmes, D.; Vinas, J.; Chagneux, N.; Lefay, C.; Phan, T. N.; Trimaille, T.; Dufils, P.-E.; Guillaneuf, Y.; Carrot, G.; Boué, F. *ACS Symp. Ser.* **2009**; *1024*, 245.

(24) Nicolas, J.; Couvreur, P.; Charleux, B. *Macromolecules* **2008**, *41*, 3758.

(25) Chiefari, J.; Chong, Y.; Ercole, F.; Krstina, J.; Jeffery, J.; Le, T. P.; Mayadunne, R. T.; Meijs, G. F.; Moad, C. L.; Moad, G. *Macromolecules* **1998**, *31*, 5559.

(26) Mayadunne, R. T.; Rizzardo, E.; Chiefari, J.; Krstina, J.; Moad, G.; Postma, A.; Thang, S. H. *Macromolecules* **2000**, *33*, 243.

(27) Braunecker, W. A.; Matyjaszewski, K. *Prog. Polym. Sci.* **2007**, *32*, 93.

(28) McCormick, C. L.; Lowe, A. B. *Acc. Chem. Res.* **2004**, *37*, 312.

(29) Trimbach, D.; Feldman, K.; Spencer, N. D.; Broer, D. J.; Bastiaansen, C. W. *Langmuir* **2003**, *19*, 10957.

(30) Letchford, K.; Burt, H. *Eur. J. Pharm. Biopharm.* **2007**, *65*, 259.

(31) Park, M.; Harrison, C.; Chaikin, P. M.; Register, R. A.; Adamson, D. H. *Science* **1997**, *276*, 1401.

(32) Hillmyer, M. A.; Lipic, P. M.; Hajduk, D. A.; Almdal, K.; Bates, F. S. *J. Am. Chem. Soc.* **1997**, *119*, 2749.

(33) Qu, Y.; Huo, H.; Li, Q.; He, X.; Li, S.; Zhang, W. *Polym. Chem.* **2014**, *5*, 5569.

(34) Perrier, S.; Armes, S. P.; Wang, X.; Malet, F.; Haddleton, D. M. *J. Polym. Sci., Part A: Polym. Chem.* **2001**, *39*, 1696.

(35) Fu, G.; Xu, L.; Yao, F.; Zhang, K.; Wang, X.; Zhu, M.; Nie, S. *ACS Appl. Mater. Interfaces* **2009**, *1*, 239.

(36) Jia, Z.; Bobrin, V. A.; Truong, N. P.; Gillard, M.; Monteiro, M. J. *J. Am. Chem. Soc.* **2014**, *136*, 5824.

(37) Hlalele, L.; Klumperman, B. *Macromolecules* **2011**, *44*, 6683.

(38) Vancoillie, G.; Pelz, S.; Holder, E.; Hoogenboom, R. *Polym. Chem.* **2012**, *3*, 1726.

Chapter 6: Epilogue

6.1 General conclusions

The discovery of alternatives to petroleum-based polymers is imperative and the design and synthesis of "green" polymers have become of increasing importance.[1] The approach we pursued included the involvement of plant-based renewable monomers.[2] The biosynthetically accessible 3M2P moiety was utilized as monomer in creating an all-carbon backbone polymer. The main objective was to test the properties and versatility of this new polymer.

The purification and optimization of the monomer synthesis were fundamental to the study (see Chapter 3). Two different approaches towards the synthesis of 3M2P were attempted. Initially, with the first synthesis route involving the Wittig reaction, two main obstacles were identified. The first being the many unsuccessful attempts in the removal of the by-product (TPPO) and the second being the formation of 3M2P-OH as a side-product. The difficulty in separating TPPO and 3M2P was attributed to strong hydrogen-bonding between the two compounds. However, a protocol was developed that led to the successful removal of TPPO. The formation of both 3M2P and the side-product 3M2P-OH, was controlled by the quantity of paraformaldehyde added. The quantities of paraformaldehyde were optimised for the synthesis of 3M2P and/or 3M2P-OH in moderate yields and the structures were confirmed by ^{1}H, ^{13}C and two-dimensional NMR spectroscopy. Monomers, 3M2P and 3M2P-OH, were obtained at a purity suitable for radical polymerizations, with yields ranging between 35-40 %. With the second synthesis route, the optimization of the last reaction step involving the dehydration of 3-(hydroxymethyl)-2-pyrrolidone, was unsuccessful. This was not investigated any further due to time constraints.

In Chapter 4, the conventional radical (co)polymerizations of 3M2P-based monomers were introduced. It was found that a mixture of 3M2P-OH and 3M2P in different ratios, proved to be soluble in water and the majority of organic solvents and therefore, statistical copolymerizations were performed on the mixtures. *In situ* ^{1}H NMR spectroscopy experiments could not confirm the incorporation or consumption of 3M2P-OH into the chains due to an overlapping peak. Only oligomeric species were obtained as indicated by the aqueous SEC of the statistical copolymerizations and further investigation was therefore abandoned. Homopolymerizations of

3M2P-OH were unsuccessful due to poor solubility. The poor solubility of 3M2P-OH could possibly be attributed to strong intra- and intermolecular forces.

Optimum conditions for the homopolymerizations of 3M2P were determined. P(3M2P), the polymer of initial interest, was obtained with very good conversions *via* conventional radical homopolymerizations. The polymer was characterized by NMR spectroscopy, SEC and the monomer consumption was monitored *via in situ* ^{1}H NMR spectroscopy experiments. Polymers were obtained with very good conversion > 80 % and high number average molecular weights ranging from approximately 52 000 – 68 000 g/mol. The *in situ* ^{1}H NMR spectroscopy revealed 99.9 % of the monomer consumed with the majority of monomer consumed within the first 200 min of the polymerization. Subsequently, various properties of P(3M2P) were investigated. The thermal stability and thermal properties were investigated *via* TGA and DSC. P(3M2P) had a very high main thermal decomposition temperature ranging between 400-500 °C, additionally exhibited a very high glass transition temperature of $T_g = 285$ °C. Furthermore, P(3M2P) proved to be very soluble in water, soluble in HFIP, partially soluble in heated DMSO and further poorly soluble in a wide variety of organic solvents. Both the high thermal stability and solubility behaviour were ascribed to the structural-rigid lactam ring and its strong ability to hydrogen bond. In addition, P(3M2P) was tested for a LCST and UCST in an aqueous medium, however no LCST nor UCST were observed in the temperature range of 25-80 °C. Finally, cytotoxicity testing was performed to evaluate this water-soluble polymer's biocompatibility, in order to expand the scope of possible applications. It was shown that P(3M2P) was non-toxic to GT1-7 cells up to the maximum concentration investigated of 1 mg/mL.

In order to investigate the versatility of 3M2P, various LRP techniques were utilized in Chapter 5. SET-LRP, NMP and RAFT techniques with varied conditions were pursued in order to create well-defined polymers with precision. The molecular weights and molecular weight distributions of the polymers were determined by ^{1}H NMR spectroscopy, where chain-end functionalities were retained and by SEC. The polymer obtained from the NMP polymerization exhibited poor control, with a $Đ = 1.65$ that could be ascribed to various different aspects such as temperature, 3M2P-alkoxyamine bond stability, *etc*. and was not investigated any further. The focus of controlled polymerizations shifted toward investigating different conditions for SET-LRP and RAFT polymerizations. Reaction conditions were thoroughly considered prior to

polymerizations and any resulting deviations from expectations, were explained. SET-LRP was performed in water and DMSO. The polymerization in DMSO achieved an overall higher conversion, molecular weight and better retention of chain-end functionalities than the aqueous polymerizations. The polymer had a M_n^{NMR} = 8 009 g/mol and a M_n^{SEC} = 11 176 g/mol, with a narrow molecular weight distribution of $Đ$ = 1.16, indicative of a successful living radical polymerization. The discrepancy between M_n^{NMR} and M_n^{SEC} was attributed to the method of calculation, where M_n^{NMR} is dependent on the retained chain-ends and M_n^{SEC} is dependent on the hydrodynamic volume of the standards (PMMA) used for calculating the calibration curve, that differs from the hydrodynamic volume of P(3M2P). RAFT polymerizations were also carried out in water and DMSO. Aqueous RAFT polymerizations proved to lose the majority of chain-end functionalities and these polymerizations were not optimized. An example of a polymer produced *via* a RAFT polymerization in DMSO achieved a M_n^{NMR} = 13 853 g/mol and a M_n^{SEC} = 14 882 g/mol, with a narrow molecular weight distribution of $Đ$ = 1.35, slightly higher than achieved *via* SET-LRP, however still indicative that control was achieved over the molecular weight distribution. The M_n^{NMR} and M_n^{SEC} were calculated in a similar fashion as polymers produced *via* SET-LRP, however showed a better correlation between the two values than produced by SET-LRP.

Additionally, a PS-*b*-P(3M2P) amphiphilic block copolymer was attempted *via* a RAFT polymerization (trithiocarbonate), in a final attempt of demonstrating the versatility and control of 3M2P-based macromolecular architectures. The block copolymer was characterized by ^{1}H NMR spectroscopy and SEC. From the SEC chromatograms it was determined that the molecular weight of the PS segment increased with 840 g/mol upon chain-extension, which is accounted for by approximately 8 3M2P-repeating units. Thus, the second hydrophilic segment consisted of an oligomeric P(3M2P) specie. Optimization of the block copolymer was not performed.

6.2 Future recommendations

Future work of 3M2P-based polymers can be extended to numerous different fields:

In future, alternative approaches to the synthesis of 3M2P, with the focus on a biosynthetic route, should be explored in order to obtain the greener synthesis of 3M2P for a more commercial production thereof.

Further investigation in the characterization of the P(3M2P) can be demonstrated by investigating *e.g.* the tacticity by ^{13}C NMR spectroscopy.[3] Chain growth polymerization such as ionic polymerizations (cationic in particular) as well as different LRP techniques not demonstrated in Chapter 5 (e.g. ATRP), will confirm the versatility of 3M2P. Sophisticated architectures *e.g.* block copolymers can be pursued and optimized *i.e.* the copolymerization of 3M2P with other monomers, as demonstrated with the preliminary block copolymer attempted.

Since P(3M2P) is non-toxic to cells and water-soluble, the polymer might be considered as part of a drug-delivery system. Additionally, P(3M2P) can be grafted onto natural biodegradable polymers in order to strengthen the latter.

6.3 References

(1) Horvath, I. T.; Anastas, P. T. *Chem. Rev.* **2007**, *107*, 2169.

(2) Coates, G. W.; Hillmyer, M. A. *Macromolecules* **2009**, *42*, 7987.

(3) Akkapeddi, M. K. *Macromolecules* **1979**, *12*, 546.